Electronic Supplementary Material (ESI) for Journal of Materials Chemistry C.

Supporting Information

2-Aryl-1,3,4-trifluoro-6,7,10,11-tetrakis(alkoxy)triphenylene: a remarkable and highly inclusive mesomorphic platform

Hui-Min Pan,[a] Jiao He,[a] Wen-Hao Yu,[a] Ping Hu,[a] Bi-Qin Wang,[a] Ke-Qing Zhao,*[a] and Bertrand Donnio*[c]

Contents

1. Materials and Methods

2. Synthesis and Characterization

3. NMR

4. HRMS

5. X-ray Crystallography

6. TGA

7. POM

8. DSC

9. S/WAXS

10. DFT

11. TOF

1. Materials and Methods

Chemicals. All commercially available starting materials were used directly without further purification. The solvents of air- and moisture-sensitive reactions were carefully distilled from appropriate drying agents before use.

Experimental. Air- and moisture-sensitive reactions were assembled on a Schlenk vacuum line using oven-dried glassware with a Teflon screw cap under Ar atmosphere. Air- and moisture-sensitive liquids and solutions were transferred by syringe. Reactions were stirred using Teflon-coated magnetic stir bars. Elevated temperatures were maintained using Thermostat-controlled air baths. Organic solutions were concentrated using a rotary evaporator with a diaphragm vacuum pump.

Analytical. ^{19}F-NMR/^{1}H-NMR/^{13}C-NMR spectra were recorded using a Varian UNITY INOVA 400/100 MHz spectrometer in $CDCl_3$, and TMS as the internal standard. High-resolution mass spectra (HRMS) spectra were recorded at the Fourier Transform ion cyclotron resonance mass spectrometer (7.0T FTICR-MS) made by IonSpec (Varian now) with MALDI as the ion source. Elemental analyses (EA) were performed on a Vario MicroSelect (Elementar Company, German). The thermal gravimetrical analysis (TGA) was measured on a TA-TGA Q500 instrument with heating rate of 10 or 20 °C/min in N_2 atmosphere. The phase transition temperatures and enthalpy changes were investigated using a TA-DSC Q100 differential scanning calorimeter (DSC) under N_2 atmosphere with heating or cooling rate of 10 °C/min. Liquid crystalline optical textures were observed on a Polarized Optical Microscope (POM) on an Olympus BH2 Polarized Optical Microscope equipped with a Mettler FP82HT hot-stages of which temperatures were controlled by XPR-201 and Mettler FP90. Temperature-variation SAXS (small-angle X-ray scattering) and WAXS (wide-angle X-ray scattering) experiments on Rigaku Smart lab. UV/Vis. absorption spectra were recorded on a Perkin Elmer Lambda 950 spectrophotometer at room temperature. Fluorescence was measured on a HORIBA Fluoromax-4p, and the quantum yields were measured by a HORIB-F-3029 Integrating Sphere, HORIBA, Kyoto, Japan. Crystal structure was measured on a Rigaku XtalAB Synergy R, DW system.

Photocurrent time-of-flight (TOF) technique uses N_2 gas laser (KEN-1520, Usho, 600 ps pulse width, λ =337 nm) and hot stage to measure compound electron and hole mobilities. The liquid crystalline sample cell with indium-tin-oxide (ITO) electrodes was mounted on a handmade hot stage, and electric bias was applied by dry cell batteries. The polarity (20 to 50 kV/cm) electric field is applied, a positive or negative charge carriers hopping through the self-organized aligned sample, causing displacement photocurrent, which was detected on a digital oscilloscope (DSO5052A, Agilent Technology) with a commercially available current amplifier (DHPCA-100, FEMTO). Thickness of the cell used for measurements was in range of 15~20 µm.

The cells were filled with the sample in its isotropic liquid state by capillary forces, and then cooled down to the columnar mesophase. POM images showed low-birefringent textures with homeotropic domains, and the laser focused on a spot with homeotropic aligned sample area.

2. Synthesis and Characterization

2.1 Synthesis of the pentafluorobiphenyl

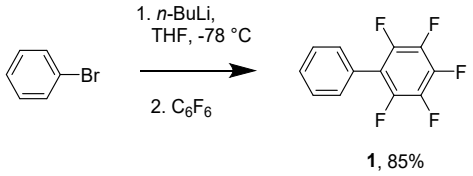

Scheme S1. Preparation of the pentafluorobiphenyl.

Bromobenzene (5.00 g, 31.80 mmol) was added in 200 mL reaction tube and THF (30 mL) was added under protection of argon. *n*-Butyllithium (2.5 M in hexane, 63.68 mmol) was slowly injected into the reaction tube with a syringe at -78 °C and the mixture was stirred for 1 h in argon, to prepare the aryl lithium reagent. Under Ar atmosphere perfluorobenzene (11.58 g, 63.74 mmol) was dissolved in THF (20 mL), then aryl lithium reagent was slowly added into the reaction system at 0 ° C and stirred at room temperature for 2 h. The reaction mixture was extracted with ether. The combined organic layers were dried over anhydrous $MgSO_4$ and concentrated in vacuo. Recrystallization with petroleum-ether, white solid **1** was obtained by sublimation and purification at 90-100 °C (6.58 g, yield 85%). **^{1}H NMR** (600 MHz, TMS, $CDCl_3$), δ (ppm) 7.52 – 7.45 (m, 3H, ArH), 7.42 (d, *J* = 7.8 Hz, 2H, ArH). **^{19}F NMR** (565 MHz, TMS, $CDCl_3$), δ (ppm) -143.22 – -143.30 (m, 2F, ArF), -155.57 – -155.64 (m, 1F, ArF) -162.19 – -162.29 (m, 2F, ArF).

2.2 Synthesis of 2,2’-dibromo-4,4’,5,5’-tetrakis(alkoxy)-1,1’-biphenyl derivatives, 2Br-**BP***n*

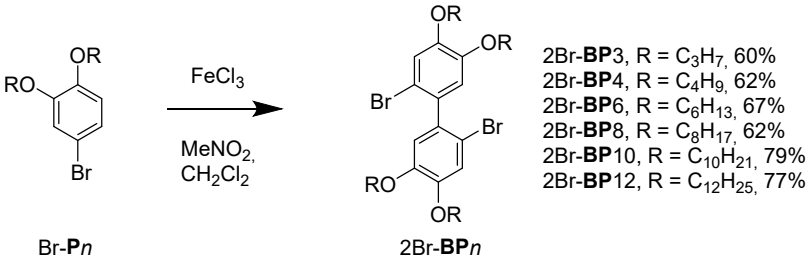

Scheme S2. Preparation of the dibromobiphenyls, 2Br-**BP***n*.

General procedure: To a stirred solution of 1-bromo-3,4-bis(alkoxy)benzene (Br-**P***n*, 1.0 equiv) in CH_2Cl_2 (60 mL), a solution of $FeCl_3$ (2.0 equiv) in CH_3NO_2 (10 mL) was added. The resulting solution was stirred at room temperature until completion of the reaction. The reaction mixture was quenched with methanol and extracted with dichloromethane. The combined organic layers were dried over anhydrous $MgSO_4$ and concentrated in vacuo. The residue was purified by column chromatography on silica gel with dichloromethane:petroleum ether (1:4.5) mixture as eluent. Recrystallization with ethanol and methanol gave white solid 2,2’-dibromo-4,4’,5,5’-tetrakis(alkoxy)-1,1’-biphenyl 2Br-**BP***n* (yields 60-80%).

2,2’-Dibromo-4,4’,5,5’-tetrakis(propyloxy)-1,1’-biphenyl(2Br-**BP**3): Br-**P**3 (3.35 mg,

6.15 mmol) was converted to the white solid 2Br-**BP**3 (2.01 g, yield 60%). **^{1}H NMR** (400 MHz, TMS, $CDCl_3$) δ (ppm) 7.10 (s, 2H, ArH), 6.76 (s, 2H, ArH),4.02 – 3.94 (m, 8H, OCH_2), 1.93 – 1.77 (m, 8H, CH_2), 1.48 – 1.27 (m, 8H, CH_2), 0.91 – 0.86 (m, 12H, CH_3).

2,2'-Dibromo-4,4',5,5'-tetrakis(butyloxy)-1,1'-biphenyl (2Br-**BP**4): Br-**P**4 (4.68 mg, 7.79 mmol) was converted to the white solid 2Br-**BP**4 (2.90 g, yield 62%). **^{1}H NMR** (400 MHz, TMS, $CDCl_3$) δ (ppm) 7.10 (s, 2H, ArH), 6.76 (s, 2H, ArH), 4.00 - 3.92 (m, 8H, OCH_2), 1.93 – 1.77 (m, 8H, CH_2), 1.08 – 1.00 (m, 12H, CH_3).

2,2'-Dibromo-4,4',5,5'-tetrakis(hexyloxy)-1,1'-biphenyl (2Br-**BP**6): Br-**P**6 (6.64 g, 9.32 mmol) was converted to the white solid 2Br-**BP**6 (4.45 g, yield 67%). **^{1}H NMR** (400 MHz, TMS, $CDCl_3$) δ (ppm) 7.10 (s, 2H, ArH), 6.76 (s, 2H, ArH), 4.03 – 3.95 (m, 8H, OCH_2), 1.87 – 1.74 (m, 8H, CH_2), 1.57 – 1.46 (m, 24H, CH_2), 1.01 – 0.94 (m, 12H, CH_3).

2,2'-Dibromo-4,4',5,5'-tetrakis(octyloxy)-1,1'-biphenyl (2Br-**BP**8): Br-**P**8 (6.87 g, 8.12 mmol) was converted to the white solid 2Br-**BP**8 (4.22 g, yield 62%). **^{1}H NMR** (400 MHz, TMS, $CDCl_3$) δ (ppm) 7.10 (s, 2H, ArH), 6.76 (s, 2H, ArH), 4.02 – 3.94 (m, 8H, OCH_2), 1.93 – 1.77 (m, 8H, CH_2), 1.50 – 1.31 (m, 40H, CH_2), 0.93 – 0.87 (m, 12H, CH_3).

2,2'-Dibromo-4,4',5,5'-tetrakis(decanoxy)-1,1'-biphenyl (2Br-**BP**10): Br-**P**10 (7.85 mg, 8.38 mmol) was converted to the white solid 2Br-**BP**10 (6.20 g, yield 79%). **^{1}H NMR** (400 MHz, TMS, $CDCl_3$) δ (ppm) 7.08 (s, 2H, ArH), 6.75 (s, 2H, ArH), 4.02– 3.93 (m, 8H, OCH_2), 1.86 – 1.76 (m, 8H, CH_2), 1.48 – 1.21 (m, 56H, CH_2), 0.91 – 0.83 (m, 12H, CH_3).

2,2'-Dibromo-4,4',5,5'-tetrakis(dodecyloxy)-1,1'-biphenyl (2Br-**BP**12): Br-**P**12 (7.01 mg, 6.68 mmol) was converted to the white solid 2Br-**BP**12 (5.40 g, yield 77%). **^{1}H NMR** (400 MHz, TMS, $CDCl_3$) δ (ppm) 7.08 (s, 2H, ArH), 6.75 (s, 2H, ArH), 4.02– 3.93 (m, 8H, OCH_2), 1.86 – 1.76 (m, 8H, CH_2), 1.48 – 1.21 (m, 72H, CH_2), 0.91 – 0.83 (m, 12H, CH_3).

2.3 Synthesis of the 2-phenyl-1,3,4-trifluorotriphenylene, **PH**0

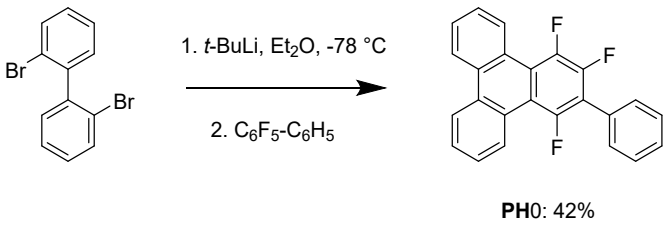

PH0: 42%

Scheme S3. Synthesis of **PH**0.

Under protection of argon, 2,2-dibromobiphenyl (0.30 g, 0.96 mmol) was charged in 50 mL reaction tube and Et_2o (10 mL) was added. *t*-Butyllithium (1.3 M in Hexane, 3.84 mmol) was slowly injected into the reaction tubes with a syringe at -78 °C and the reaction mixture was stirred at -78 °C for 2 h. Ph-C_6F_5 (0.54 g, 1.44 mmol) was added and the reaction solution continuing stirred at -78 °C for 0.5 h, then at room temperature for 10 h. The reaction mixture was extracted with dichloromethane. The combined organic layers were dried over anhydrous $MgSO_4$ and concentrated in vacuo. The crude product was separated and purified by silica gel column chromatography with (dichloromethane:petroleum ether = 1:3) as eluent, recrystallization with ethyl acetate and ethanol gave white solid (0.15 g，yield 42%).

^{1}H NMR (400 MHz, $CDCl_3$) δ (ppm) 9.06 – 9.01 (m, 1H, ArH), 9.00 – 8.95 (m, 1H, ArH), 8.66 – 8.65 (m, 1H, ArH), 8.64 – 8.63 (m, 1H, ArH), 7.76 – 7.47 (m, 9H, ArH). **^{19}F NMR** (565 MHz, $CDCl_3$) δ (ppm) -113.98 (d, *J* = 14.4 Hz, 1F, ArF), -139.27 (d, *J* = 19.5 Hz, 1F, ArF), -140.51 (t, *J* = 17.3 Hz, 1F, ArF). **^{13}C NMR** (151 MHz, $CDCl_3$) δ (ppm) 154.10, 152 .39, 147.42, 146.78, 145.89, 145.15,130.80, 130.57, 130.38, 128.74, 128.56, 128.48, 128.48, 128.21, 128.12, 128.01, 127.91, 127.74, 126.59 (d, *J* = 18.6 Hz), 123.20, 120.59 (t, *J* = 5.0 Hz), 126.66 – 126.53 (m), 116.39 (d, *J* = 13.4 Hz). **HRMS (MALDI)** Calcd for $C_{24}H_{13}F_3$ $[M]^+$ m/z: 358.0969 (100%), 359.1003 (26.0%), 360.1036 (3.2%); found 358.0964 (100%), 359.0998 (25%), 360.1033 (3.3%).

2.4 Synthesis of the 2-phenyl-1,3,4-trifluoro-6,7,10,11-tetra (alkoxy) triphenylene derivatives, **PH***n*

General procedure: Under protection of argon, 2Br-**BP***n* (1.0 equiv) was added in 50 mL reaction tube and then THF (10 mL) was added. *n*-Butyllithium (2.5 M in Hexane, 4.0 equiv) was slowly injected into the reaction tubes with a syringe at -78 °C and the reaction mixture was stirred at -78 °C for 2 h. C_6F_5-C_6H_5 (4.0 equiv) was added and the reaction solution continuing stirred at -78 °C for 0.5 h, then at room temperature for 10 h. The reaction mixture was extracted with dichloromethane. The combined organic layers were dried over anhydrous $MgSO_4$ and concentrated in vacuo. The crude product was separated and purified by silica gel column chromatography with (dichloromethane:petroleum ether = 1:3) as eluent, recrystallization with ethyl acetate and ethanol gave white solid **PH***n* (yields 60-90%).

2-Phenyl-1,3,4-trifluoro-6,7,10,11-tetra (propyloxy) triphenylene (**PH**3). 2Br-**BP**3 (0.30 g, 0.55 mmol) was converted to the white solid **PH**3 (0.23 g, yield 70%). **^{1}H NMR** (400 MHz, TMS, $CDCl_3$) δ (ppm) 8.50 (d, *J* = 5.6 Hz, 1H, ArH), 8.45 (d, *J* = 6.0 Hz, 1H, ArH), 7.82 (s, 2H, ArH), 7.62 (d, *J* = 7.4 Hz, 2H, ArH), 7.56 (t, *J* = 7.4 Hz, 2H, ArH), 7.51 (t, *J* = 8.0 Hz, 1H, ArH), 4.24 – 4.10 (m, 8H, OCH_2), 2.03 – 1.91 (m, 8H, CH_2), 1.18 – 1.07 (m, 12H, CH_3). **^{19}F NMR** (376 MHz, TMS, $CDCl_3$) δ (ppm) -115.44 – -116.13 (m, 1F, ArF), -141.73 (d, *J* = 18.6 Hz, 1F, ArF), -142.37 (s, 1F, ArF). **^{13}C NMR** (151 MHz, $CDCl_3$) δ (ppm) 153.50, 151.83, 149.78, 149.22, 148.60, 148.44, 146.38 – 146.07 (m), 144.80 – 144.45(m), 130.70, 129.16, 128.52, 128.39, 125.46, 124.96, 120.72 – 119.71 (m), 119.71 – 119.29 (m), 116.85 – 110.98 (m), 106.43, 106.10. **HRMS (MALDI)** calcd for $C_{36}H_{37}F_3O_4$ $[M]^+$ m/z: 590.2644 (100%), 591.2677 (38.9%), 592.2711 (7.4%); found 590.2640 (100%), 591.2673 (39%), 592.2707 (7.3%). **Elemental Analysis** ($C_{36}H_{37}F_3O_4$, MW 590.68): calcd C 73.20%, H 6.31%; found C 73.15%, H 5.85%.

2-Phenyl-1,3,4-trifluoro-6,7,10,11-tetra(butyloxy)triphenylene (**PH**4). 2Br-**BP**4 (0.40 g, 0.67 mmol) was converted to the white solid **PH**4 (0.38 g, yield 87%). **^{1}H NMR** (400 MHz, TMS, $CDCl_3$) δ (ppm) 8.50 (d, *J* = 5.7 Hz, 1H, ArH), 8.45 (d, *J* = 6.1 Hz, 1H, ArH), 7.82 (s, 2H, ArH), 7.61 (d, *J* = 7.6 Hz, 2H, ArH), 7.56 (t, *J* = 7.5 Hz, 2H, ArH), 7.49 (t, *J* = 7.2 Hz, 1H, ArH), 4.29 – 4.14 (m, 8H, OCH_2), 2.00 – 1.83 (m, 8H, CH_2), 1.65 – 1.51 (m, 8H, CH_2), 1.10 – 0.94 (m, 12H, CH_3). **^{19}F NMR** (376 MHz, TMS, $CDCl_3$) δ (ppm) -115.70 (s, 1F, ArF), -141.74 (d, *J* = 18.9 Hz, 1F, ArF), -142.37 (s, 1F, ArF). **^{13}C NMR** (151 MHz, CDCl3) δ (ppm) 153.47, 151.84, 149.76, 149.21, 148.59, 148.43, 146.39 – 146.01 (m), 144.72 – 144.43 (m), 130.72, 129.17, 128.50, 128.38,125.41, 124.93, 120.28 – 119.72

(m), 117.04 – 116.81 (m), 115.59, 111.40 – 110.68 (m), 106.29, 105.96. **HRMS (MALDI)** calcd for $C_{40}H_{45}F_3O_4$ $[M]^+$ m/z: 646.3270 (100%), 647.3303 (43.3%), 648.3337 (9.1%), 649.3371 (1.3%); found 646.3261 (100%), 647.3294 (53%), 648.3328 (14%), 649.3362 (1%). **Elemental Analysis** ($C_{40}H_{45}F_3O_4$, MW 646.33): calcd C 74.28%, H 7.01%; found C 74.10%, H 6.53%.

2-Phenyl-1,3,4-trifluoro-6,7,10,11-tetra(hexyloxy)triphenylene (**PH**6). 2Br-**BP**6 (0.40 g, 0.56 mmol) was converted to the white solid **PH**6 (0.27 g, yield 64%). **^{1}H NMR** (400 MHz, TMS, $CDCl_3$) δ (ppm) 8.49 (d, *J* = 5.8 Hz, 1H, ArH), 8.44 (d, *J* = 6.1 Hz, 1H, ArH), 7.81 (s, 2H, ArH), 7.61 (d, *J* = 7.4 Hz, 2H, ArH), 7.56 (t, *J* = 7.5 Hz, 2H, ArH), 7.50 (t, 1H, ArH), 4.29 – 4.17 (m, 6H, OCH_2), 4.13 (t, *J* = 6.4 Hz, 2H, OCH_2), 2.00 – 1.85 (m, 8H, CH_2), 1.65 – 1.47 (m, 8H, CH_2), 1.42 – 1.34 (m, 16H, CH_2), 0.99 – 0.86 (m, 12H, CH_3). **^{19}F NMR** (376 MHz, TMS, $CDCl_3$) δ (ppm) -115.67 (s, 1F, ArF), -141.76 (d, *J* = 19.3, 1F, ArF), -142.35 (s, 1F, ArF). **^{13}C NMR** (151 MHz, $CDCl_3$) δ (ppm) 153.51, 151.86, 149.84, 149.27, 148.66, 148.51, 146.46 – 145.59 (m), 144.92 – 144.49 (m), 130.69, 129.16, 128.53, 128.41, 125.50, 124.98, 120.34 – 119.80 (m), 117.16 – 116.88 (m), 115.60, 111.44 – 110.98 (m), 106.46, 106.14. **HRMS (MALDI)** calcd for $C_{48}H_{61}F_3O_4$ $[M]^+$ m/z: 758.4522 (100%), 759.4555 (51.9%), 760.4589 (13.2%), 761.4623 (2.2%); found 758.4533 (100%), 759.4566 (54%), 760.4600 (15%), 761.4634 (1.5%). **Elemental Analysis** ($C_{48}H_{61}F_3O_4$, MW 759.01): calcd C 75.96%, H 8.10%; found C 75.79%, H 7.59%.

2-Phenyl-1,3,4-trifluoro-6,7,10,11-tetra(octyloxy)triphenylene (**PH**8). 2Br-**BP**8 (0.40 g, 0.48 mmol) was converted to the white solid **PH**8 (0.34 g, yield 80%). **^{1}H NMR** (400 MHz, TMS, $CDCl_3$) δ (ppm) 8.49 (m, 1H, ArH), 8.43 (d, *J* = 6.3 Hz, 1H, ArH), 7.85 – 7.77 (m, 2H, ArH), 7.62 (d, *J* = 7.5 Hz, 2H, ArH), 7.56 (t, *J* = 7.4 Hz, 2H, ArH), 7.49 (t, *J* = 7.2 Hz, 1H, ArH), 4.29 – 4.17 (m, 6H, OCH_2), 4.13 (t, *J* = 6.3 Hz, 2H, OCH_2), 2.00 – 1.85 (m, 8H, CH_2), 1.65 – 1.49 (m, 8H, CH_2), 1.46 – 1.22 (m, 32H, CH_2), 0.98 – 0.82 (m, 12H, CH_3). **^{19}F NMR** (376 MHz, TMS, $CDCl_3$) δ (ppm) -115.50 – -116.06 (m, 1F, ArF), -141.77 (d, *J* = 12 Hz, 1F, ArF), -142.34 (t, *J* = 14.5 Hz, 1F, ArF). **^{13}C NMR** (151 MHz, $CDCl_3$) δ (ppm) 153.50, 151.87, 149.83, 149.26, 148.65, 148.50, 146.47 – 146.01 (m), 144.85 – 144.56 (m), 130.70, 129.17, 128.52, 128.40, 125.48, 124.98, 120.35 – 119.79 (m), 117.14 – 116.87(m), 115.58, 111.46 – 110.98 (m), 106.46, 106.13. **HRMS (MALDI)** calcd for $C_{56}H_{77}F_3O_4$ $[M]^+$ m/z: 870.5774 (100%), 871.5808 (60.6%), 872.5841 (18.0%),873.5875 (3.5%); found 870.5782 (100%), 871.5829 (65%), 872.5860 (19%), 873.5887 (3.3%). **Elemental Analysis** ($C_{56}H_{77}F_3O_4$, MW 871.22): calcd C 77.20%, H 8.91%; found C 77.00%, H 8.42%.

2-Phenyl-1,3,4-trifluoro-6,7,10,11-tetra(decyloxy)triphenylene (**PH**10). 2Br-**BP**10 (0.40 g, 0.43 mmol) was converted to the white solid **PH**10 (0.33 g, yield 79%). **^{1}H NMR** (400 MHz, TMS, $CDCl_3$) δ (ppm) 8.49 (d, *J* = 5.9 Hz, 1H, ArH), 8.44 (d, *J* = 6.2 Hz, 1H, ArH), 7.82 (d, *J* = 1.3 Hz, 2H, ArH), 7.61 (d, *J* = 7.5 Hz, 2H, ArH), 7.56 (t, *J* = 7.4 Hz, 2H, ArH), 7.50 (t, *J* = 8.0 Hz, 1H, ArH), 4.29 – 4.17 (m, 6H, OCH_2), 4.13 (t, *J* = 6.5 Hz, 2H, OCH_2), 2.00 – 1.86 (m, 8H, CH_2), 1.60 – 1.48 (m, 8H, CH_2), 1.44 – 1.23 (m, 48H, CH_2), 0.94 – 0.82 (m, 12H, CH_3). **^{19}F NMR** (376 MHz, TMS, $CDCl_3$) δ (ppm) -115.68 (t, *J* = 12 Hz, 1F, ArF), -141.71 – -141.77 (m, 1F, ArF), -142.19 – -142.47 (m, 1F, ArF). **^{13}C NMR** (151 MHz, $CDCl_3$) δ (ppm) 153.51, 151.87, 149.77, 149.22, 148.61, 148.45, 146.35 –

146.03 (m), 144.85 – 144.36 (m), 130.72, 129.18, 128.50, 128.38, 125.42, 124.95, 120.30 – 119.77 (m), 115.62, 111.40 – 111.84 (m), 106.36, 106.02. **HRMS (MALDI)** calcd for $C_{64}H_{93}F_3O_4$ $[M]^+$ m/z: 982.7026 (100%), 983.7060 (69.2%), 984.7093 (23.6%); found 982.7033 (100%), 983.7067 (81%), 984.7100 (30%). **Elemental Analysis** ($C_{64}H_{93}F_3O_4$, MW 983.44): calcd C 78.16%, H 9.53%; found C 78.17%, H 9.43%.

2-Phenyl-1,3,4-trifluoro-6,7,10,11-tetra(dodecyloxy)triphenylene (**PH**12). 2Br-**BP**12 (0.30 g, 0.29 mmol) was converted to the white solid **PH**12 (0.19 g, yield 61%). **^{1}H NMR** (400 MHz, TMS, $CDCl_3$) δ (ppm) 8.47 (d, *J* = 5.7 Hz, 1H, ArH), 8.43 (d, *J* = 6.2 Hz, 1H, ArH), 7.80 (s, 2H, ArH), 7.62 (d, *J* = 7.4 Hz, 2H, ArH), 7.56 (t, *J* = 7.4 Hz, 2H, ArH), 7.49 (t, *J* = 7.2 Hz, 1H, ArH), 4.27 – 4.17 (m, 6H, OCH_2), 4.13 (t, *J* = 6.5 Hz, 2H, OCH_2), 1.92 (m, 8H, CH_2), 1.63 – 1.47 (m, 10H, CH_2), 1.43 – 1.24 (m, 62H, CH_2), 0.88 (t, *J* = 6.6 Hz, 12H, CH_3). **^{19}F NMR** (376 MHz, TMS, $CDCl_3$) δ (ppm) -115.68 (d, *J* = 12 Hz, 1F, ArF), -141.73 (d, *J* = 19.7, 1F, ArF), -142.17 – -142.50 (m, 1F, ArF). **^{13}C NMR** (151 MHz, $CDCl_3$) δ (ppm) 153.54, 151.89, 149.85, 149.29, 148.68, 148.51, 146.14, 144.49, 130.69, 129.17, 128.54, 128.41, 125.52, 125.00, 120.38 – 119.83(m), 116.96, 115.67, 111.48, 111.26, 106.49, 106.16. **HRMS (MALDI)** calcd for $C_{72}H_{109}F_3O_4$ $[M]^+$ m/z: 1094.8278 (100%), 1095.8312 (77.9%), 1096.8345 (29.9%), 1097.8379 (7.5%), 1098.8412 1.4%); found 1094.8256 (100%), 1095.8290 (87%), 1096.8323 (36%), 1097.8357 (9.5%), 1098.8390 (1.6%). **Elemental Analysis** ($C_{72}H_{109}F_3O_4$, MW 1095.66): calcd C 78.93%, H 10.03%; found C 79.02%, H 9.91%.

2.5 Synthesis of 2,3,6,7-tetrakis(hexyloxy)-10-phenyltriphenylene, **BP**6

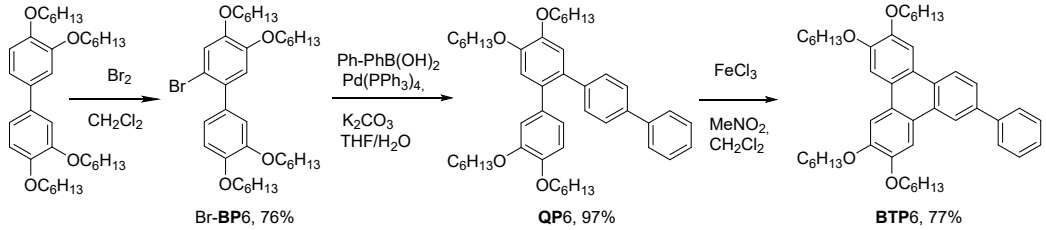

Scheme S4. Preparation of **BTP**6.

Synthesis of 2-bromo-3',4,4',5-tetrahexyloxy-1,1'-biphenyl (Br-**BP**6): 3,3',4,4'-tetra (hexyloxy)-1,1'-biphenyl (2.50 g, 4.6 mmol) was dissolved in dry CH_2Cl_2 (100 mL), and bromine (0.77 g, 4.8 mmol) diluted with CH_2Cl_2 was added slowly (1 drop for 2 seconds). The resulting solution was stirred at room temperature until completion of the reaction. The reaction mixture was quenched with aqueous sodium hydrogen sulfite and extracted with dichloromethane. The combined organic layers were dried over anhydrous $MgSO_4$ and concentrated in vacuum. The crude product was purified by column chromatography on silica gel with (dichloromethane:petroleum ether = 1:2) mixture as eluent. Recrystallized from ethanol and methanol gave white solid (2.20 g, yield 76%). **^{1}H NMR** (400 MHz, TMS, $CDCl_3$) δ (ppm) 7.11 (s, 1H, ArH), 6.95 (s, 1H, ArH), 6.92 – 6.87 (m, 2H, ArH), 6.84 (s, 1H, ArH), 4.05 – 3.94 (m, 8H, OCH_2), 1.87 – 1.76 (m, 8H, CH_2), 1.49 – 1.44 (m, 8H, CH_2), 1.39 – 1.28 (m, 16H, CH_2), 0.96 – 0.85 (m, 12H, CH_3).

Synthesis of the 3,4,4',5'-tetrakis(hexyloxy)-1,1':2',1'':4'',1'''-quaterphenyl **(QP**6**)**.

Under argon, 4-biphenyl-boric acid (0.19 g, 0.95mmol.), Br-**BP**6 (0.40 g, 0.63 mmol), K_2CO_3 (1.74 g, 12.62 mmol.), $Pd(PPh_3)_4$ (0.07 g, 0.06 mmol), THF (10 mL)/H_2O(3 mL) were added in a reaction tube. The resulting solution was stirred at 70 °C for 48 h. The reaction mixture was cooled to room temperature and extracted with dichloromethane. The combined organic layers were dried over anhydrous $MgSO_4$ and concentrated in vacuum. The crude product was separated and purified by silica gel column chromatography with (dichloromethane:petroleum ether = 1:3) as eluent, recrystallization with ethanol and methanol gave white solid **QP**6 (0.43 g, yield 97%). **^{1}H NMR** (400 MHz, TMS, $CDCl_3$) δ (ppm) 7.57 (d, *J* = 7.6 Hz, 2H, ArH), 7.50 – 7.38 (m, 4H, ArH), 7.32 (t, *J* = 7.3 Hz, 1H, ArH), 7.21 (d, *J* = 8.0 Hz, 2H, ArH), 6.98 (s, 2H, ArH), 6.79 (s, 2H, ArH), 6.55 (s, 1H, ArH), 4.13 – 4.03 (m, 4H, OCH_2), 3.96 (t, *J* = 6.7 Hz, 2H, OCH_2), 3.61 (t, *J* = 6.7 Hz, 2H, OCH_2), 1.89 - 1.76(m, 6H, CH_2), 1.59 (d, *J* = 14.8 Hz, 2H, CH_2), 1.50 - 1.42 (m, 6H, CH_2), 1.36 - 1.21 (m, 18H, CH_2), 0.99 – 0.78 (m, 12H, CH_3). **^{13}C NMR** (151 MHz, $CDCl_3$) δ (ppm) 148.49, 148.23, 147.69, 140.93, 140.80, 138.83, 134.17, 133.05, 132.51, 130.35, 128.75, 127.17, 126.92, 126.59, 121.86, 116.33, 116.03, 116.13, 113.29.

Synthesis of 2,3,6,7-tetrakis(hexyloxy)-10-phenyltriphenylene (**BTP**6). To a stirred solution of **QP**6 (0.20 g，0.28 mmol) was added in 100 mL reaction tube and CH_2Cl_2 (30 mL) was added, a solution of $FeCl_3$ (0.07 g，0.42 mmol) in CH_3NO_2 (10 mL) was added. The resulting solution was stirred at room temperature until completion of the reaction. The reaction mixture was quenched with methanol and extracted with dichloromethane. The combined organic layers were dried over anhydrous $MgSO_4$ and concentrated in vacuo. The residue was purified by column chromatography on silica gel with (dichloromethane:petroleum ether = 1:4.5) mixture as eluent. Recrystallization with ethanol and ethyl acetate gave white solid **BTP**6 (0.15 g, yield 77 %). **^{1}H NMR** (400 MHz, TMS, $CDCl_3$) δ (ppm) 8.63 (s, 1H, ArH), 8.54 (d, *J* = 8.4 Hz, 1H, ArH), 8.08 (s, 1H, ArH), 8.03 (s, 1H, ArH), 7.85 (s, 2H, ArH), 7.80 (d, *J* = 7.4 Hz, 3H, ArH), 7.54 (t, *J* = 7.4 Hz, 2H, ArH), 7.43 (t, *J* = 7.1 Hz, 1H, ArH), 4.26 (t, *J* = 5.9 Hz, 8H, OCH_2), 2.00 – 1.93 (m, 6H, CH_2), 1.59 (s, 8H, CH_2), 1.41 (d, *J* = 2.7 Hz, 14H, CH_2), 1.26 (s, 4H, CH_2), 0.96 - 0.88 (m, 12H, CH_3). **^{13}C NMR** (151 MHz, $CDCl_3$) δ (ppm) 149.53, 141.64, 138.74, 128.91, 127.54, 127.33, 125.23, 124.49, 123.52, 121.43, 107.05. **HRMS (MALDI)** calcd for $C_{48}H_{64}O_4$ $[M]^+$ m/z: 704.4805 (100%), 705.4838 (51.9%), 706.4872 (13.2%), 707.4905 (2.2%); found 704.4810 (100%), 705.4840 (49%), 706.4870 (11%), 707.4901 (2%).

2.6 Synthesis of 1,2,3,4-tetrafluoro-6,7,10,11-tetrakis(octyloxy)triphenylene, 4*F*-**TP**8

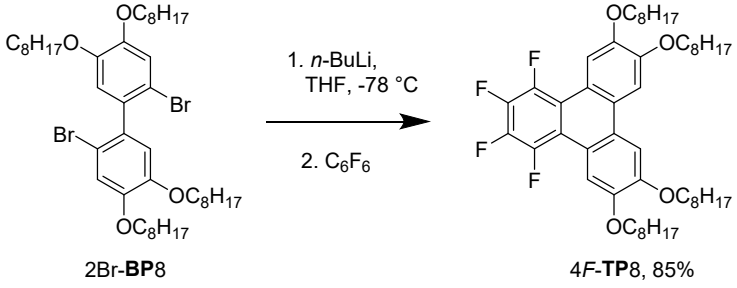

2Br-**BP**8 4*F*-**TP**8, 85%

Scheme S5. Preparation of the tetrafluorotriphenylenes, 4*F*-**TP**8.

2,2'-Dibromo-4,4',5,5'-tetrakis(octyloxy)-1,1'-biphenyl (2Br-**BP**8, 3.00 g, 4.21 mmol) was weighed in 50 mL reaction tubes and solvent THF (10 mL) was added under protection of argon. *n*-Butyllithium (2.5 M hexane, 16.80 mmol) was slowly injected into the reaction tube with a syringe at -78 °C. After reacting for 2 h perfluorobenzene (1.57 g, 8.44 mmol) was added into the reaction mixture and continued to react at -78 °C for 0.5 h, then the resulting solution was stirred at room temperature for 10 h. The reaction mixture was extracted with chloroform, the combined organic layers were dried with anhydrous $MgSO_4$ and concentrated in vacuo. The crude product was purified by silica gel column chromatography with (dichloromethane:petroleum ether = 1:3) as eluent, recrystallization with ethyl acetate and ethanol gave white solid (2.48 g, yield 85%). **^{1}H NMR** (400 MHz, TMS, $CDCl_3$) δ (ppm) 8.35 (s, 2H, ArH), 7.77 (s, 2H, ArH), 4.25 – 4.15 (m, 8H, OCH_2), 1.99 – 1.89 (m, 8H, CH_2), 1.62 – 1.51 (m, 10H, CH_2), 1.47 – 1.30 (m, 30H, CH_2), 0.90 (t, *J* = 6.8 Hz, 12H, CH_3). **^{19}F NMR** (565 MHz, TMS, $CDCl_3$) δ (ppm) -139.87 (d, *J* = 13.2 Hz, 2F, ArF), -159.69 (t, *J* = 22.8 Hz, 2F, ArF).

2.7 Synthesis of 2-aryl-1,3,4-trifluorotriphenylene derivatives

1,2,4-Trifluoro-3-(naphthalen-1-yl)-6,7,10,11-tetrakis(octyloxy)triphenylene (**NAA**8). Under protection of argon, 1-bromonaphthalene (0.10 g, 0.49 mmol) was charged in a 50 mL reaction tube and THF (10 mL) was added. *n*-Butyllithium (2.5 M hexane, 0.97 mmol) was slowly injected into the reaction tube with a syringe at -78 °C and the reaction mixture was stirred at -78 °C for 0.5 h, then continued to react at room temperature for 3 h. 4*F*-**TP**8 (0.20 g, 0.24 mmol) was added and the reaction solution continued under stirring at 55 °C for 10 h. The reaction mixture was cooled to room temperature and extracted with dichloromethane. The combined organic layers were dried over anhydrous $MgSO_4$ and concentrated in vacuo. The crude product was separated and purified by silica gel column chromatography with (dichloromethane:petroleum ether = 1:3) as eluent; recrystallization with ethyl acetate and ethanol gave white solid (0.17 g, yield 74%). **^{1}H NMR** (400 MHz, TMS, $CDCl_3$) δ (ppm) 8.56 (d, *J* = 5.9 Hz, 1H, ArH), 8.42 (d, *J* = 6.3 Hz, 1H, ArH), 8.03 (d, *J* = 7.2 Hz, 1H, ArH), 7.98 (d, *J* = 8.1 Hz, 1H, ArH), 7.85 (s, 2H, ArH), 7.68 – 7.63 (m, 3H, ArH), 7.55 (t, *J* = 7.4 Hz, 1H, ArH), 7.48 (t, *J* = 8 Hz, 1H, ArH), 4.30 – 4.21(m, 6H, OCH_2), 4.05 (t, *J* = 6.5 Hz, 2H, OCH_2), 2.01 – 1.95 (m, 6H, CH_2), 1.86 – 1.78 (m, 2H, CH_2), 1.64 – 1.52 (m, 8H, CH_2), 1.46 – 1.23 (m, 32H, CH_2), 0.95 – 0.82 (m, 12H, CH_3). **^{19}F NMR** (565 MHz, TMS, $CDCl_3$) δ (ppm) -112.03 (s, 1F, ArF), -138.88 (s, 1F, ArF), -142.18 (s, 1F, ArF). **^{13}C NMR** (151 MHz, $CDCl_3$) δ (ppm) 154.13, 152.49, 149.97, 149.35, 148.80, 148.58, 146.17, 145.25, 144.40, 133.65, 132.09, 129.38, 128.93, 128.47, 126.86, 126.73, 126.16, 125.64, 125.41, 125.29, 125.04, 120.33 (d, *J* = 29.6 Hz), 115.74 – 115.36 (m), 111.39 – 111.12 (m), 106.63, 106.23. **HRMS (MALDI)** calcd for $C_{60}H_{79}F_3O_4$ $[M]^+$ m/z: 920.5930 (100.0%), 921.5964 (64.9%), 922.5998 (20.7%); found 920.5936 (100%), 921.5973 (73%). **Elemental Analysis** ($C_{60}H_{79}F_3O_4$, MW 921.28): calcd C 78.22%, H 8.64%; found C 78.13%, H 8.30%.

1,2,4-Trifluoro-3-(naphthalen-2-yl)-6,7,10,11-tetrakis(octyloxy)triphenylene (**NAB**8). As for **NAA**8: 2-bromonaphthalene (0.10 g, 0.49 mmol), THF (10 mL), *n*-Butyllithium (2.5 M hexane, 0.97 mmol), 4*F*-**TP**8 (0.20 g, 0.24 mmol). Extraction in dichloromethane

and purification by silica gel column chromatography with dichloromethane:petroleum ether = 1:3 as eluent; recrystallization with ethyl acetate and ethanol gave white solid (0.16 g, yield 72%). **^{1}H NMR** (400 MHz, TMS, $CDCl_3$) δ (ppm) 8.46 (dd, *J* = 15.4, 5.9 Hz, 2H, ArH), 8.11 (s, 1H, ArH), 8.01 (d, *J* = 8.5 Hz, 1H, ArH), 7.95 (dd, *J* = 8.7, 5.3 Hz, 2H, ArH), 7.80 (s, 2H, ArH), 7.71 (d, *J* = 8.3 Hz, 1H, ArH), 7.60 – 7.53 (m, 2H, ArH), 4.29 – 4.09 (m, 8H, OCH_2), 2.00 – 1.84 (m, 8H, CH_2), 1.60 – 1.26 (m, 40H, CH_2), 0.90 – 0.85 (m, 12H, CH_3). **^{19}F NMR** (565 MHz, TMS, $CDCl_3$) δ (ppm) -115.30 – -115.61 (m, 1F, ArF) -141.57 (d, *J* = 19.5 Hz, 1F, ArF), -142.22 (t, *J* = 14.4 Hz, 1F, ArF). **^{13}C NMR** (151 MHz, $CDCl_3$) δ (ppm) 153.70, 152.05, 149.81, 149.26, 148.63, 148.48, 146.20, 144.61, 133.11 (d, *J* = 17.6 Hz), 130.29, 128.33, 127.99 (d, *J* = 26.8 Hz), 127.76, 126.73, 126.63 (d, *J* = 23.2 Hz), 126.37, 125.47, 124.98, 120.58 – 119.82 (m), 116.99, 115.66, 111.46 – 111.22 (m), 106.45 – 106.40 (m), 106.22 (d, *J* = 50.0 Hz). **HRMS (MALDI)** calcd for $C_{60}H_{79}F_3O_4$ $[M]^+$ m/z: 920.5930 (100.0%), 921.5964 (64.9%), 922.5998 (20.7%); found 920.5913 (100%), 921.5973 (73%). **Elemental Analysis** ($C_{60}H_{79}F_3O_4$, MW 921.28): calcd. C 78.22%, H 8.64%, found C 77.84%, H 8.18%.

1,2,4-Trifluoro-6,7,10,11-tetrakis(octyloxy)-3-(triphenylene-2-yl)triphenylene (**TP**8). As for **NAA**8: 2-bromotriphenylene (0.15 g, 0.49 mmol), THF (10 mL), *n*-Butyllithium (2.5 M hexane, 0.97 mmol), 4*F*-**TP**8 (0.20 g, 0.24 mmol). Extraction in dichloromethane and purification by silica gel column chromatography with (dichloromethane:petroleum ether = 1:3) as eluent; recrystallization with ethyl acetate and ethanol gave white solid (0.18 g, yield 74%). **^{1}H NMR** (400 MHz, TMS, $CDCl_3$) δ (ppm) 8.92 (s, 1H, ArH), 8.80 – 8.65 (m, 5H, ArH), 8.46 (s, 2H, ArH), 7.89 (d, *J* = 8.1 Hz, 1H, ArH), 7.80 – 7.65 (m, 6H, ArH), 4.29 – 4.08 (m, 8H, OCH_2), 2.00 – 1.83 (m, 8H, CH_2), 1.60 – 1.22 (m, 40H, CH_2), 0.96 – 0.79 (m, 12H, CH_3). **^{19}F NMR** (565 MHz, TMS, $CDCl_3$) δ (ppm) -115.42 (d, *J* = 3.3 Hz, 1F, ArF), -141.47 (d, *J* = 18.0 Hz, 1F, ArF), -142.08 (d, *J* = 13.8 Hz, 1F, ArF). **^{13}C NMR** (151 MHz, $CDCl_3$) δ (ppm) 153.66, 151.99, 149.74, 149.22, 148.58, 148.39, 146.58 – 146.36 (m) , 144.96 – 144.53(m), 144.93 (d, *J* = 9.5 Hz), 144.57 (d, *J* = 13.6 Hz), 129.99 (d, *J* = 13.9 Hz), 129.73 (d, *J* = 14.1 Hz), 129.53, 129.35 (d, *J* = 12.2 Hz), 127.91, 127.46 (d, *J* = 11.9 Hz), 127.28, 125.86, 125.41, 124.96, 123.55, 123.42, 123.32 – 123.22 (m), 120.23 – 119.85 (m), 117.04 – 116.76(m), 115.66, 111.38 – 110.78 (m), 106.23, 105.90. **HRMS (MALDI)** calcd for $C_{68}H_{83}F_3O_4$ $[M]^+$ m/z: 1020.6243 (100.0%), 1021.6277 (73.5%), 1022.6311 (26.6%); found 1020.6218 (100%), 1021.6254 (78%). **Elemental Analysis** ($C_{68}H_{83}F_3O_4$, MW 1021.40): calcd C 79.96%, H 8.19%; found C 79.57%, H 7.92%.

1,2,4-Trifluoro-6,7,10,11-tetrakis(octyloxy)-3-(pyren-1-yl)triphenylene (**PY**8). As for **NAA**8: 1-bromopyrene (0.17 g, 0.61 mmol), THF (10 mL), *n*-Butyllithium (2.5 M hexane, 1.22 mmol), 4*F*-**TP**8 (0.25 g, 0.30 mmol). Extraction in dichloromethane and purification by silica gel column chromatography with (dichloromethane:petroleum ether = 1:3) as eluent, recrystallization with ethyl acetate and ethanol gave white solid (0.24 g, yield 78%). **^{1}H NMR** (400 MHz, TMS, $CDCl_3$) δ (ppm) 8.58 (d, *J* = 5.7 Hz, 1H, ArH), 8.44 (d, *J* = 6.1 Hz, 1H, ArH), 8.35 (d, *J* = 7.8 Hz, 1H, ArH), 8.27 – 8.14 (m, 5H, ArH), 8.09 – 8.03 (m, 2H, ArH), 7.29 – 7.85 (m, 3H, ArH), 4.31 – 4.24 (m, 6H, OCH_2), 4.03 (t, *J* = 6.2 Hz, 2H, OCH_2), 2.03 – 1.93 (m, 6H, CH_2), 1.83 – 1.76 (m, 2H, CH_2), 1.63 – 1.52 (m,

8H, CH_2), 1.43 – 1.18 (m, 32H, CH_2), 0.95 – 0.86 (m, 9H, CH_3), 0.80 (d, *J* = 6.9 Hz, 3H, CH_3). **^{19}F NMR** (565 MHz, TMS, $CDCl_3$) δ (ppm) -112.03 (d, *J* = 14.0 Hz, 1F, ArF), -138.76 – -138.80 (m, 1F, ArF), -142.07 (t, *J* = 15.1 Hz, 1F, ArF). **^{13}C NMR** (151 MHz, $CDCl_3$) δ (ppm) 154.21, 152.59, 150.00, 149.36, 148.80, 148.60, 146.17, 145.42, 144.55, 131.82, 131.26, 130.86, 129.93, 128.66, 128.34, 128.18, 127.33, 126.16, 125.64 (d, *J* = 9.2 Hz), 125.45, 125.07, 124.69 (dd, *J* = 31.4, 11.5 Hz), 123.88, 120.52 – 120.26 (m), 116.17 – 115.96 (m), 111.34, 111.14, 106.63, 106.22. **HRMS (MALDI)** calcd for $C_{66}H_{81}F_3O_4$ $[M]^+$ m/z: 994.6087 (100.0%), 995.6121 (71.4%), 996.6154 (25.1%); found 994.6075 (100%), 995.6110 (75%). **Elemental Analysis** ($C_{66}H_{81}F_3O_4$, MW 995.37): calcd C 79.64%, H 8.20%; found C 79.61%, H 8.06%.

1,2,4-Trifluoro-6,7,10,11-tetrakis(octyloxy)-3-(4-triphenylethylene-yl)triphenylene (**TPE**8). As for **NAA**8: (2-(4-bromophenyl)ethene-1,1,2-triyl)tribenzene (0.25 g, 0.61 mmol), THF (10 mL), *n*-Butyllithium (2.5 M hexane, 1.22 mmol), 4*F*-**TP**8 (0.25 g, 0.30 mmol). Extraction in dichloromethane and purification by silica gel column chromatography with dichloromethane:petroleum ether = 1:3 as eluent; recrystallization with ethyl acetate and ethanol gave white solid (0.24 g, yield 75%). **^{1}H NMR** (400 MHz, TMS, $CDCl_3$) δ (ppm) 8.50 (d, *J* = 5.9 Hz, 1H, ArH), 8.44 (d, *J* = 6.3 Hz, 1H, ArH), 7.83 (s, 2H, ArH), 7.57 – 7.52 (m, 1H, ArH), 7.44 – 7.42 (m, 2H, ArH), 7.38 – 7.27 (m, 5H, ArH), 7.15 – 7.06 (m, 5H, ArH), 7.00 (t, *J* = 6.2 Hz, 3H, ArH), 6.84 – 6.76 (m, 3H, ArH), 4.28 – 4.12 (m, 8H, OCH_2), 1.99 – 1.85 (m, 8H, CH_2), 1.57 – 1.27 (m, 40H, CH_2), 0.95 – 0.83 (m, 12H, CH_3). **^{19}F NMR** (565 MHz, TMS, $CDCl_3$) δ (ppm) -115.34 – -115.61 (m, 1F, ArF), -141.25 – -141.48 (m, 1F, ArF), -142.48 (t, *J* = 14.5 Hz, 1F, ArF). **^{13}C NMR** (151 MHz, $CDCl_3$) δ (ppm) 153.54, 151.87, 149.91, 149.33, 148.65 (d, *J* = 16.4 Hz), 143.98, 143.18, 142.19, 141.12, 140.09, 137.40, 130.81 (d, *J* = 8.5 Hz), 130.16, 129.91 (d, *J* = 21.3 Hz), 129.19 (d, *J* = 8.0 Hz), 127.93, 127.67, 127.50 (d, *J* = 27.8 Hz), 127.06, 126.75, 126.49, 125.57, 125.05, 120.50, 120.28 , 119.71, 117.13, 115.66, 111.62, 111.38, 111.18, 106.67, 106.36. **HRMS (MALDI)** calcd for $C_{76}H_{91}F_3O_4$ $[M]^+$ m/z: 1124.6869 (100%), 1125.6903 (82.2%), 1126.6937 (33.3%); found 1124.6863 (100%), 1125.6903 (88%). **Elemental Analysis** ($C_{76}H_{91}F_3O_4$, MW 1125.56): calcd C 81.10%, H 8.15%; found C 80.87%, H 7.95%.

1,2,4-Trifluoro-6,7,10,11-tetrakis(octyloxy)-3-(benzo[b]thiophene-2-yl)triphenylene (**BT**8). As for **NAA**8: 2-bromobenzo[b]thiophene (0.13 g, 0.61 mmol), THF (10 mL), *n*-Butyllithium (2.5 M hexane, 0.97 mmol), 4*F*-**TP**8 (0.25 g, 0.30 mmol). Extraction in dichloromethane and purification by silica gel column chromatography with (dichloromethane:petroleum ether = 1:3) as eluent; recrystallization with ethyl acetate and ethanol gave white solid (0.18 g, yield 63%). **^{1}H NMR** (600 MHz, TMS, $CDCl_3$) δ (ppm) 8.43 (d, *J* = 5.5 Hz, 2H, ArH), 7.91 (t, *J* = 8.8 Hz, 2H, ArH), 7.84 (s, 1H, ArH), 7.78 (d, *J* = 7.8 Hz, 2H, ArH), 7.45 – 7.38 (m, 2H, ArH), 4.26 – 4.16 (m, 8H, OCH_2), 1.98 – 1.85 (m, 8H, CH_2), 1.58 – 1.55 (m, 10H, CH_2), 1.42 – 1.32 (m, 30H, CH_2), 0.91 – 0.87 (m, 12H, CH_3). **^{19}F NMR** (565 MHz, TMS, $CDCl_3$) δ (ppm) -111.56 (d, *J* = 10.3 Hz, 1F, ArF), -138.50 (d, *J* = 18.5 Hz, 1F, ArF), -141.97 (t, *J* = 13.3 Hz, 1F, ArF). **^{13}C NMR** (151 MHz, $CDCl_3$) δ (ppm) 154.88, 153.19, 149.64, 148.49, 132.30, 130.74, 129.59, 128.16, 127.49, 127.33, 126.48, 126.15, 125.76, 124.82, 123.77 – 123.59 (m), 120.77, 118.67,

118.19, 112.99 – 111.92 (m), 106.83. **HRMS (MALDI)** calcd for $C_{58}H_{77}F_3O_4S$ $[M]^+$ m/z: 926.5495 (100%), 927.5528 (62.7%), 928.5562 (19.3%); found 926.5506 (100%), 927.5546 (65%), 928.5580 (21%). **Elemental Analysis** ($C_{58}H_{77}F_3O_4S$, MW 927.31): calcd C 75.12%, H 8.37%, S 3.46%; found C 74.69%, H 8.30%, S 3.44%.

3. ^{1}H NMR

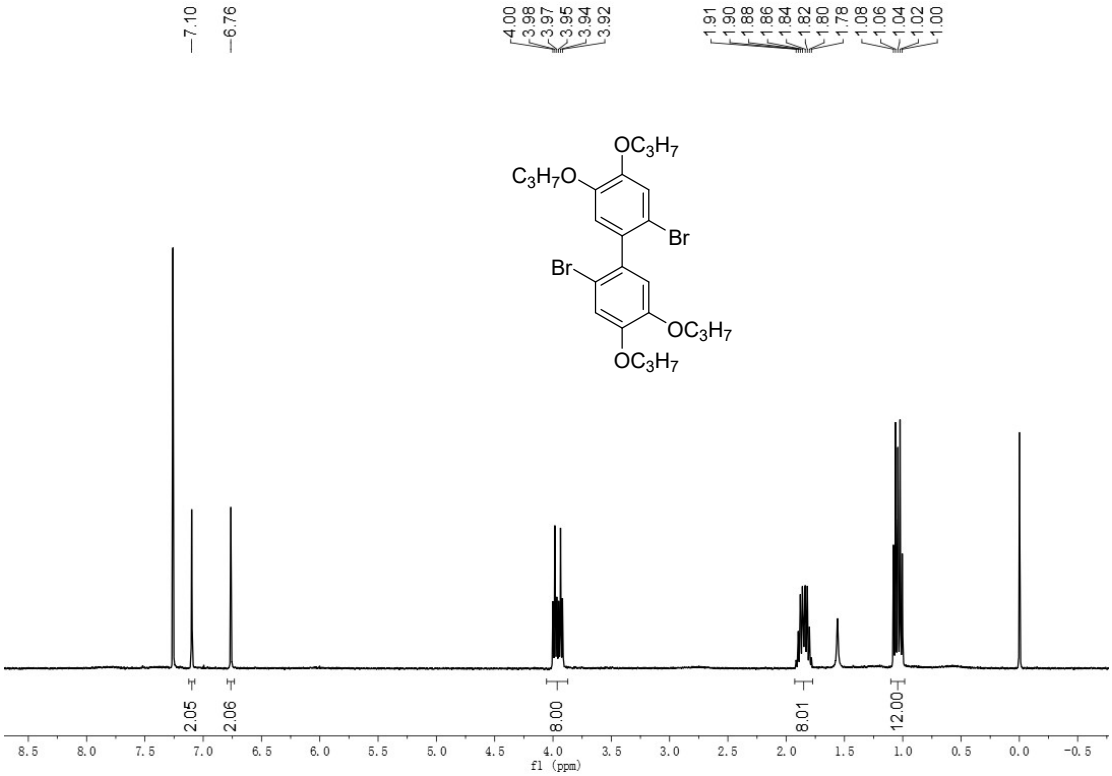

Figure S1 ^{1}H NMR ($CDCl_3$, 400MHz) spectrum of 2Br-**BP**3.

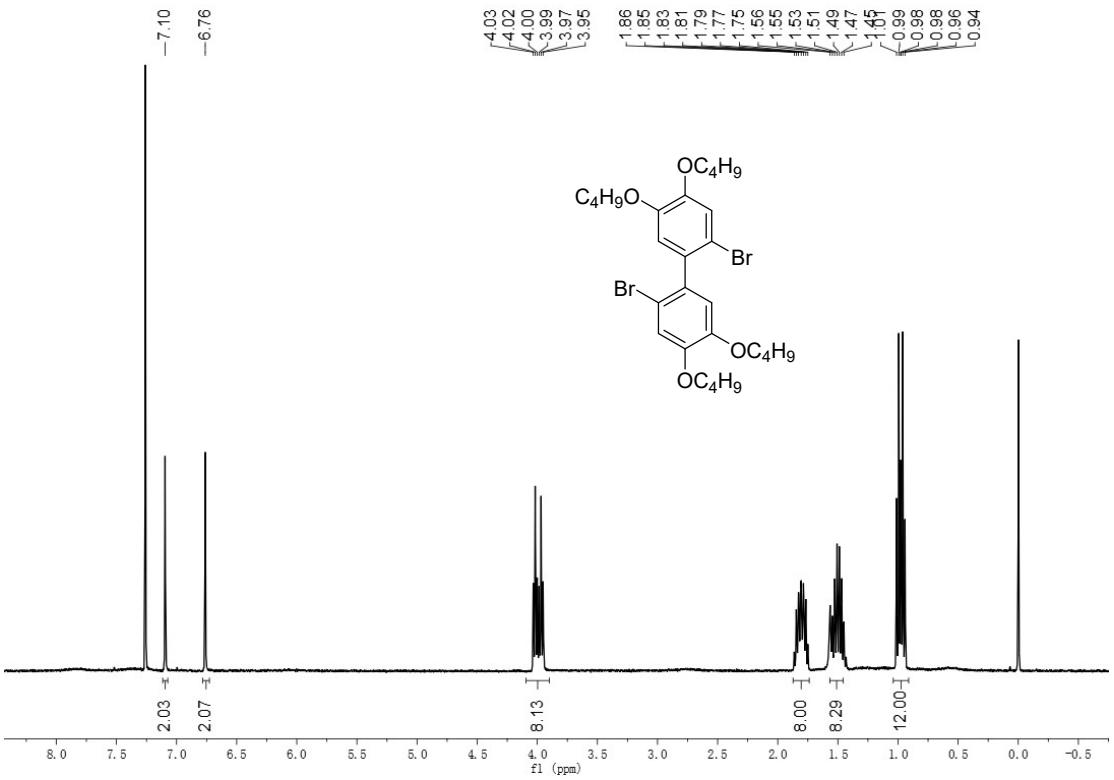

Figure S2 ^{1}H NMR ($CDCl_3$, 400 MHz) spectrum of 2Br-**BP**4.

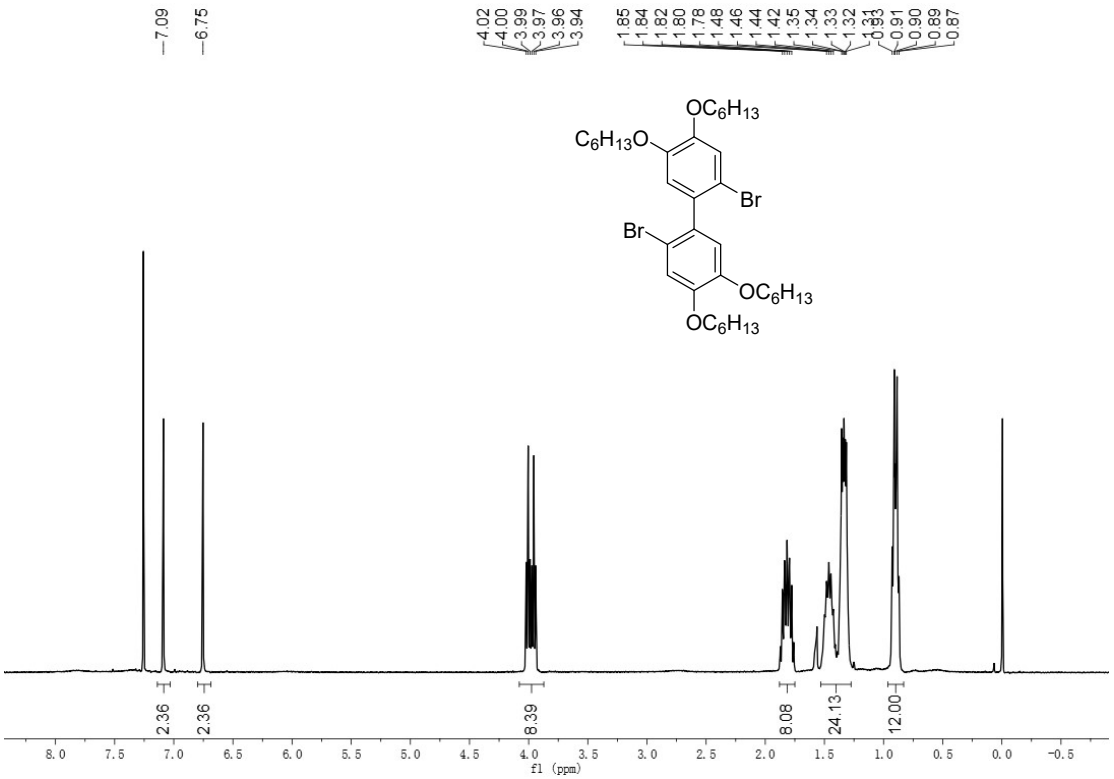

Figure S3 ^{1}H NMR (CDCl3, 400 MHz) spectrum of 2Br-**BP**6.

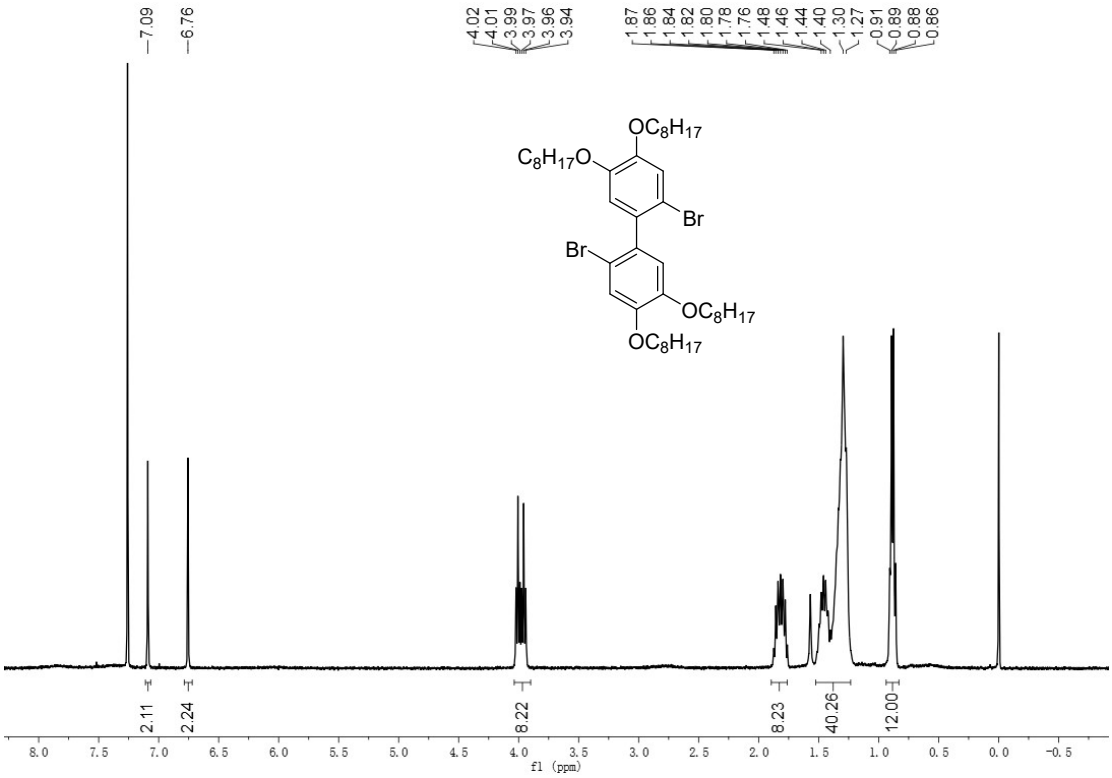

Figure S4 ^{1}H NMR ($CDCl_3$, 400 MHz) spectrum of 2Br-**BP**8.

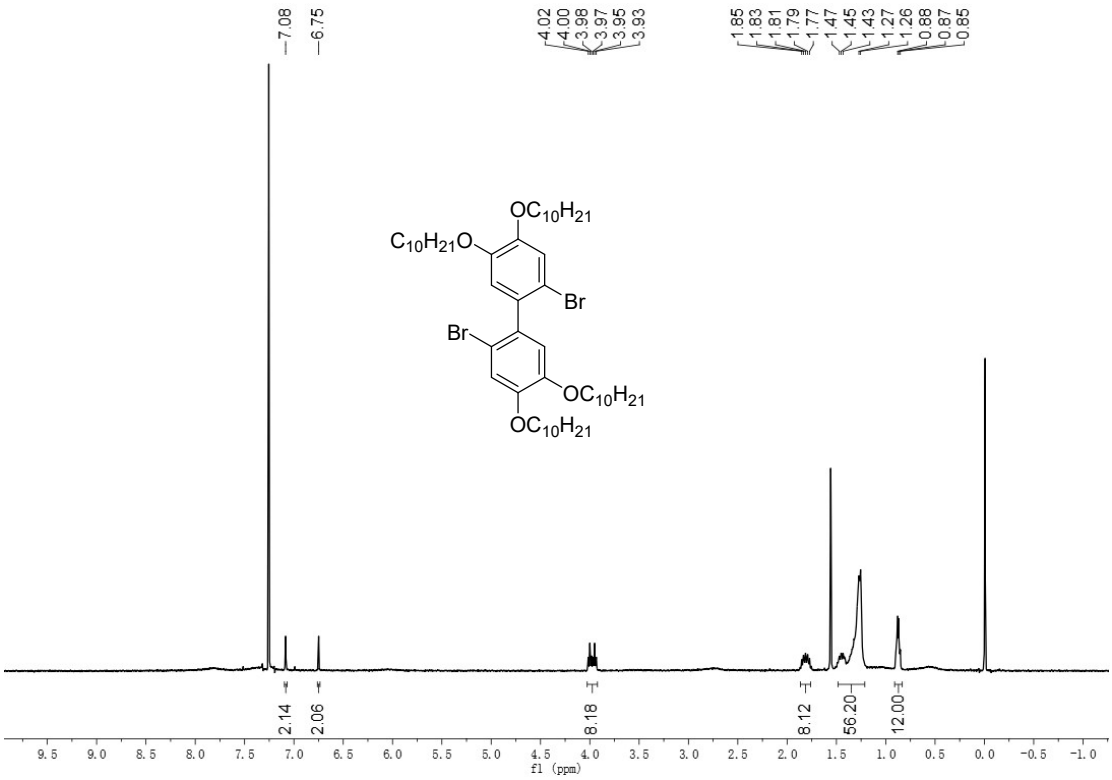

Figure S5 ^{1}H NMR ($CDCl_3$, 400 MHz) spectrum of 2Br-**BP**10.

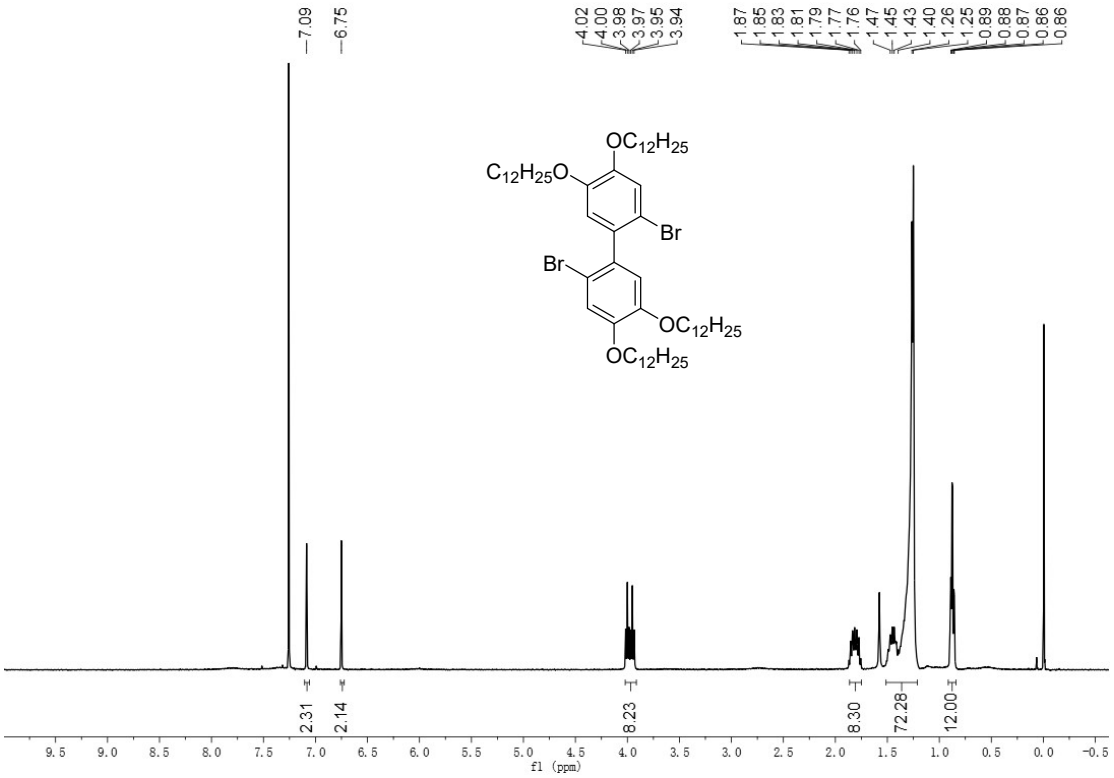

Figure S6 ^{1}H NMR ($CDCl_3$, 400 MHz) spectrum of 2Br-**BP**12.

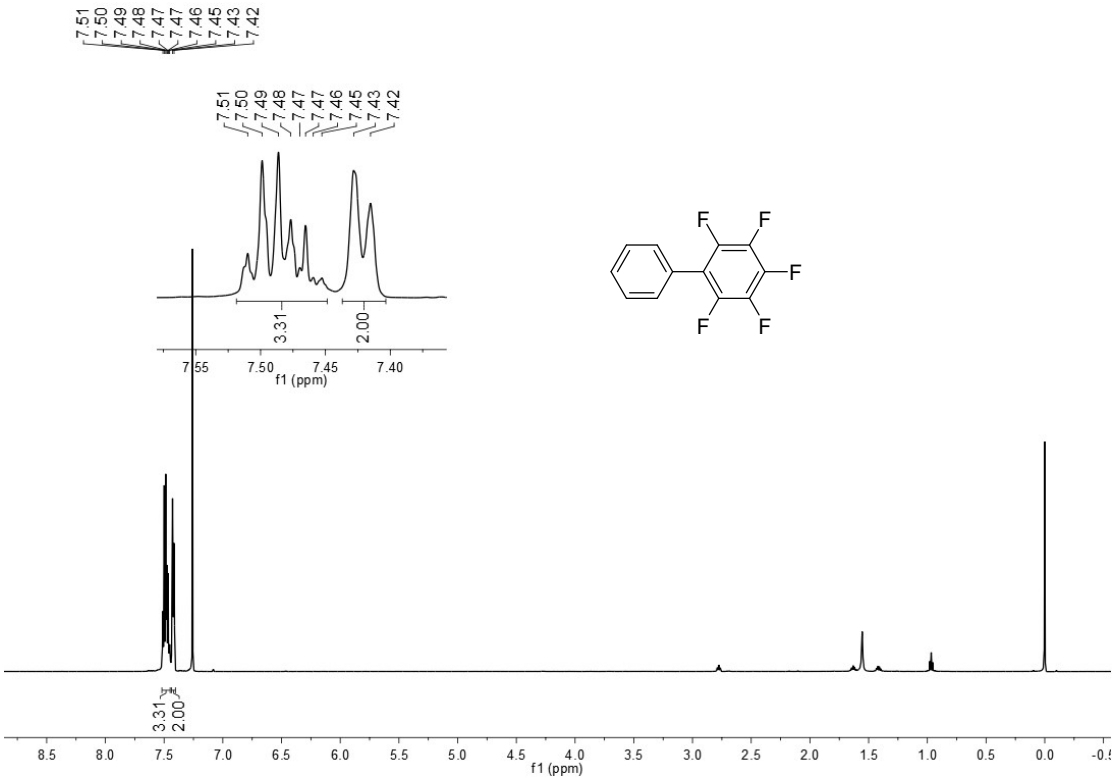

Figure S7 ^{1}H NMR ($CDCl_3$, 600 MHz) spectrum of Ph-C_6F_5.

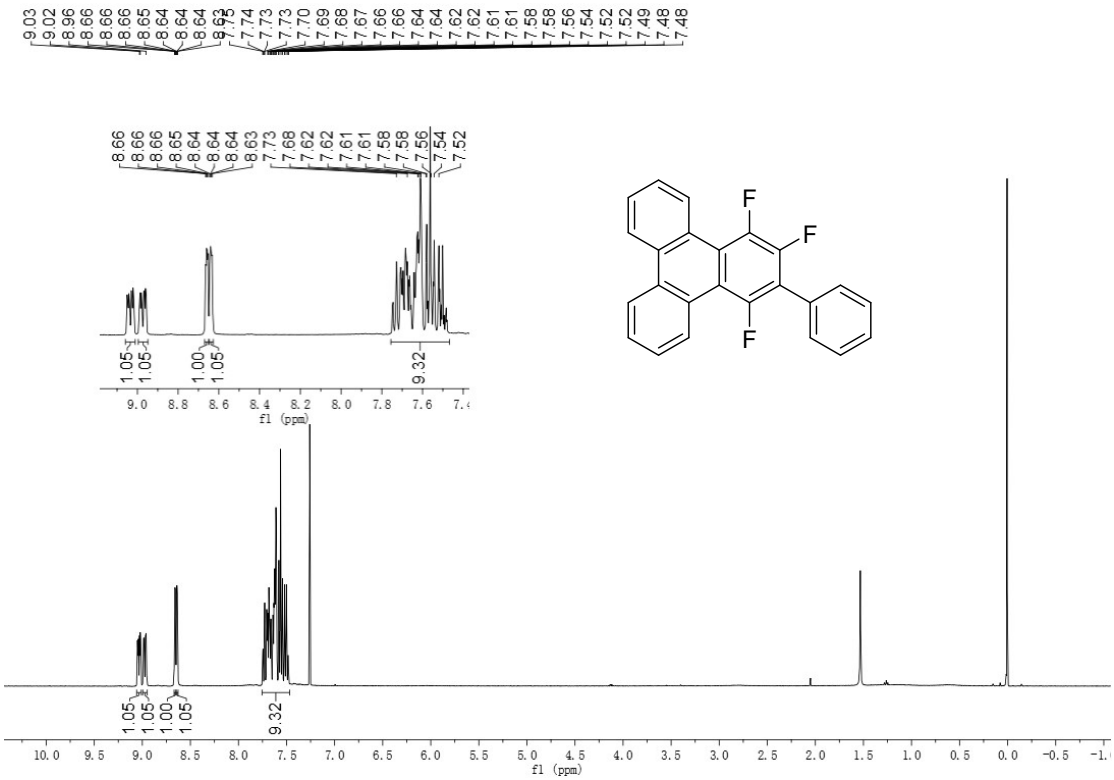

Figure S8 ^{1}H NMR ($CDCl_3$, 400MHz) spectrum of **PH**0**.**

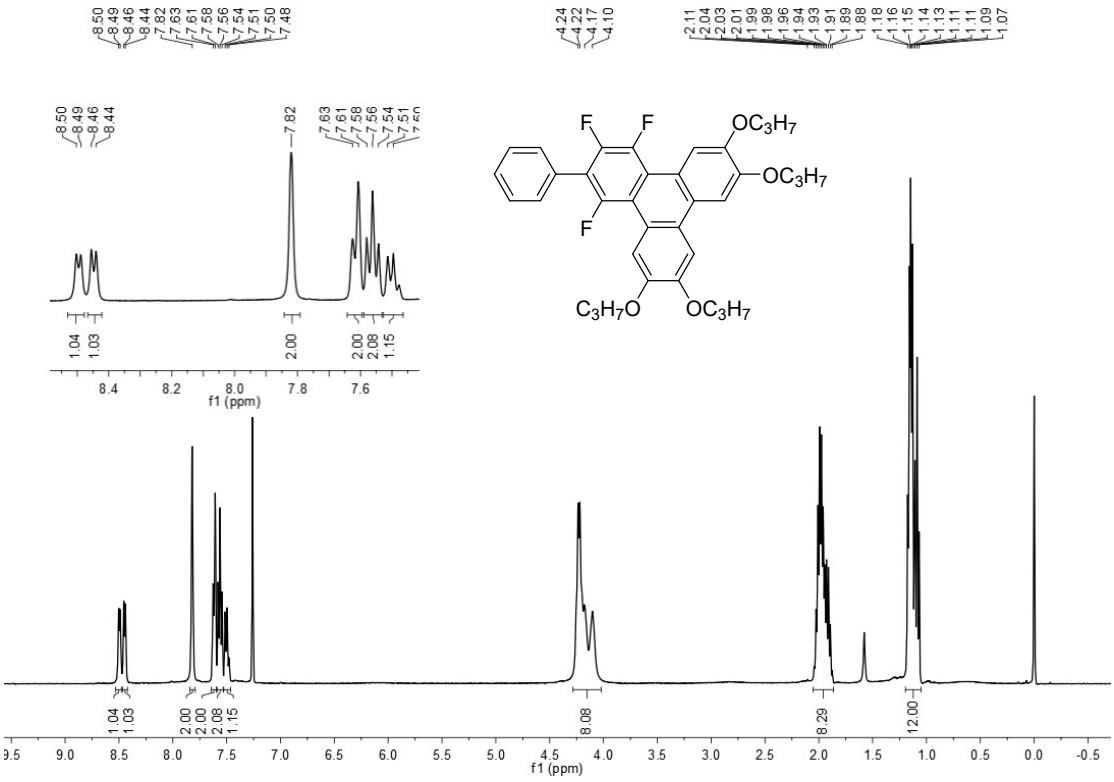

Figure S9 ^{1}H NMR ($CDCl_3$, 400 MHz) spectrum of **PH**3.

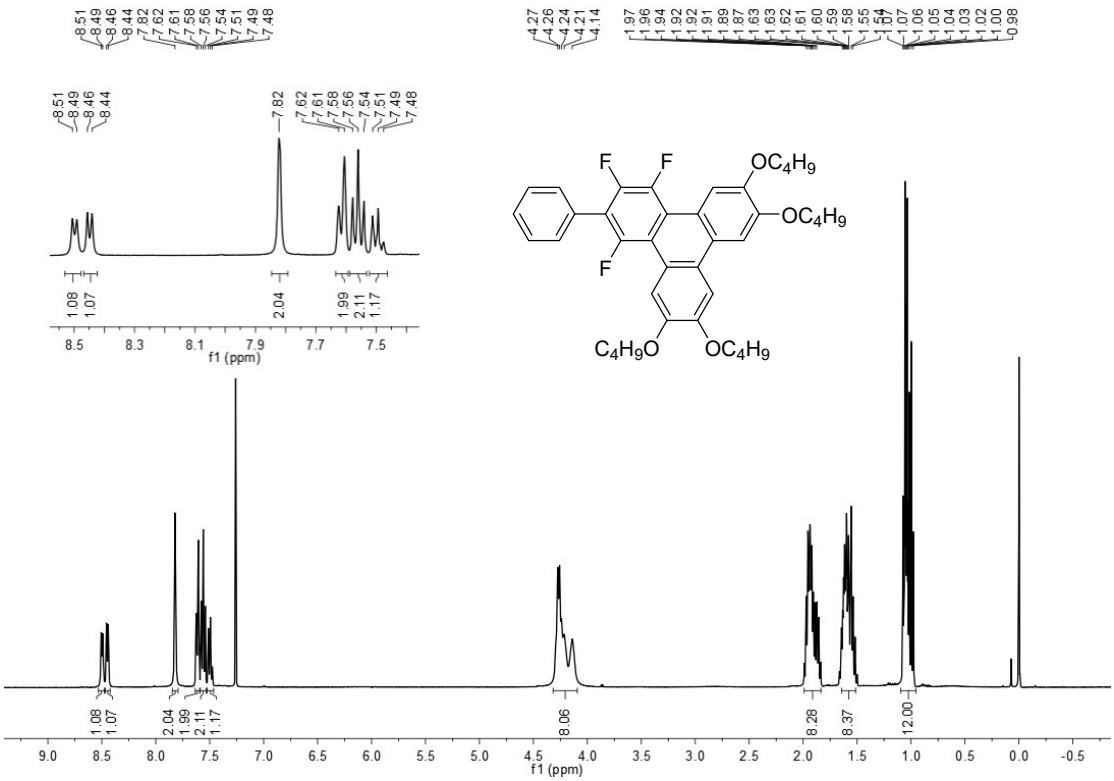

Figure S10 ^{1}H NMR ($CDCl_3$, 400 MHz) spectrum of **PH**4.

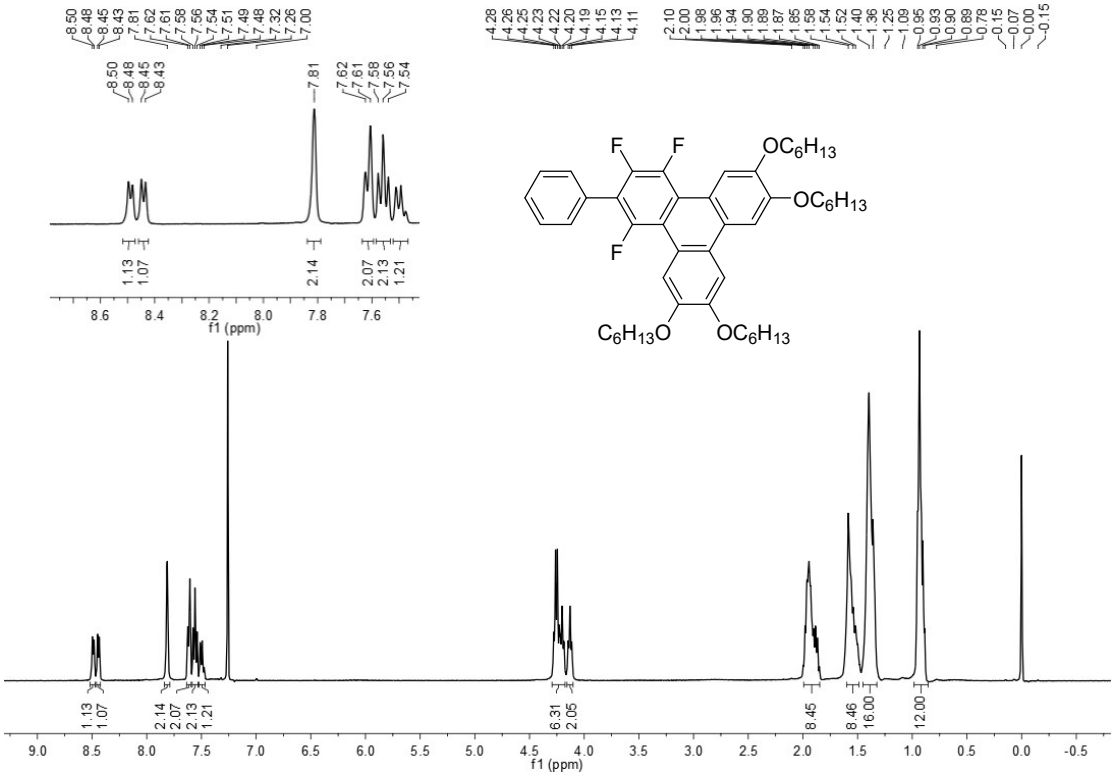

Figure S11 ^{1}H NMR ($CDCl_3$, 400 MHz) spectrum of **PH**6.

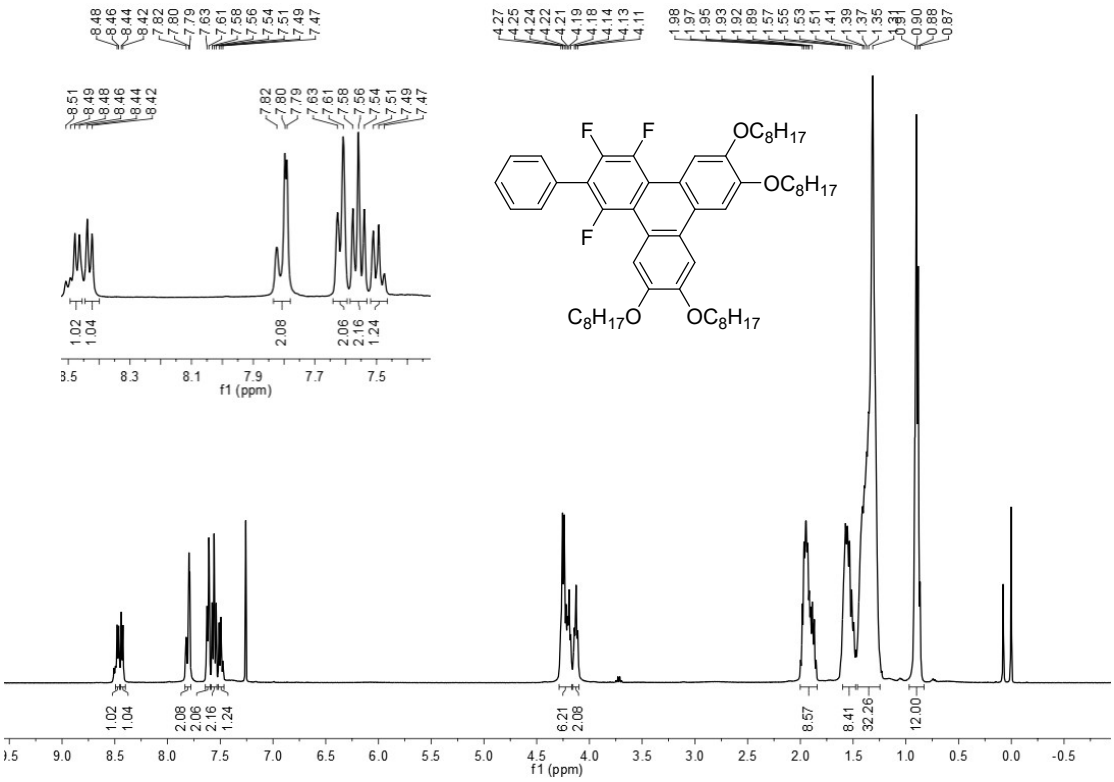

Figure S12 ^{1}H NMR ($CDCl_3$, 400 MHz) spectrum of **PH**8.

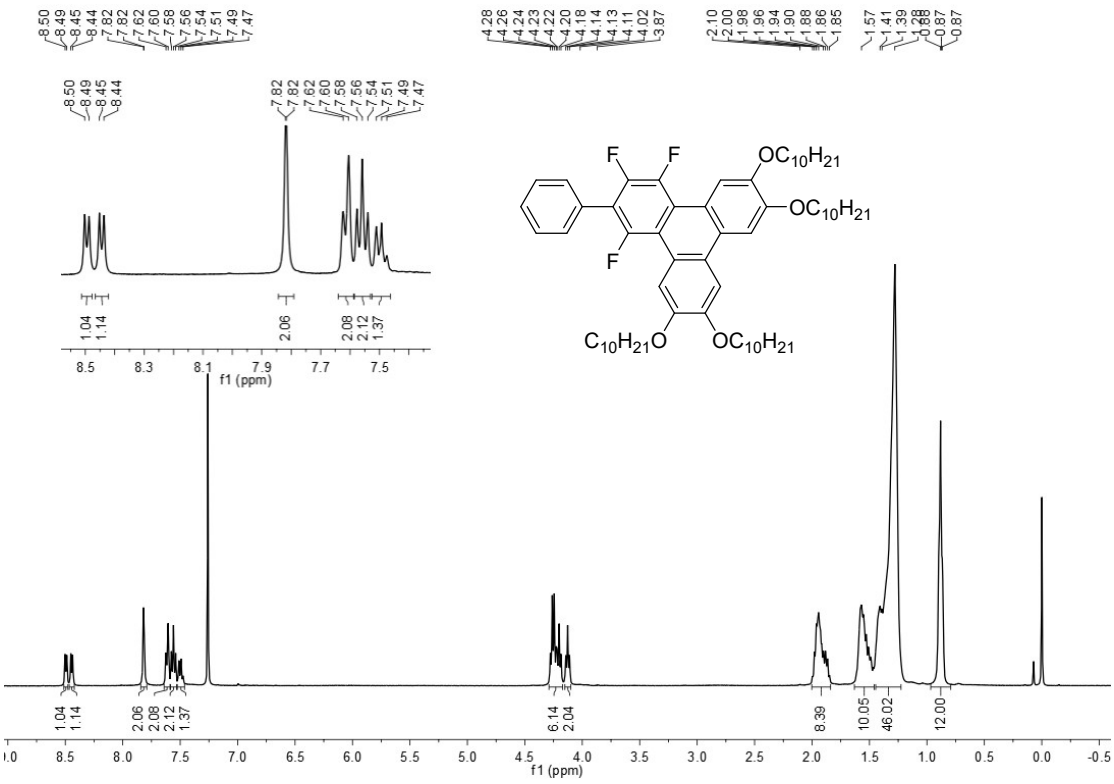

Figure S13 ^{1}H NMR ($CDCl_3$, 400 MHz) spectrum of **PH**10.

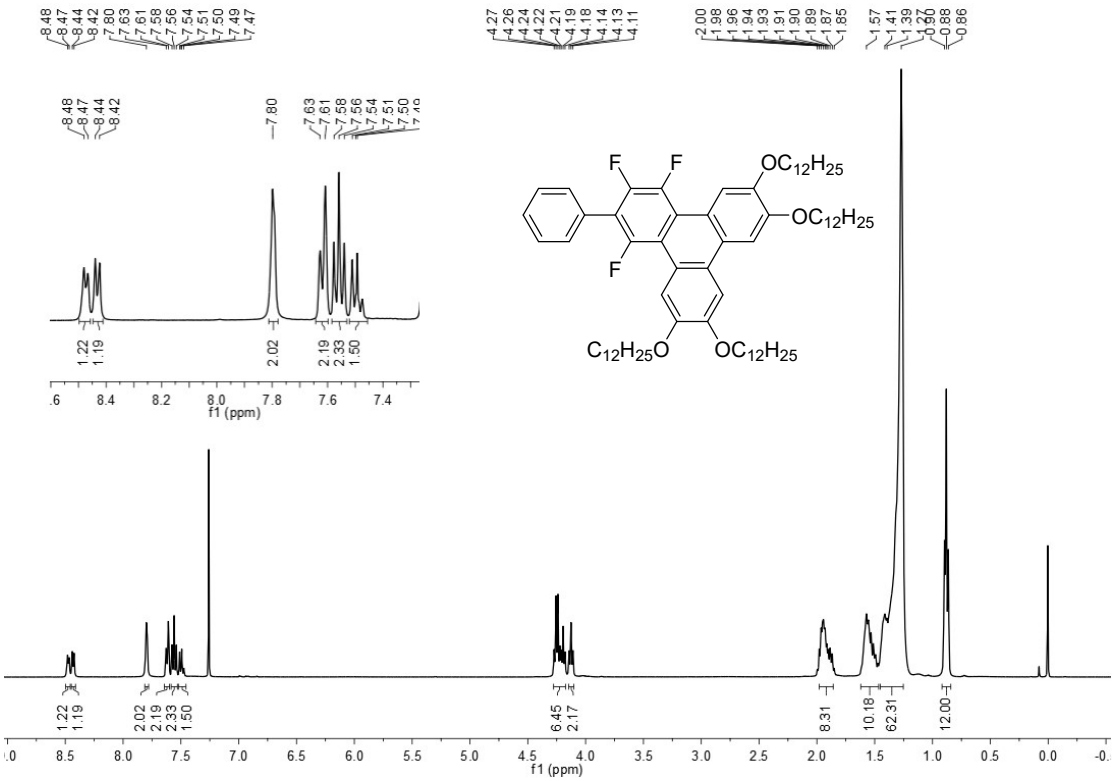

Figure S14 ^{1}H NMR ($CDCl_3$, 400 MHz) spectrum of **PH**12.

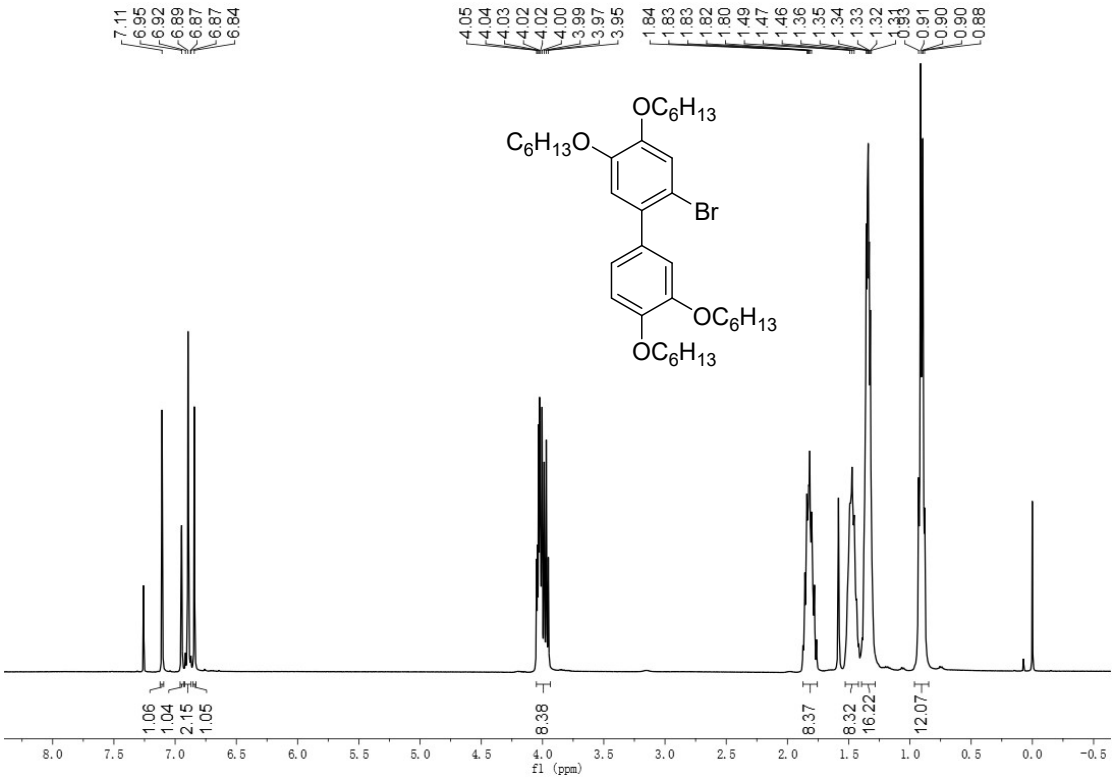

Figure S15 ^{1}H NMR ($CDCl_3$, 400 MHz) spectrum of Br-**BP**6.

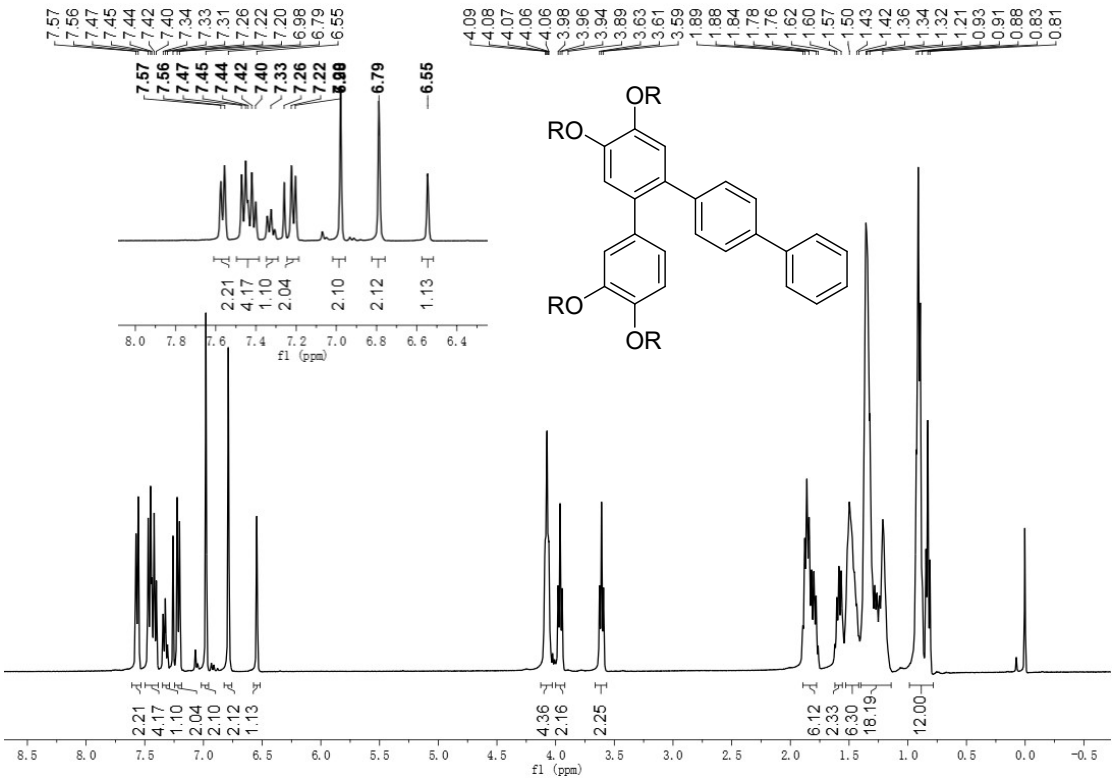

Figure S16 ^{1}H NMR ($CDCl_3$, 400 MHz) spectrum of **QP**6.

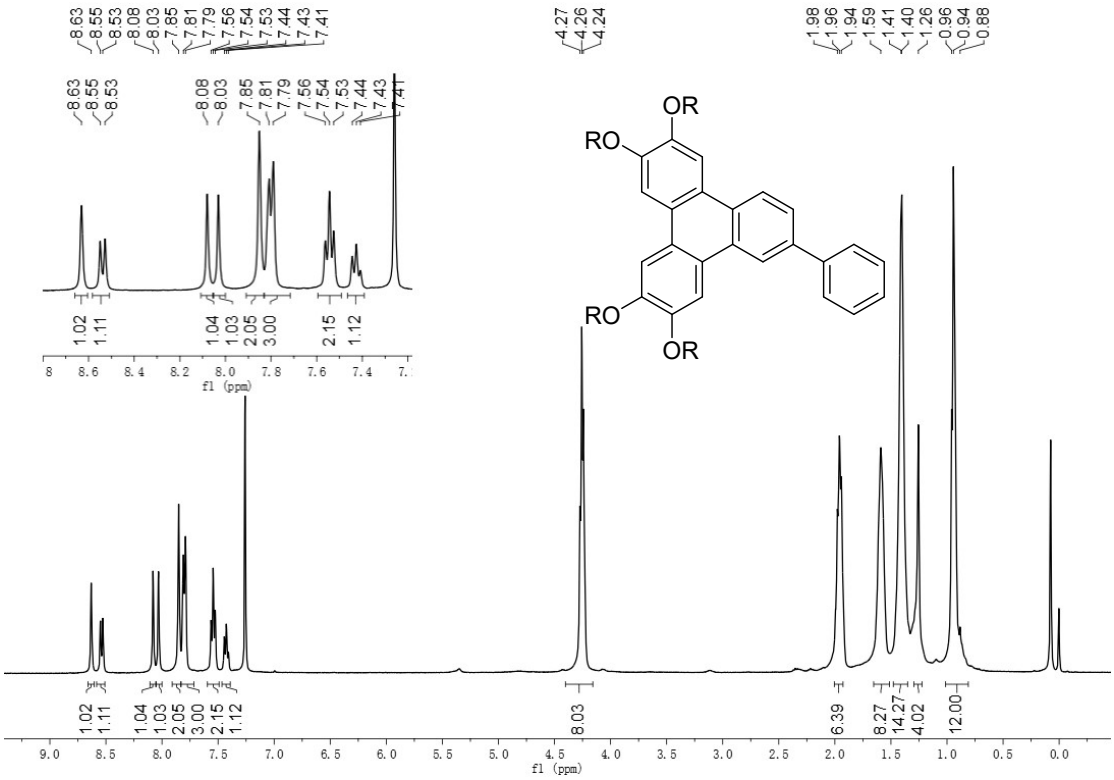

Figure S17 ^{1}H NMR ($CDCl_3$, 400 MHz) spectrum of **BTP**6.

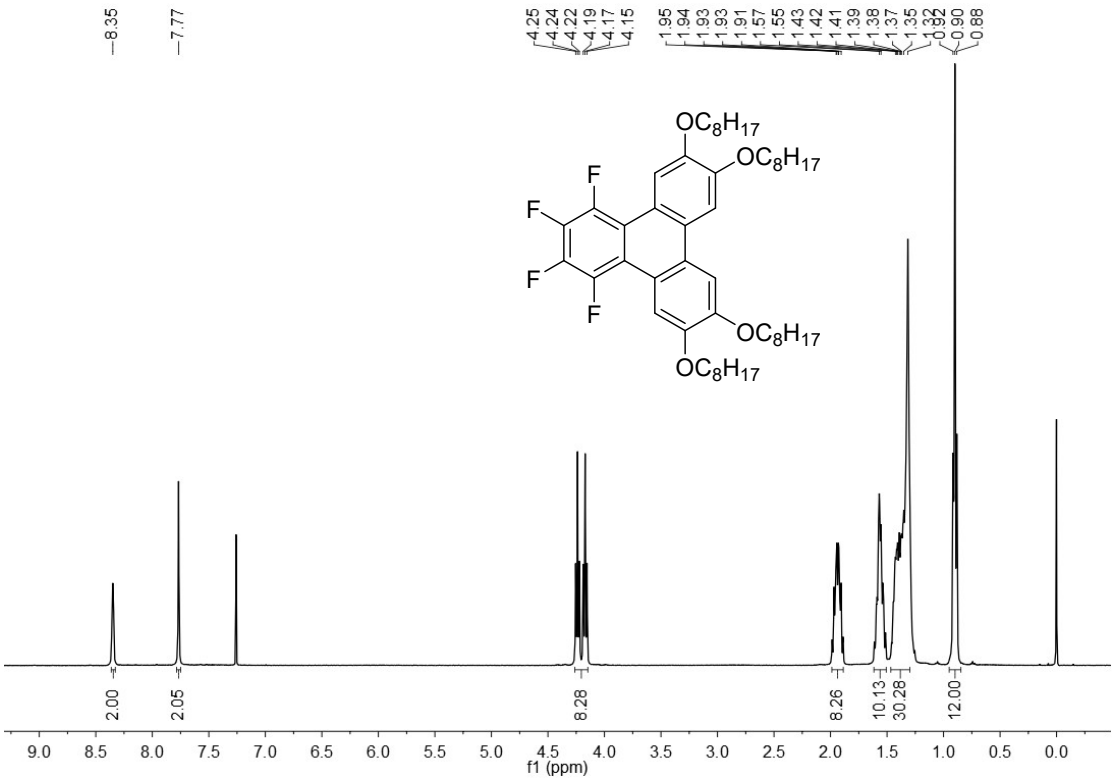

Figure S18 ^{1}H NMR ($CDCl_3$, 400 MHz) spectrum of 4*F*-**TP**8.

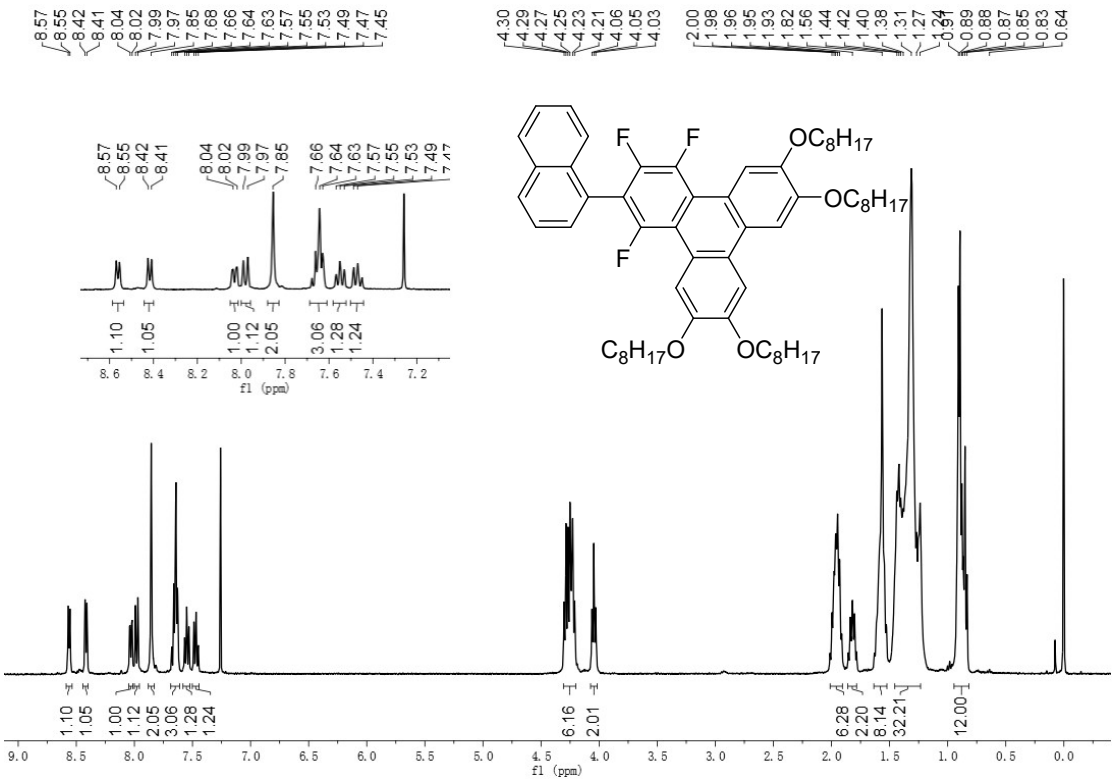

Figure S19 ^{1}H NMR ($CDCl_3$, 400 MHz) spectrum of **NAA**8.

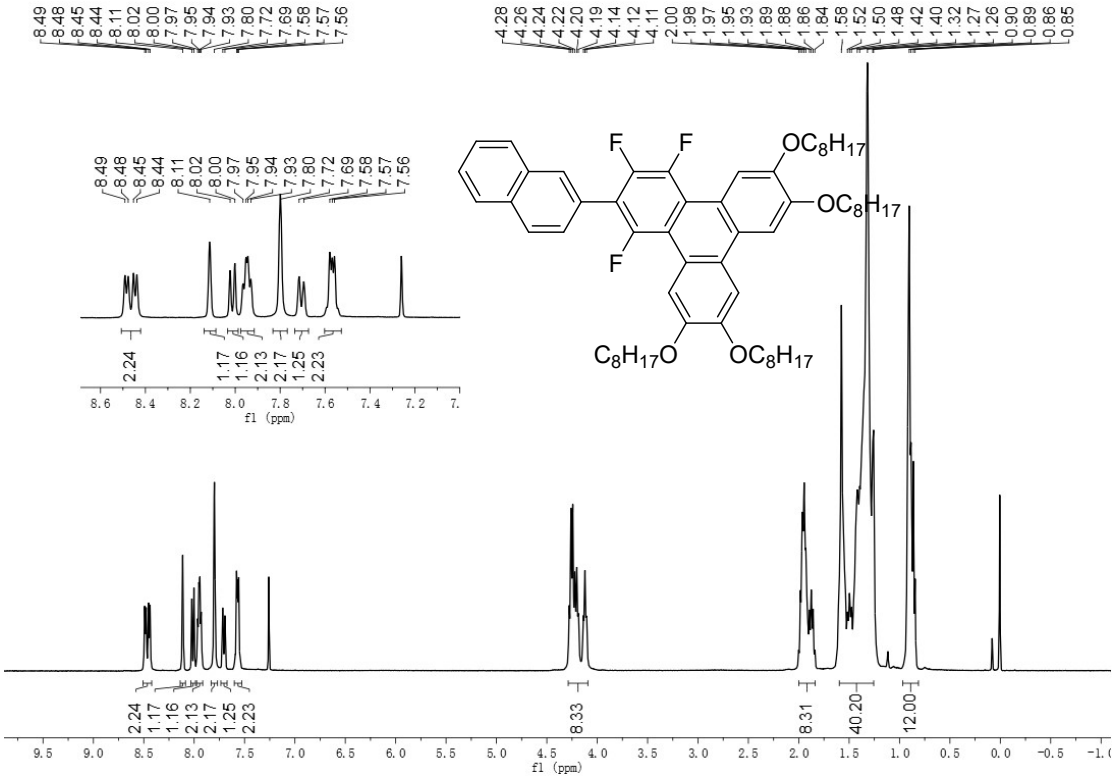

Figure S20 ^{1}H NMR ($CDCl_3$, 400 MHz) spectrum of **NAB**8.

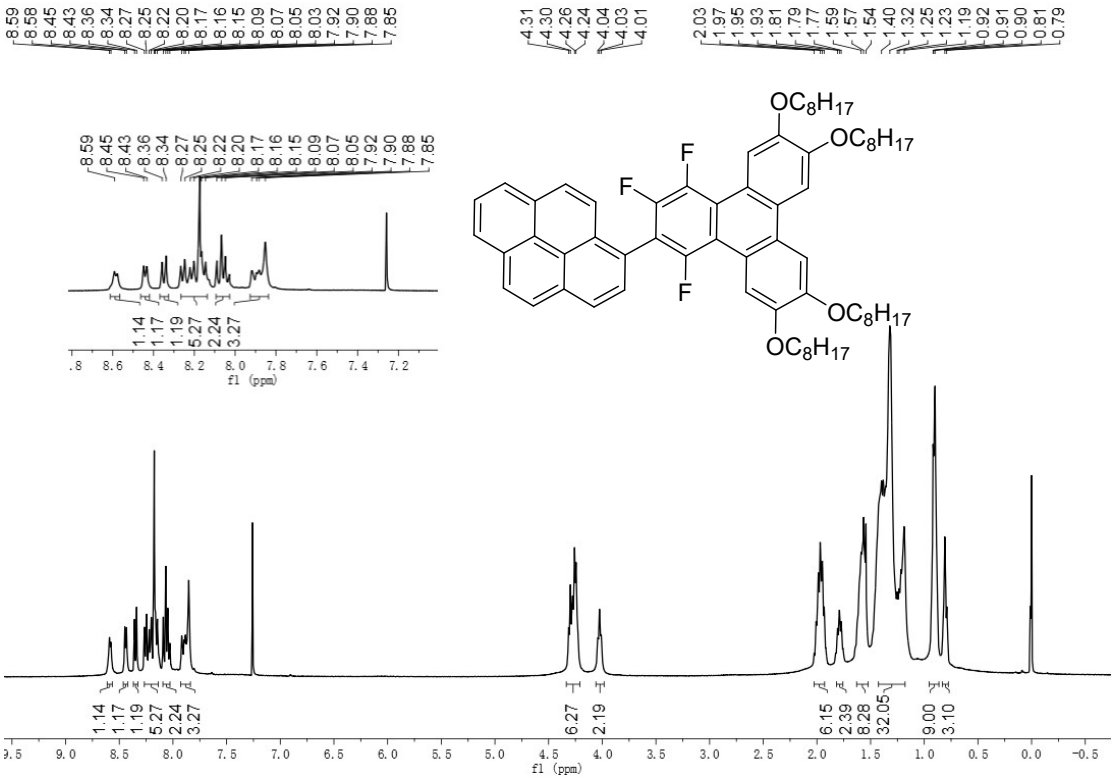

Figure S21 ^{1}H NMR ($CDCl_3$, 400 MHz) spectrum of **PY**8.

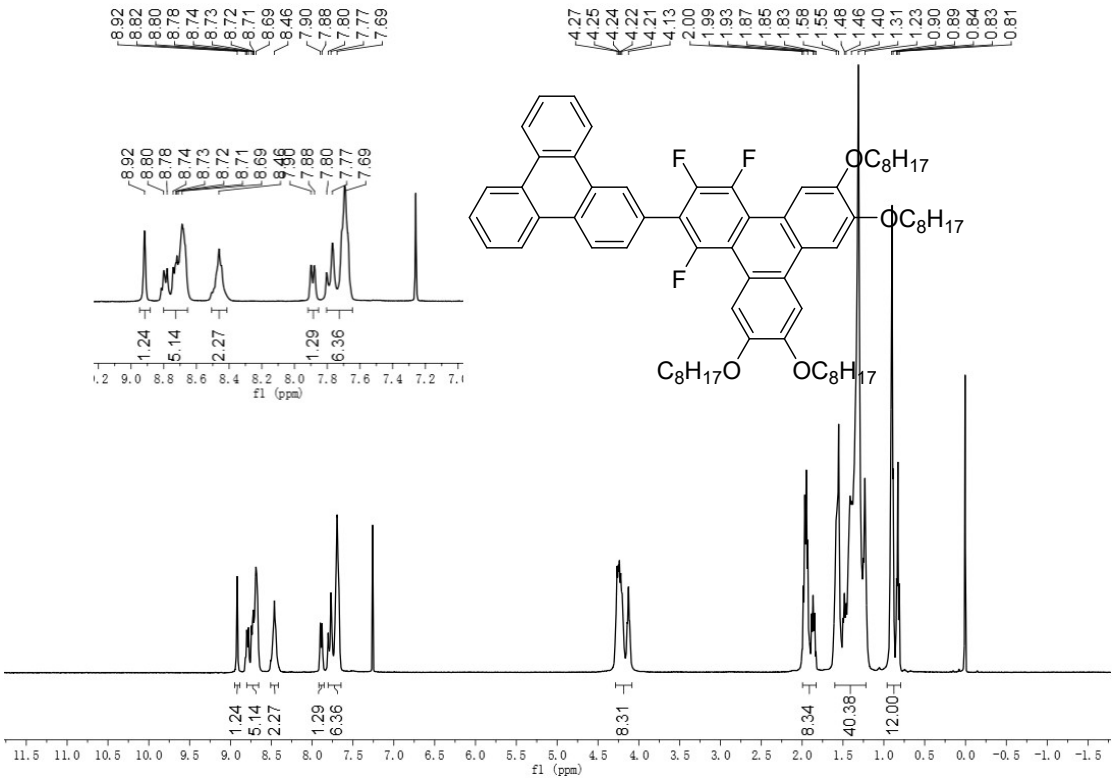

Figure S22 ^{1}H NMR ($CDCl_3$, 400 MHz) spectrum of **TP**8.

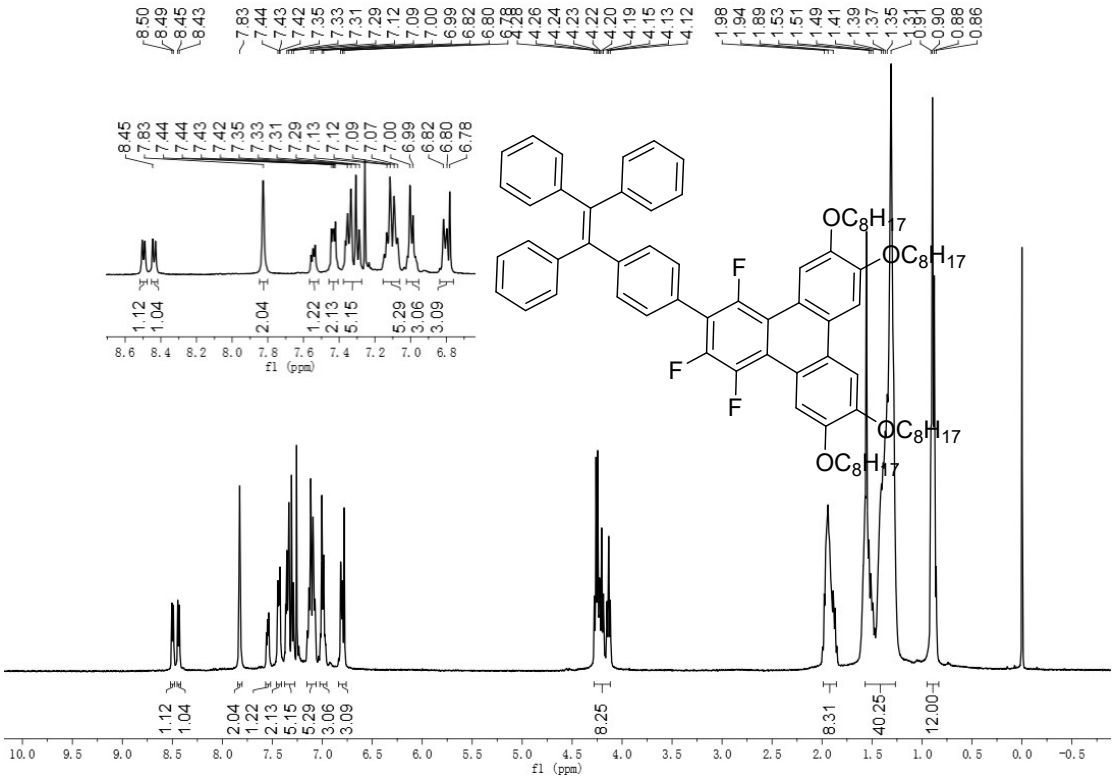

Figure S23 ^{1}H NMR ($CDCl_3$, 400 MHz) spectrum of **TPE**8.

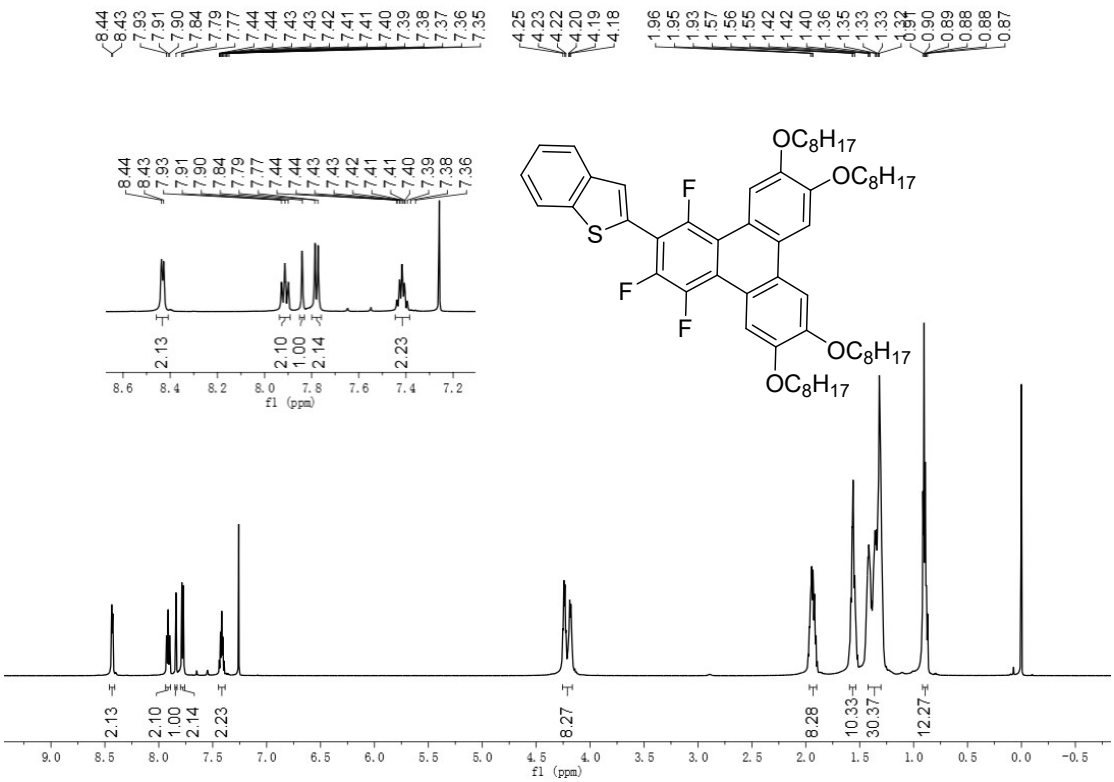

Figure S24 ^{1}H NMR ($CDCl_3$, 400 MHz) spectrum of **BT**8.

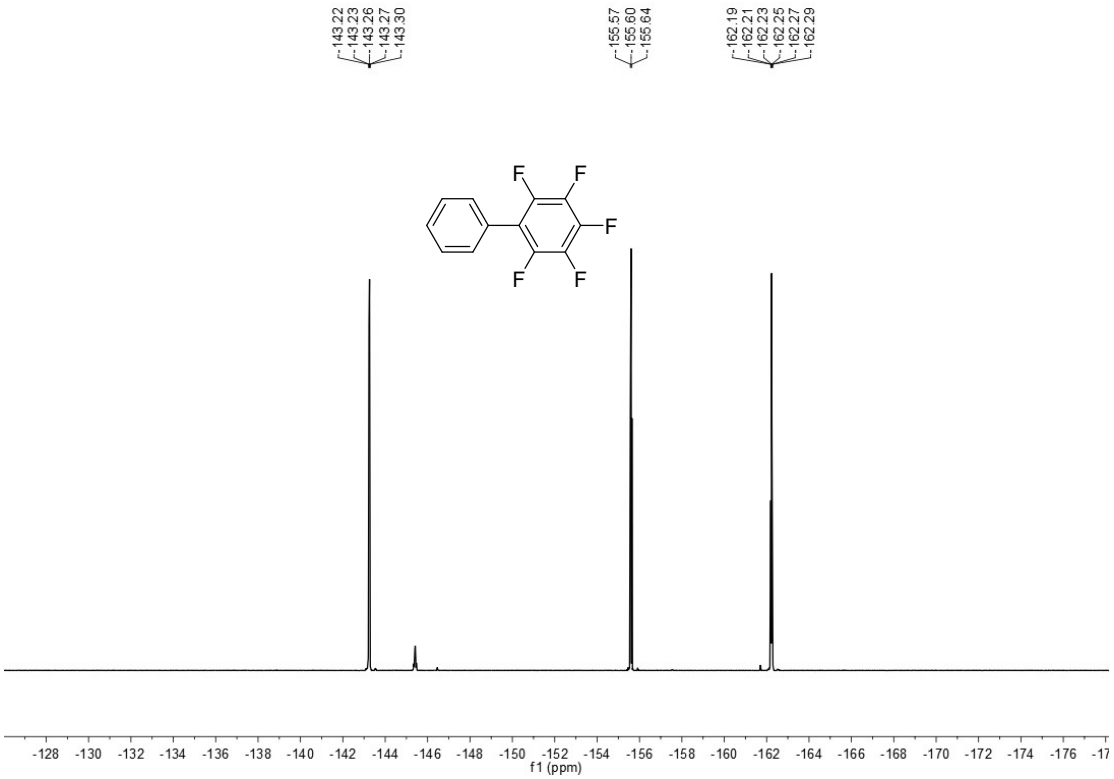

Figure S25 ^{19}F NMR ($CDCl_3$, 565 MHz) spectrum of Ph-C_6F_5.

Figure S26 ^{19}F NMR ($CDCl_3$, 565 MHz) spectrum of **PH**0.

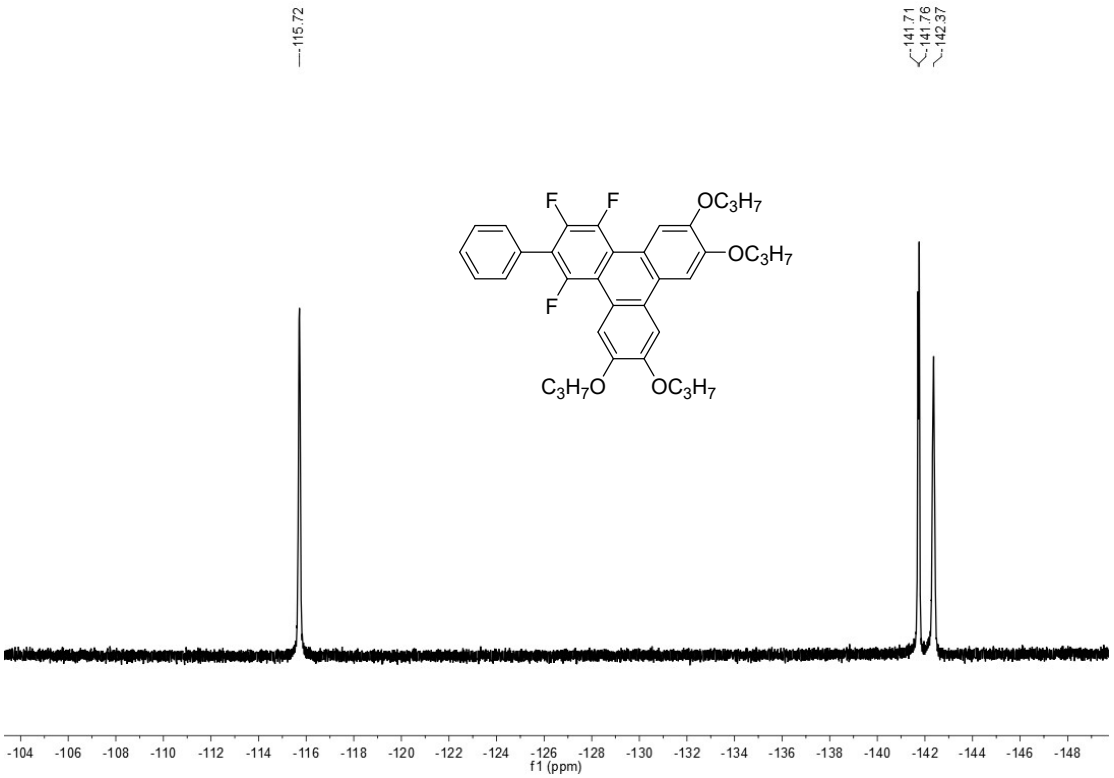

Figure S27 ^{19}F NMR ($CDCl_3$, 376 MHz) spectrum of **PH**3.

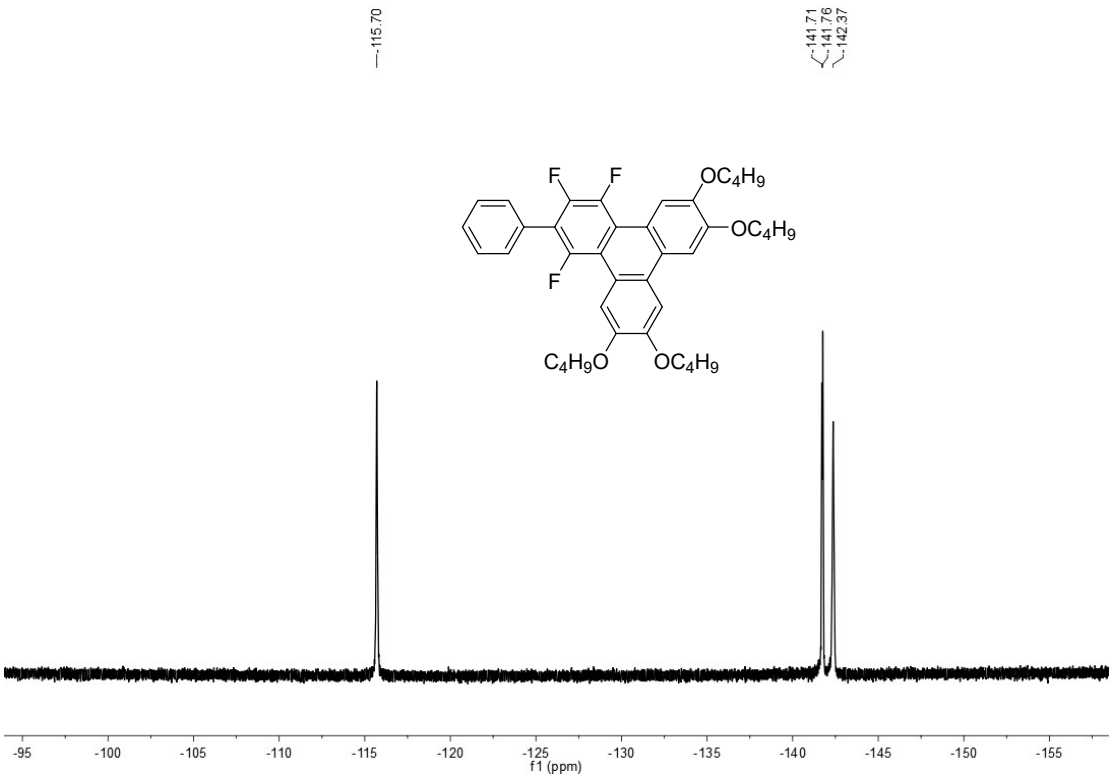

Figure S28 ^{19}F NMR ($CDCl_3$, 376 MHz) spectrum of **PH**4.

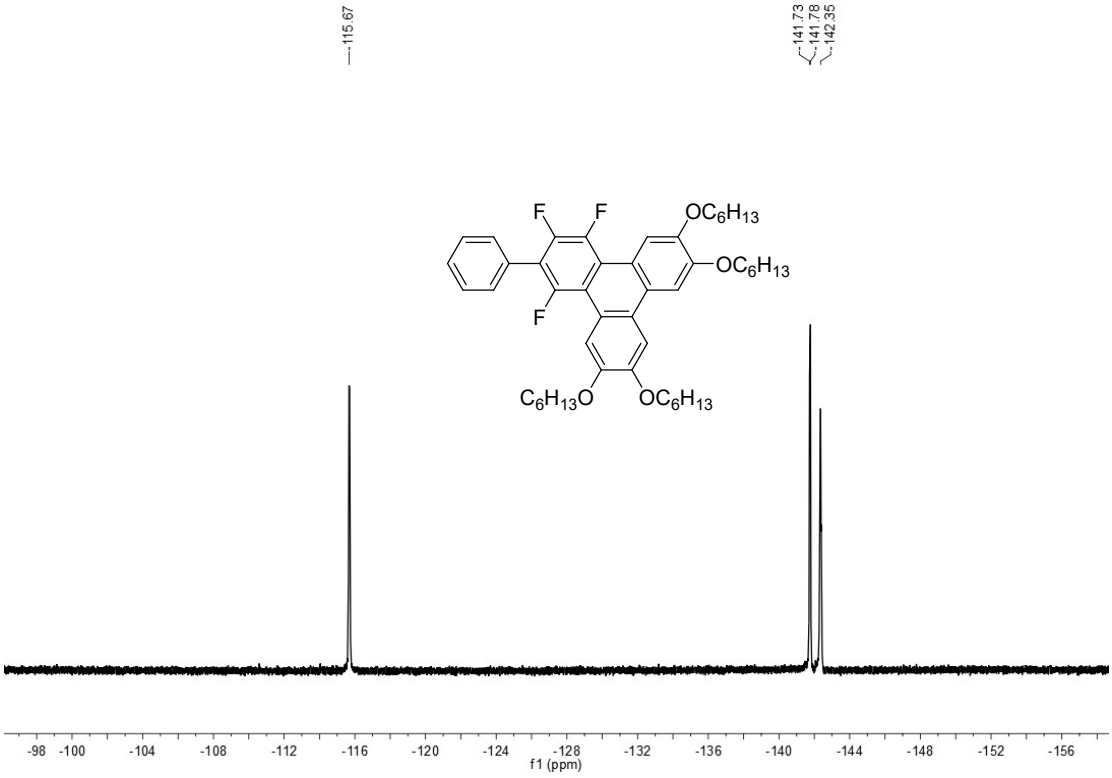

Figure S29 ^{19}F NMR ($CDCl_3$, 376 MHz) spectrum of **PH**6.

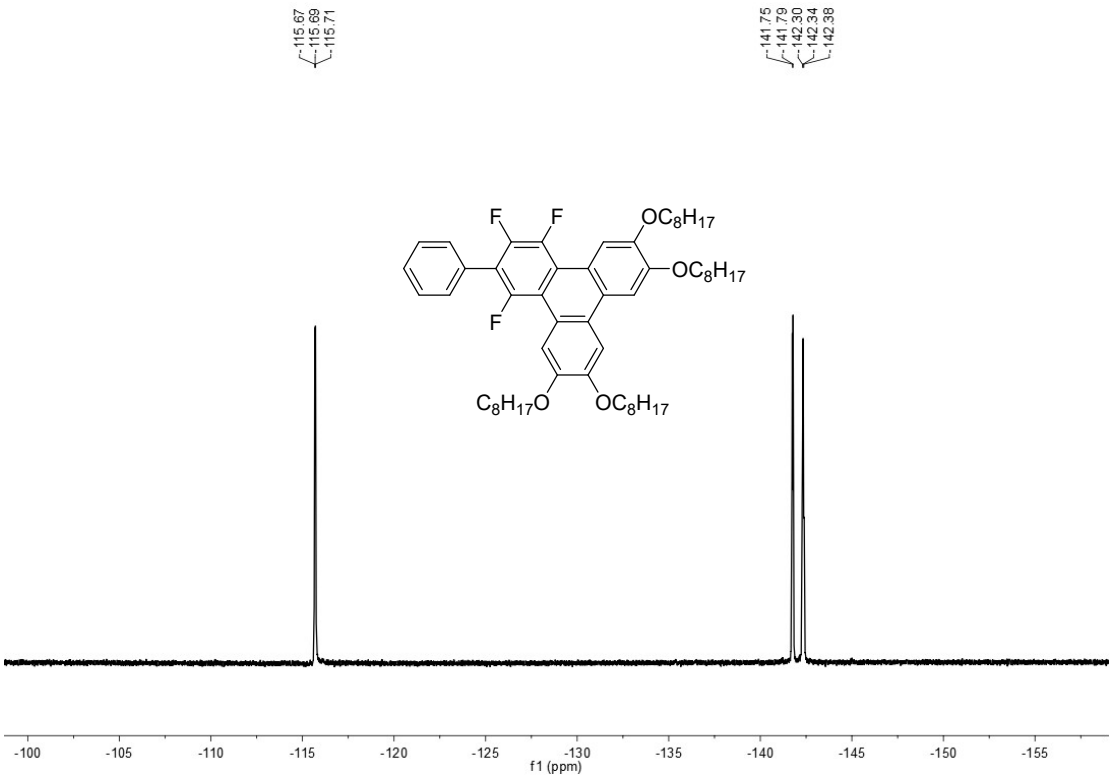

Figure S30 ^{19}F NMR ($CDCl_3$, 376 MHz) spectrum of **PH**8.

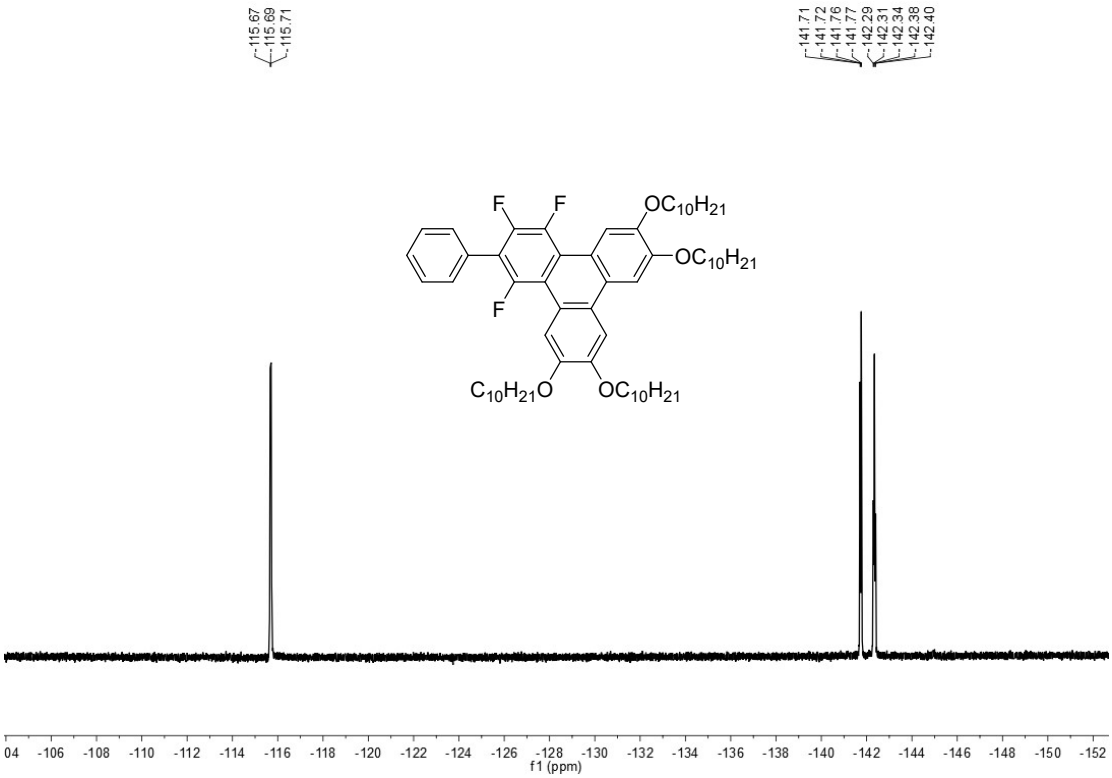

Figure S31 ^{19}F NMR ($CDCl_3$, 376 MHz) spectrum of **PH**10.

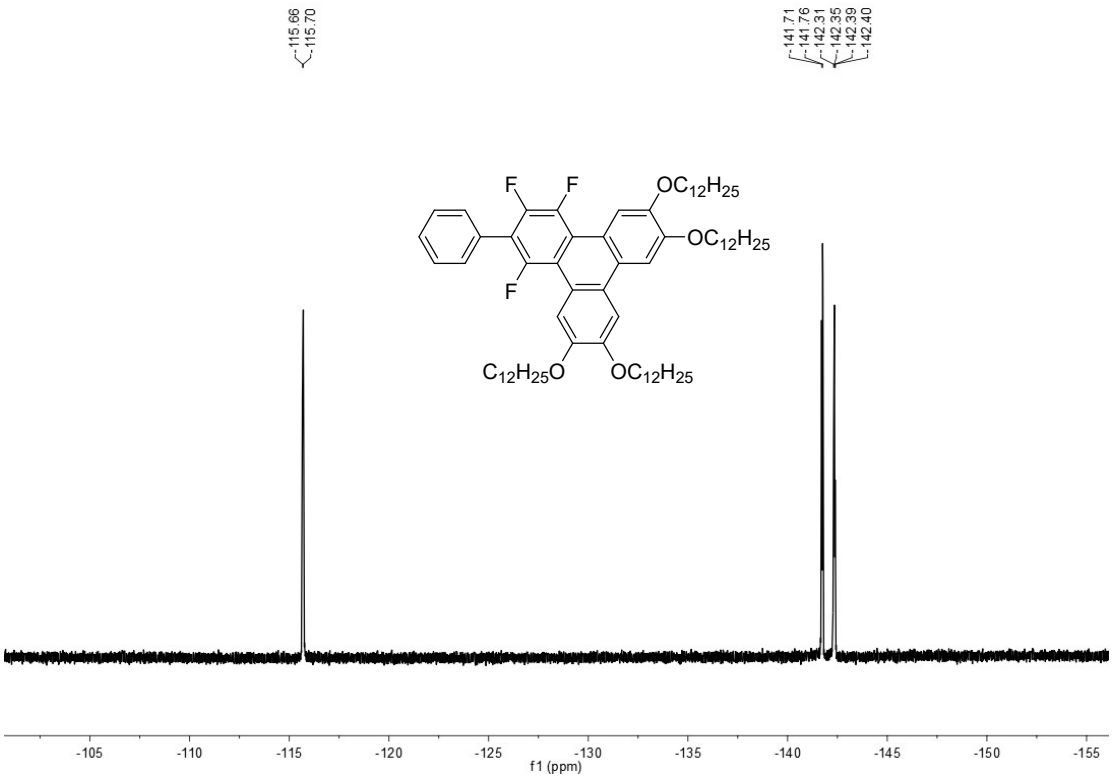

Figure S32 ^{19}F NMR ($CDCl_3$, 376 MHz) spectrum of **PH**12.

Figure S33 ^{19}F NMR ($CDCl_3$,565 MHz) spectrum of 4*F*-**TP**8.

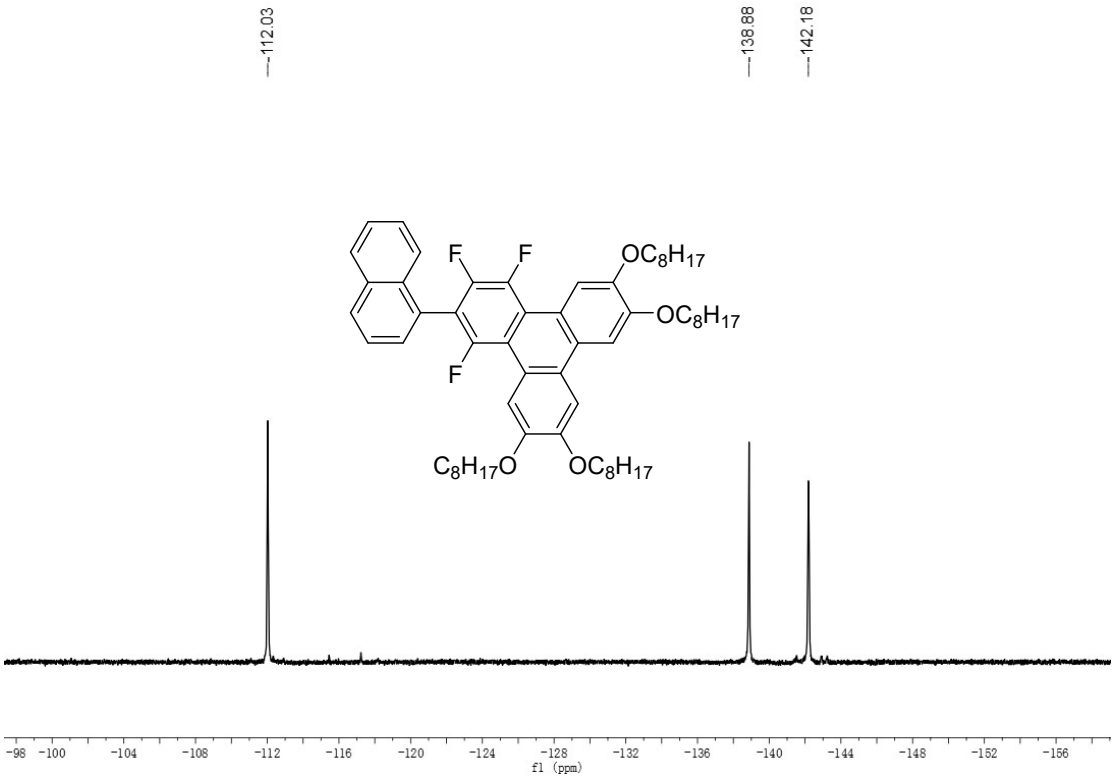

Figure S34 ^{19}F NMR ($CDCl_3$, 565 MHz) spectrum of **NAA**8.

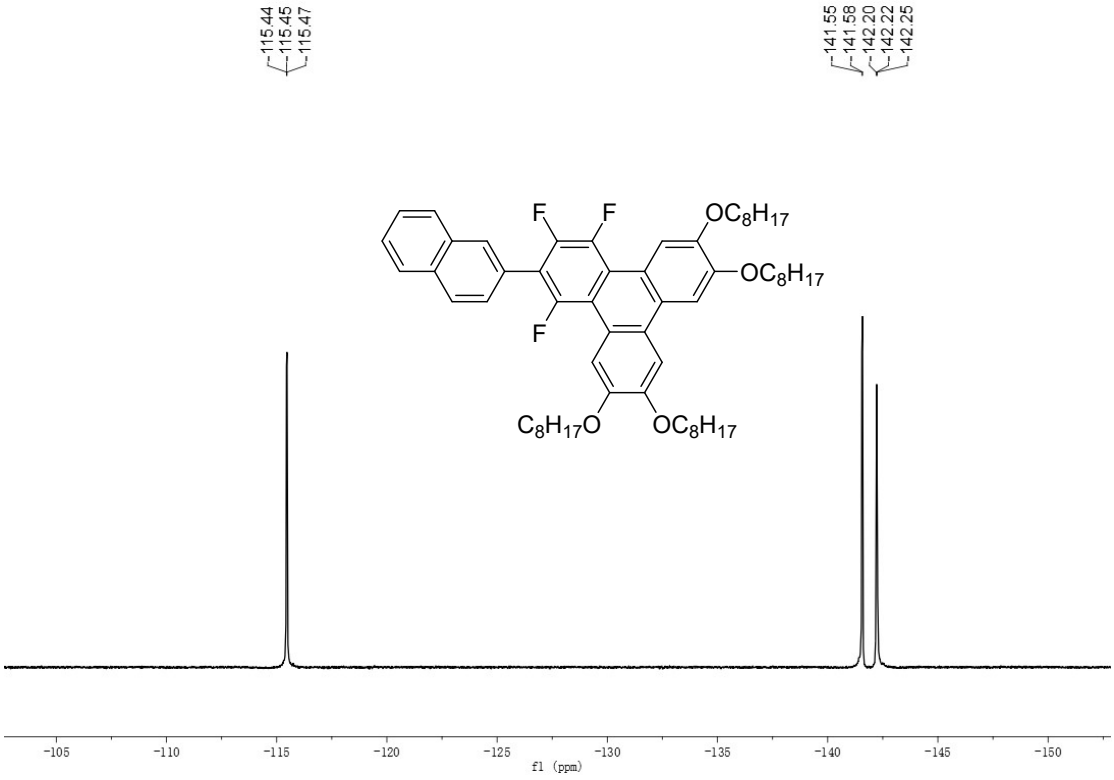

Figure S35 ^{19}F NMR ($CDCl_3$, 565 MHz) spectrum of **NAB**8.

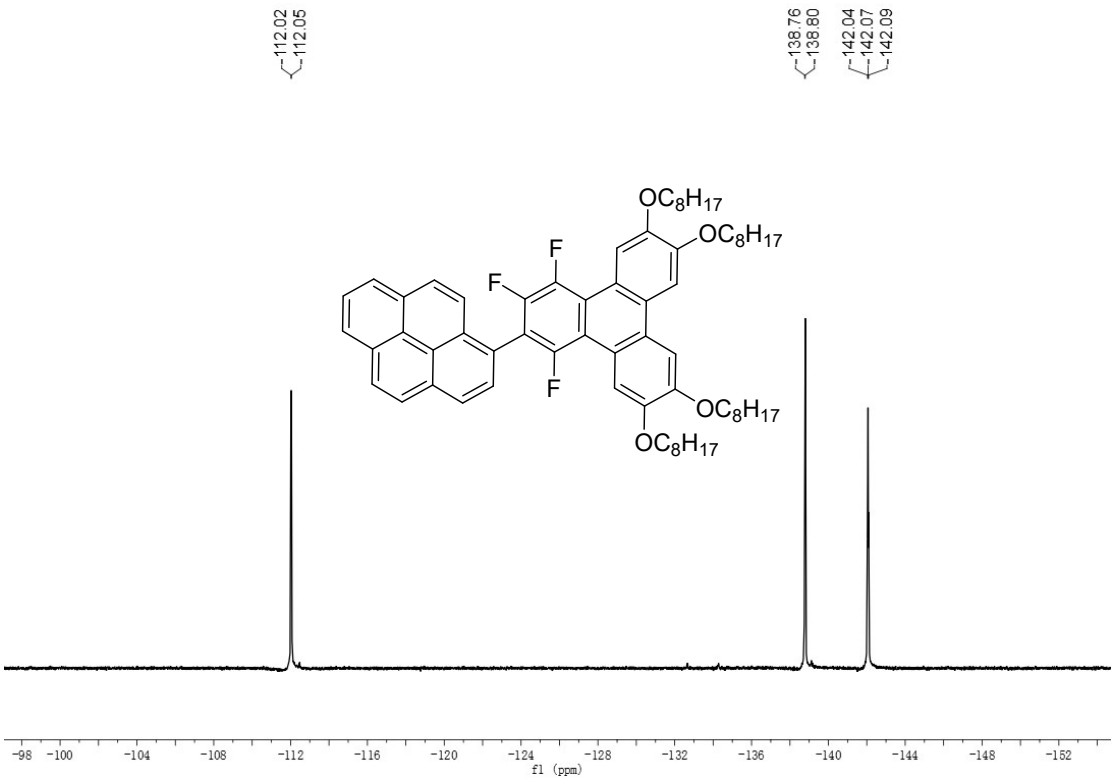

Figure S36 ^{19}F NMR ($CDCl_3$, 565 MHz) spectrum of **PY**8.

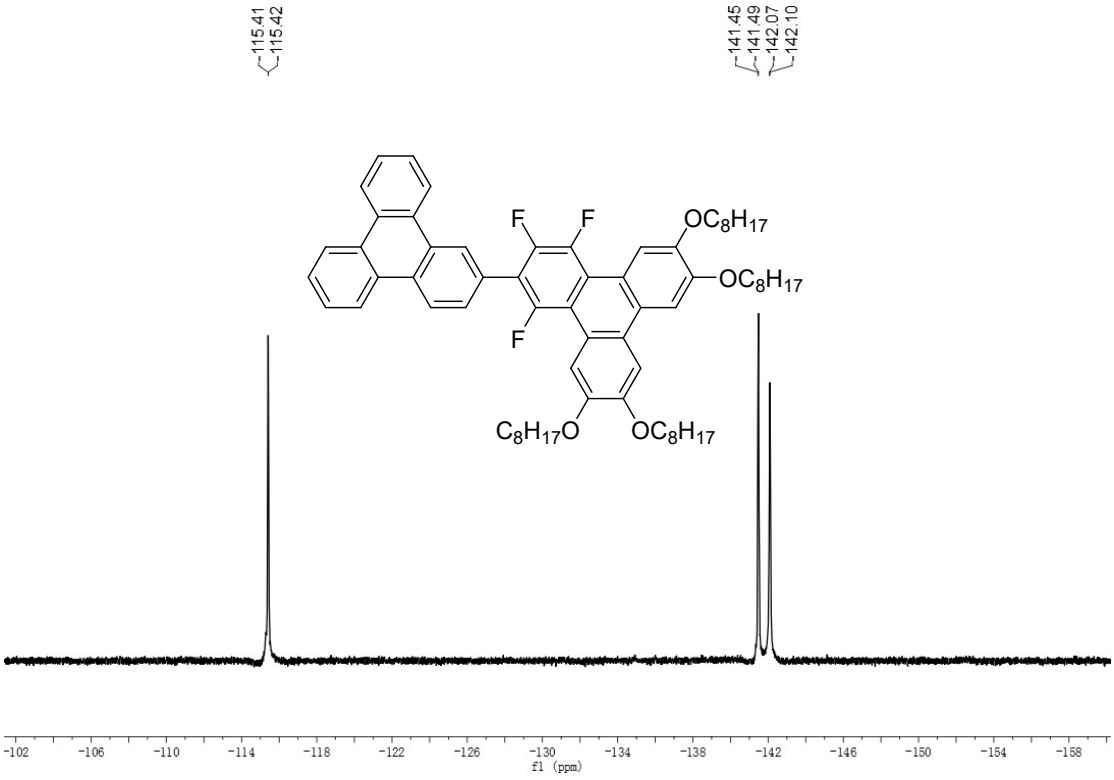

Figure S37 ^{19}F NMR ($CDCl_3$, 565 MHz) spectrum of **TP**8.

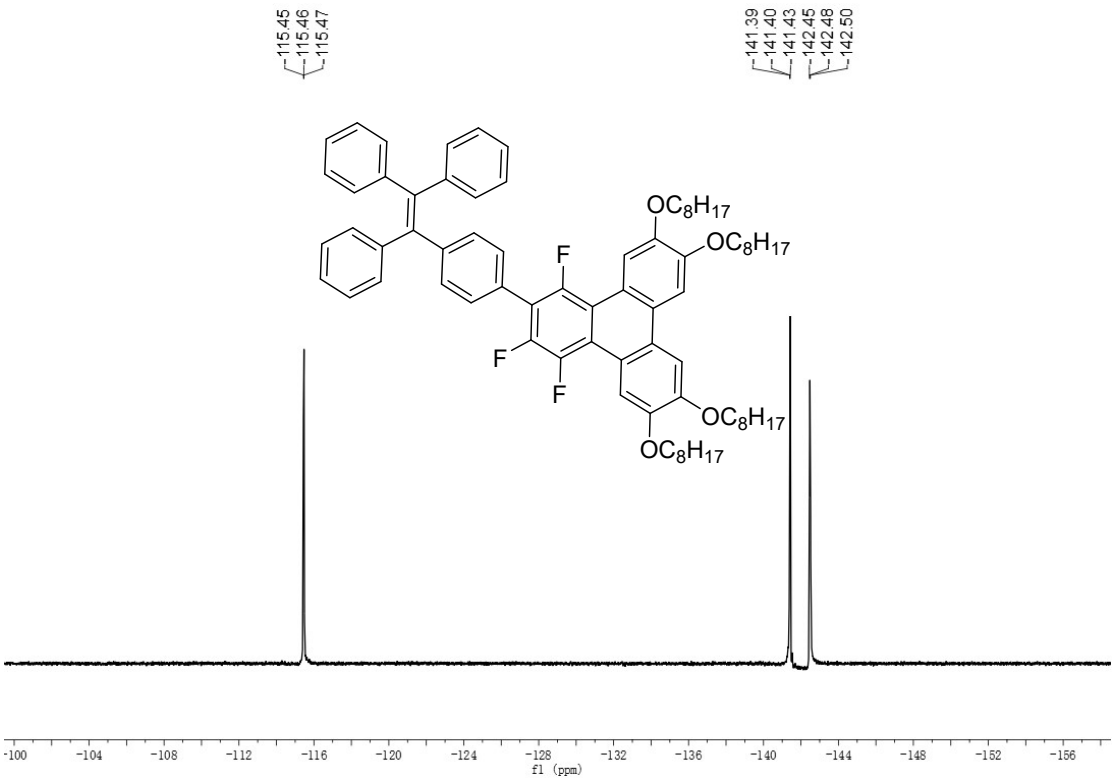

Figure S38 ^{19}F NMR ($CDCl_3$, 565 MHz) spectrum of **TPE**8.

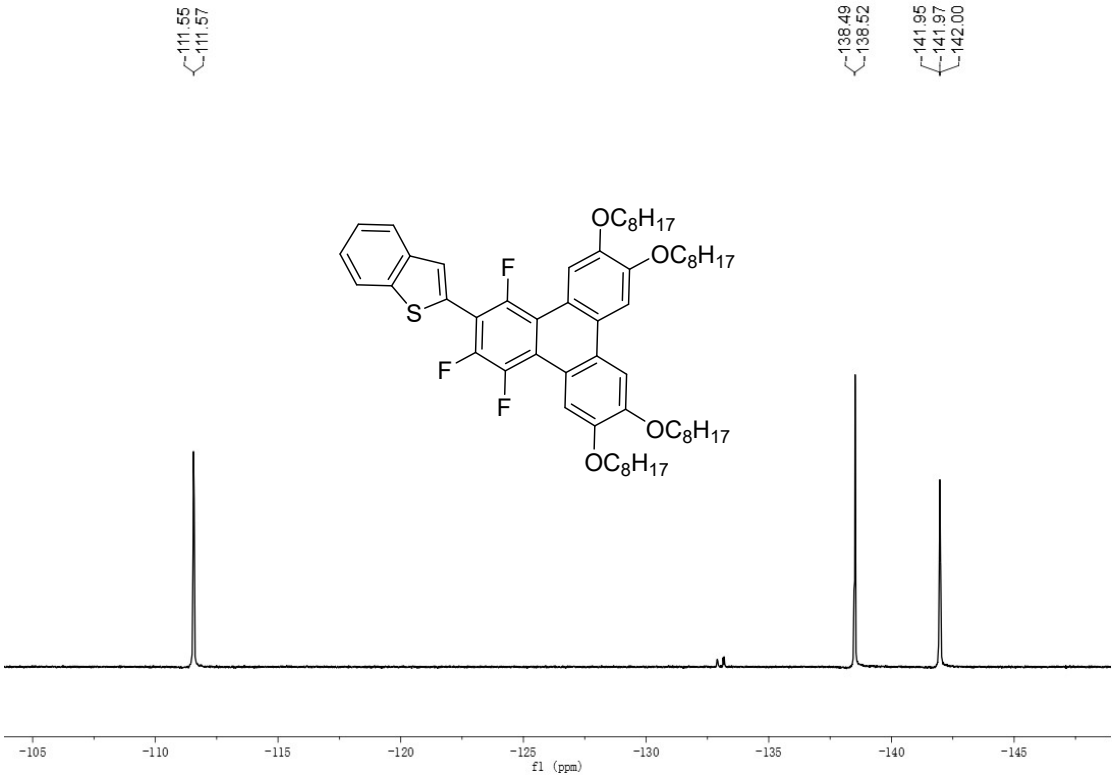

Figure S39 ^{19}F NMR ($CDCl_3$, 565 MHz) spectrum of **BT**8.

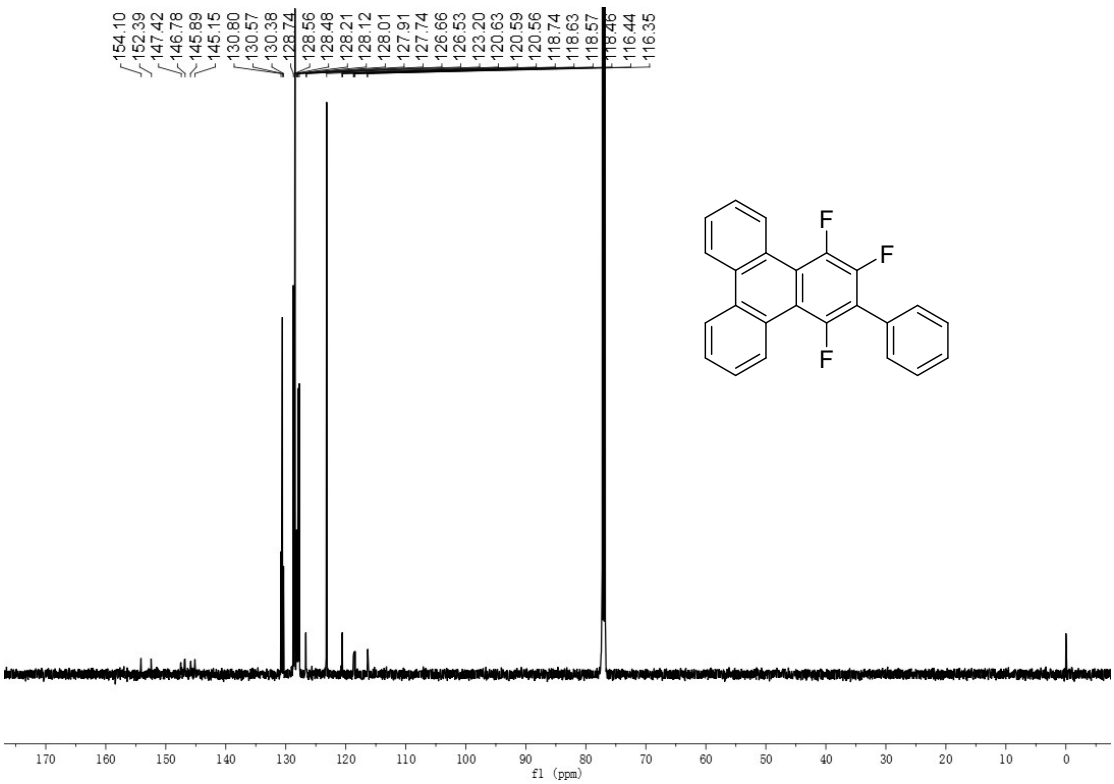

Figure S40 ^{13}C NMR ($CDCl_3$, 151 MHz) spectrum of **PH**0.

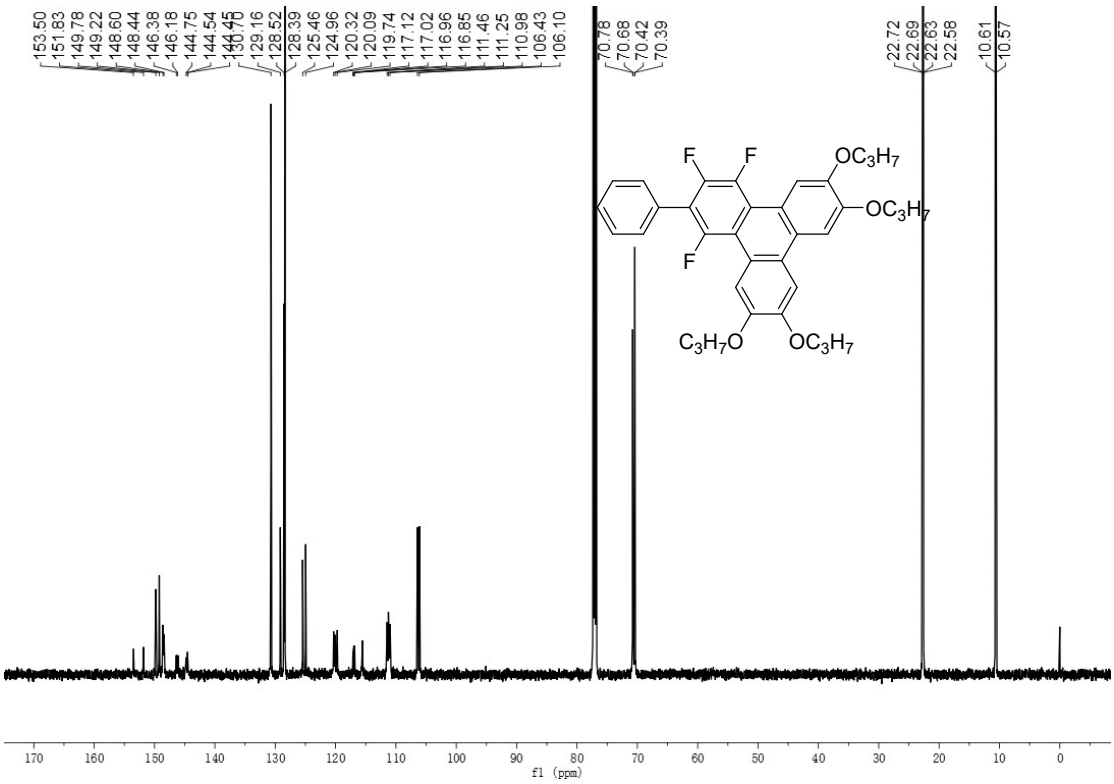

Figure S41 ^{13}C NMR ($CDCl_3$, 151 MHz) spectrum of **PH**3.

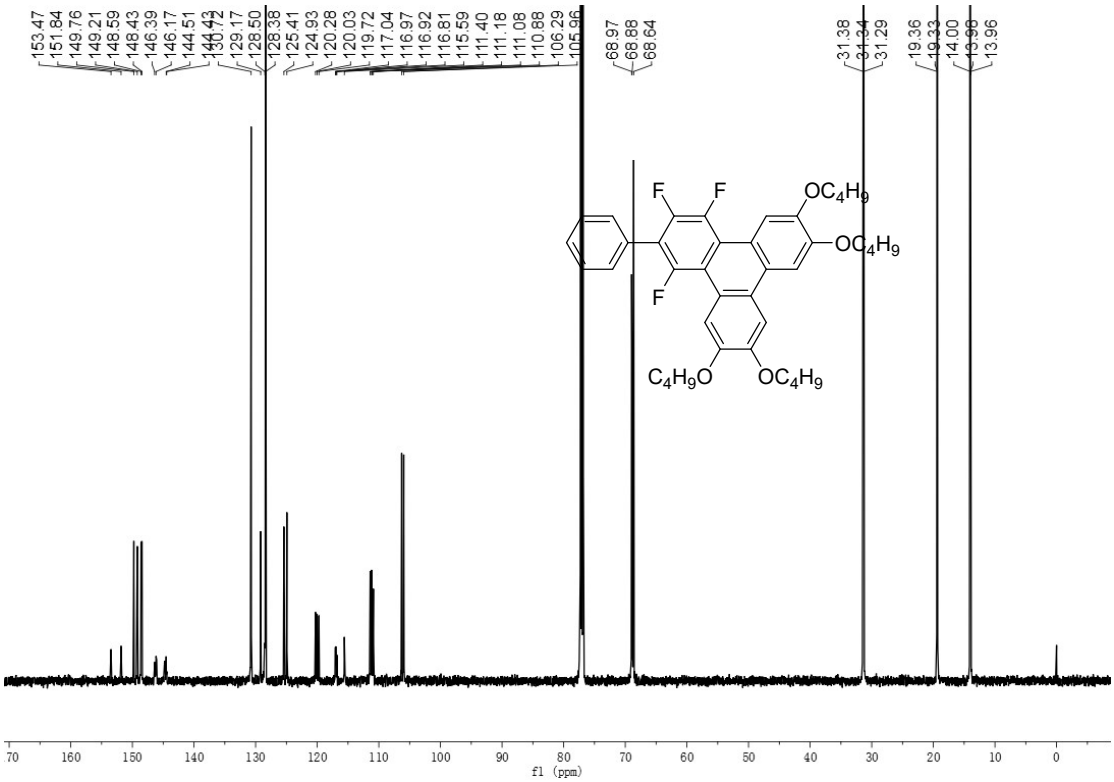

Figure S42 ^{13}C NMR ($CDCl_3$, 151 MHz) spectrum of **PH**4.

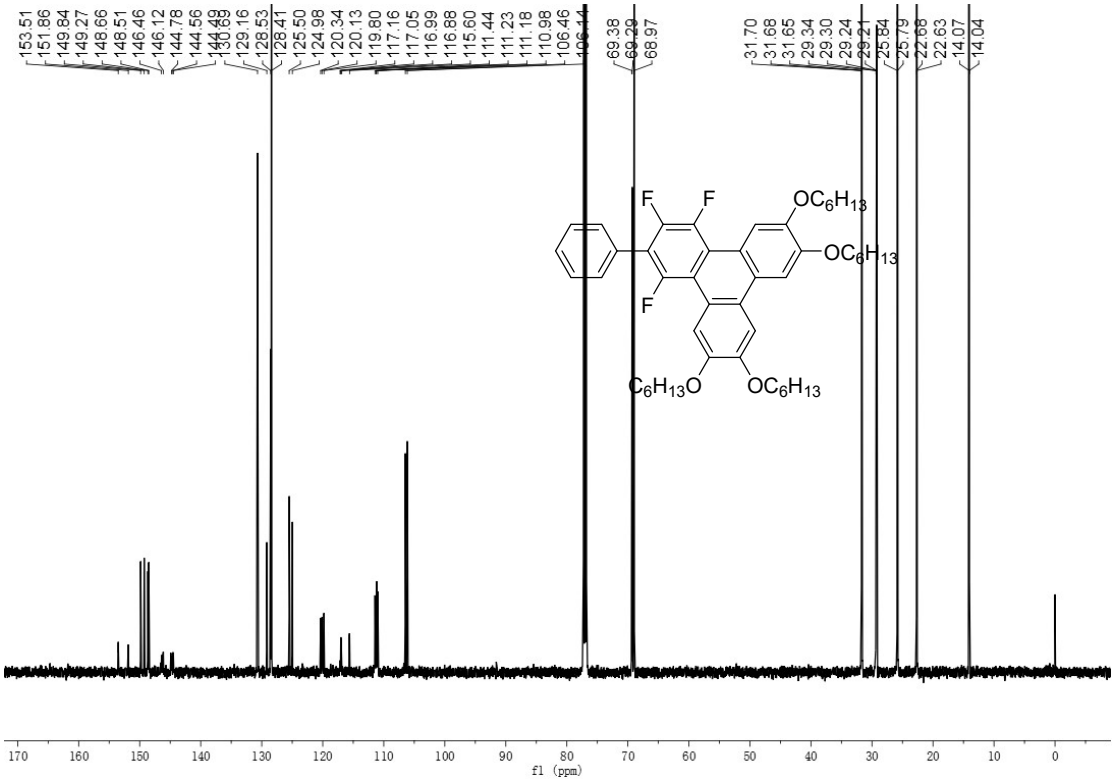

Figure S43 ^{13}C NMR ($CDCl_3$, 151 MHz) spectrum of **PH**6.

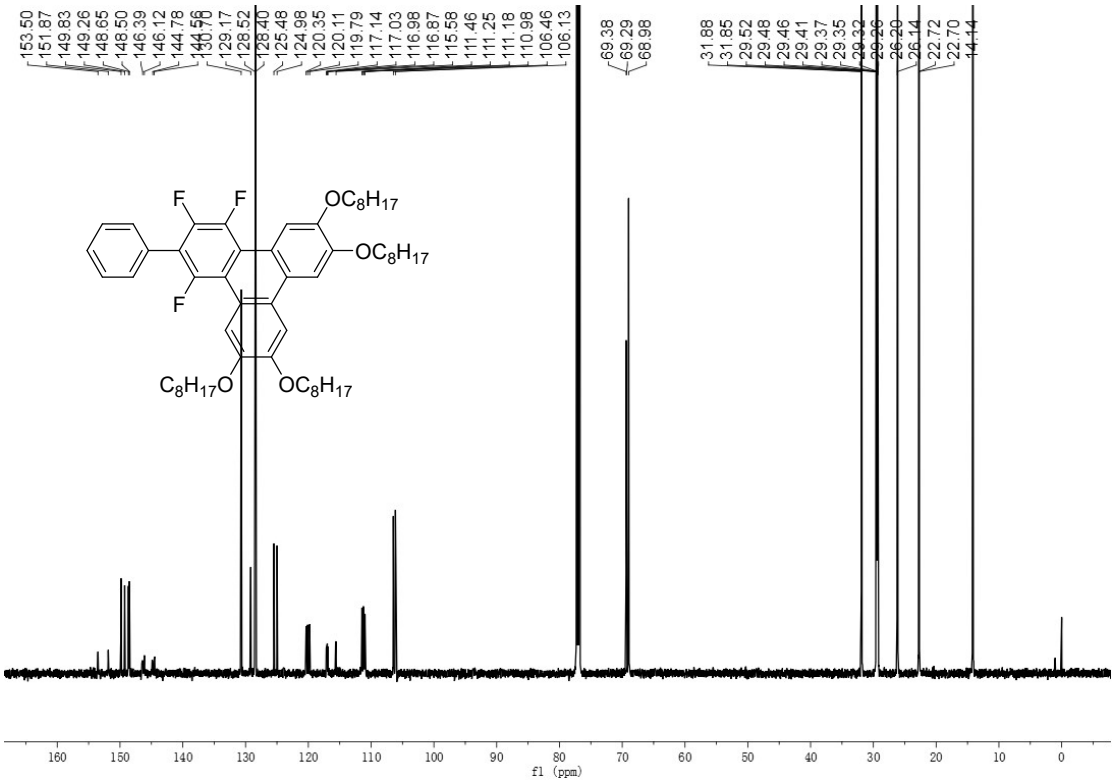

Figure S44 ^{13}C NMR ($CDCl_3$, 151 MHz) spectrum of **PH**8.

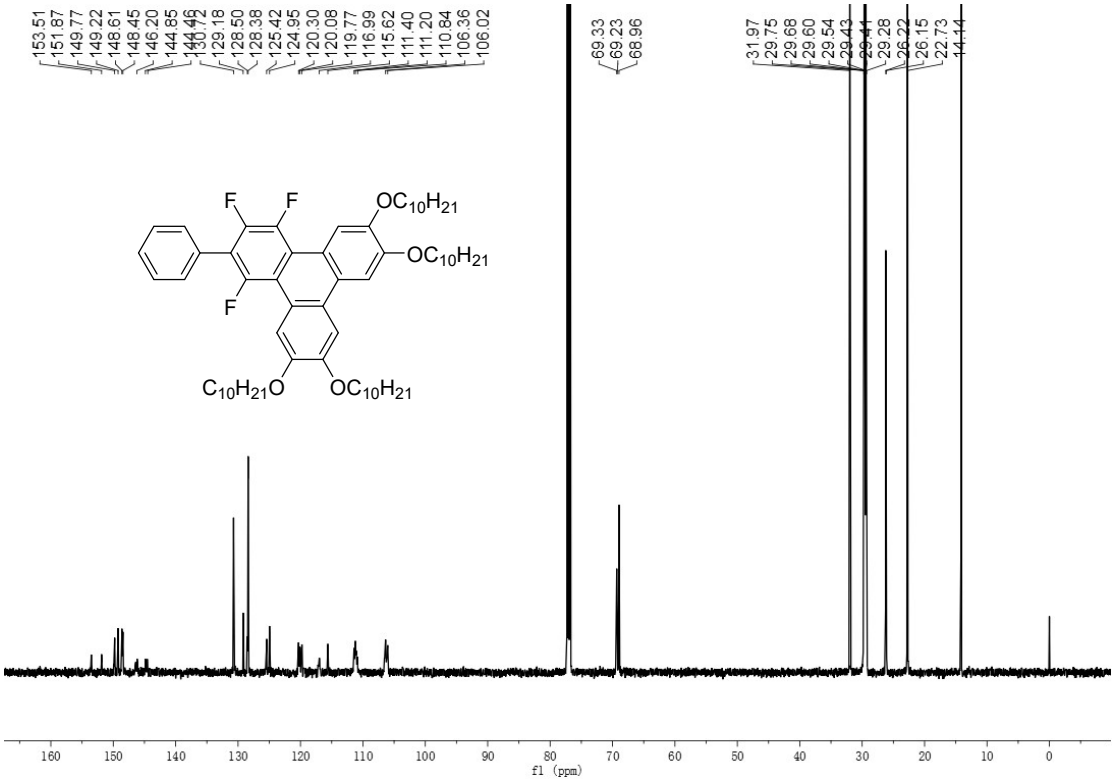

Figure S45 ^{13}C NMR ($CDCl_3$, 151 MHz) spectrum of **PH**10.

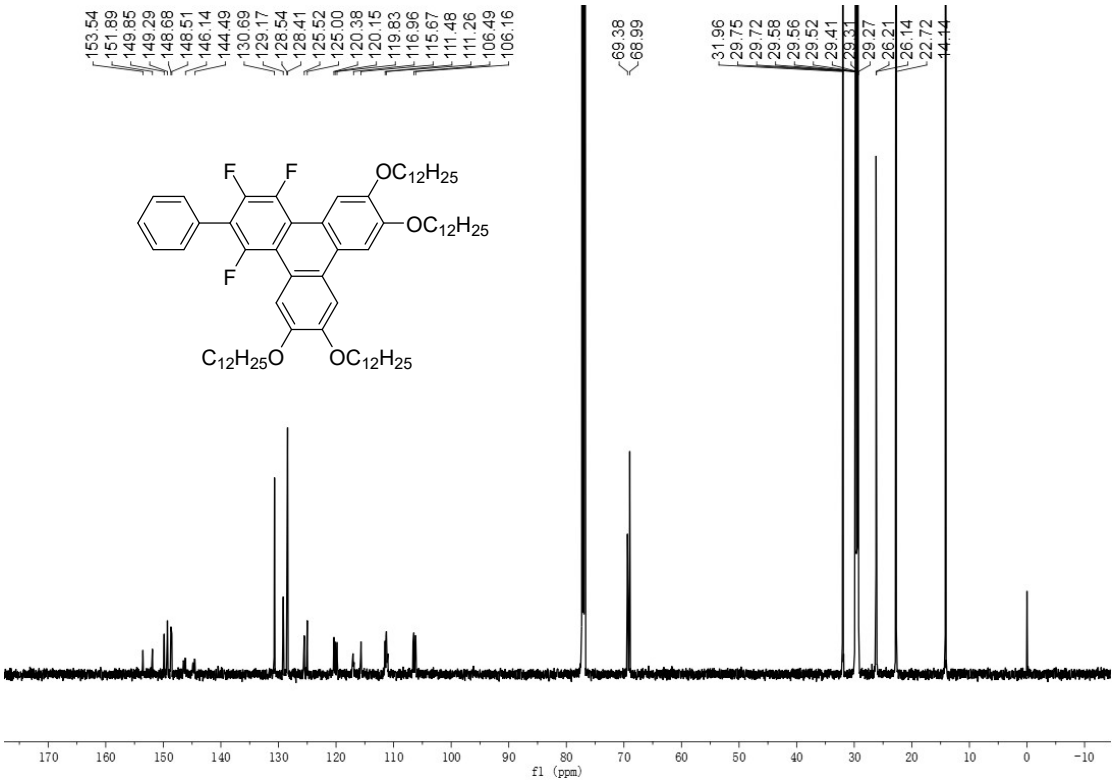

Figure S46 ^{13}C NMR ($CDCl_3$, 151 MHz) spectrum of **PH**12.

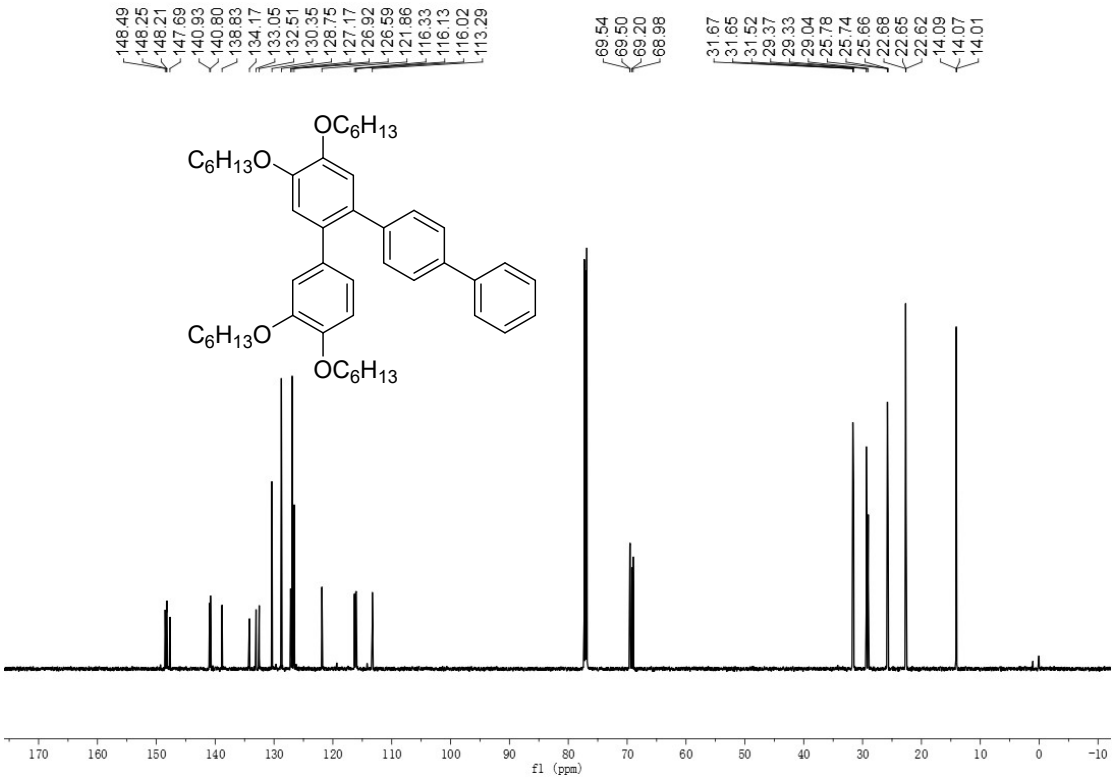

Figure S47 ^{13}C NMR ($CDCl_3$, 151 MHz) spectrum of **QP**6.

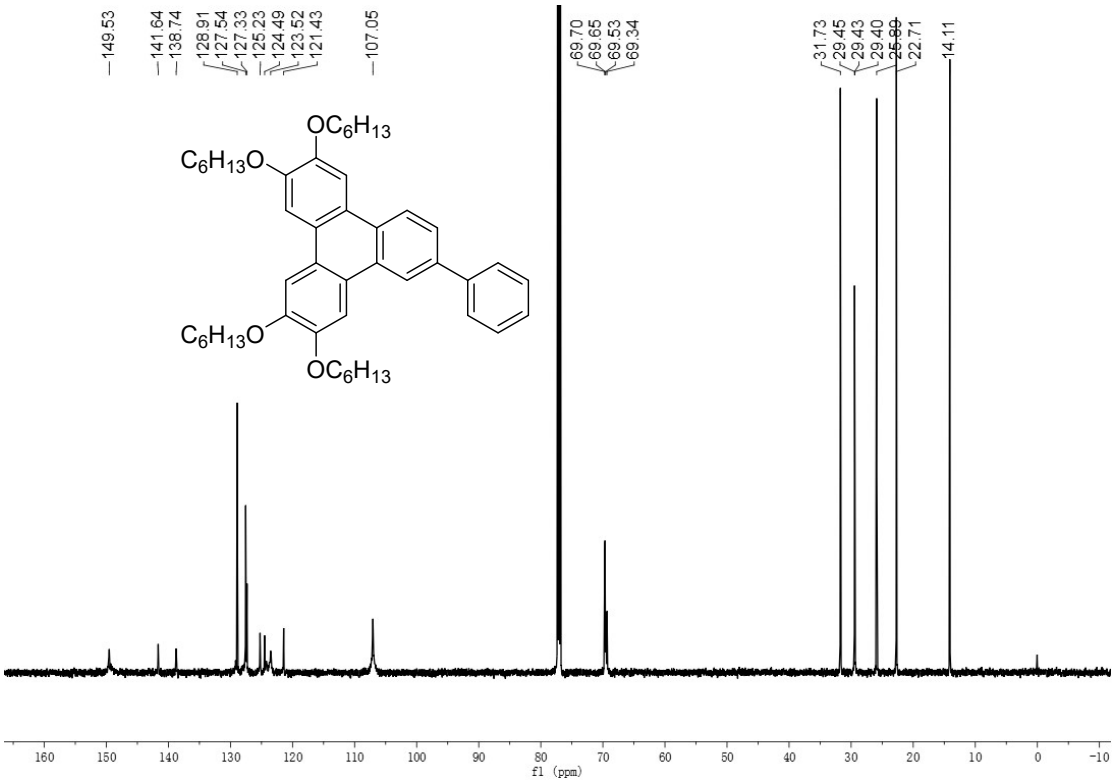

Figure S48 ^{13}C NMR ($CDCl_3$, 151 MHz) spectrum of **BTP**6.

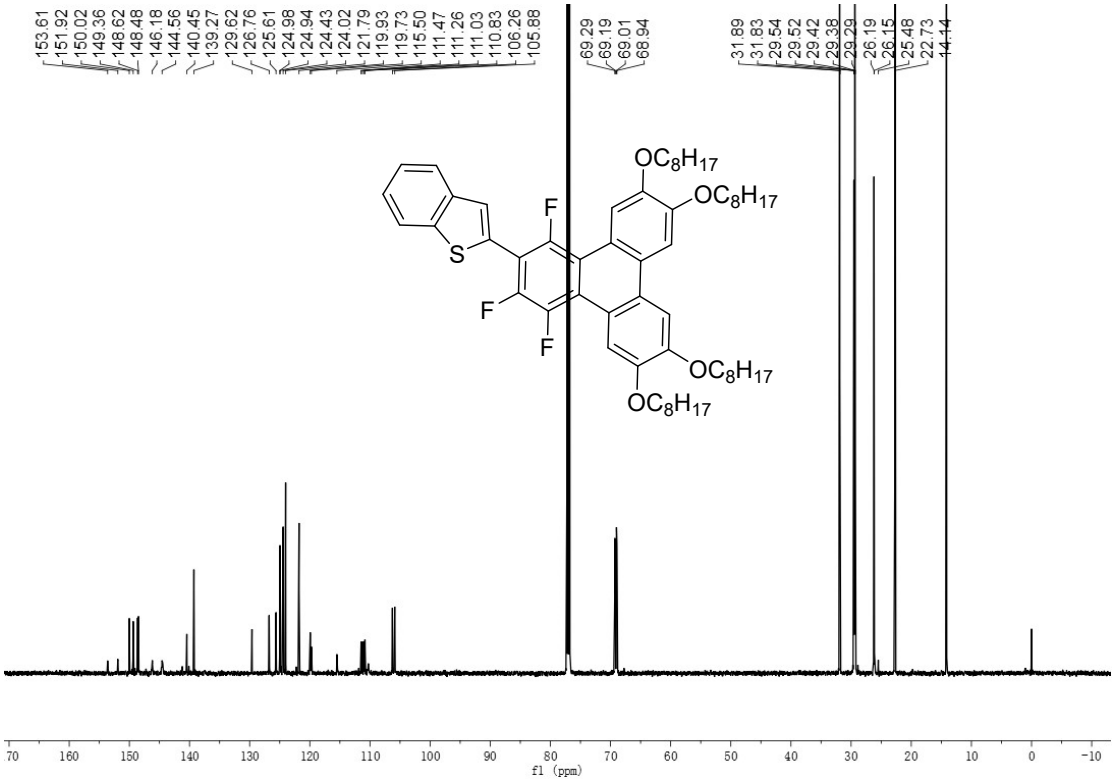

Figure S49 ^{13}C NMR ($CDCl_3$, 151 MHz) spectrum of **BT**8.

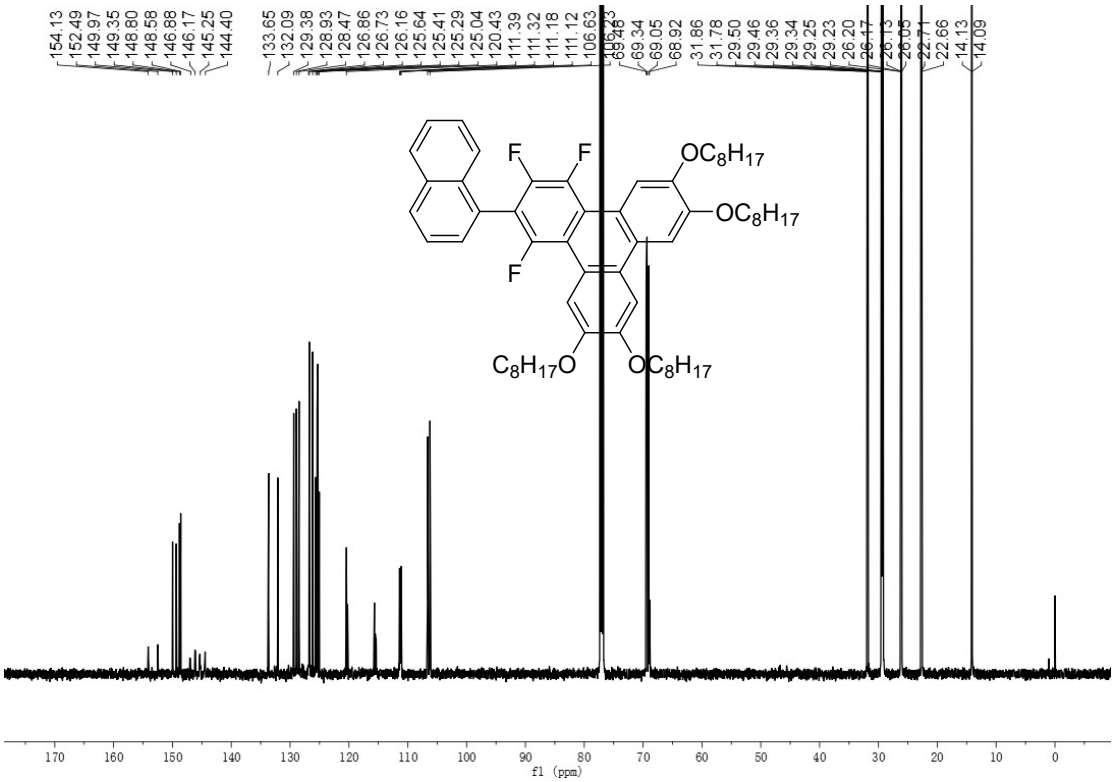

Figure S50 ^{13}C NMR ($CDCl_3$, 151 MHz) spectrum of **NAA**8.

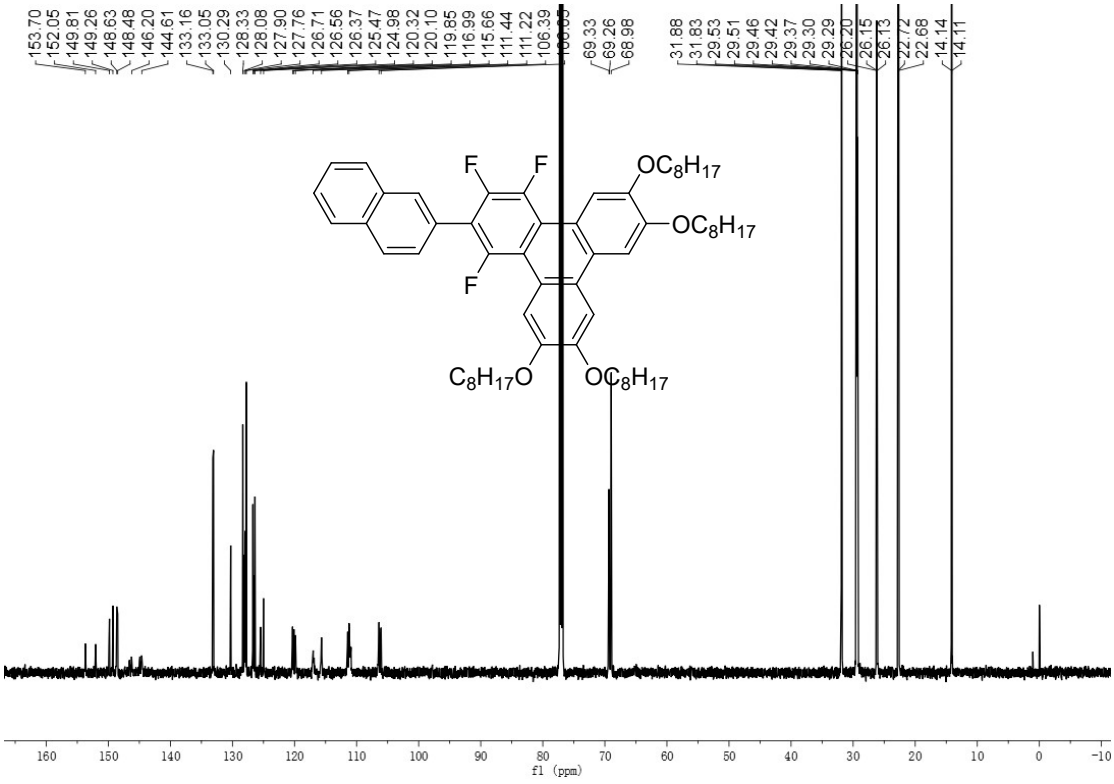

Figure S51 ^{13}C NMR ($CDCl_3$, 151 MHz) spectrum of **NAB**8.

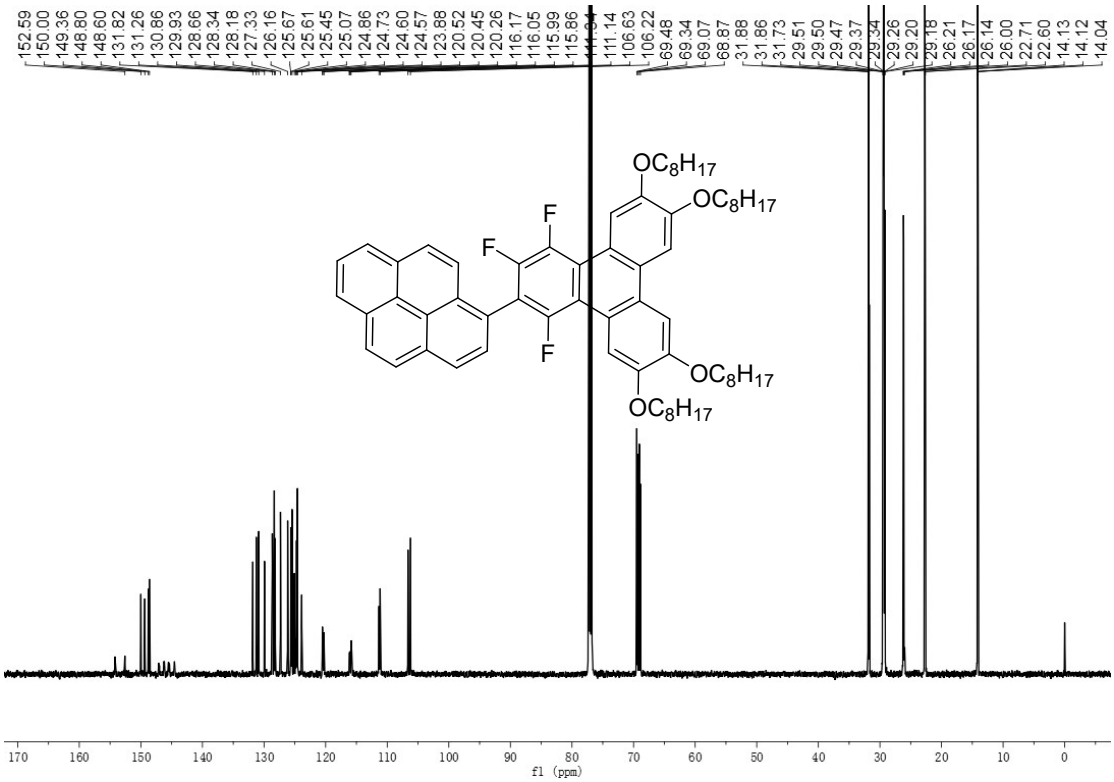

Figure S52 ^{13}C NMR ($CDCl_3$, 151 MHz) spectrum of **PY**8.

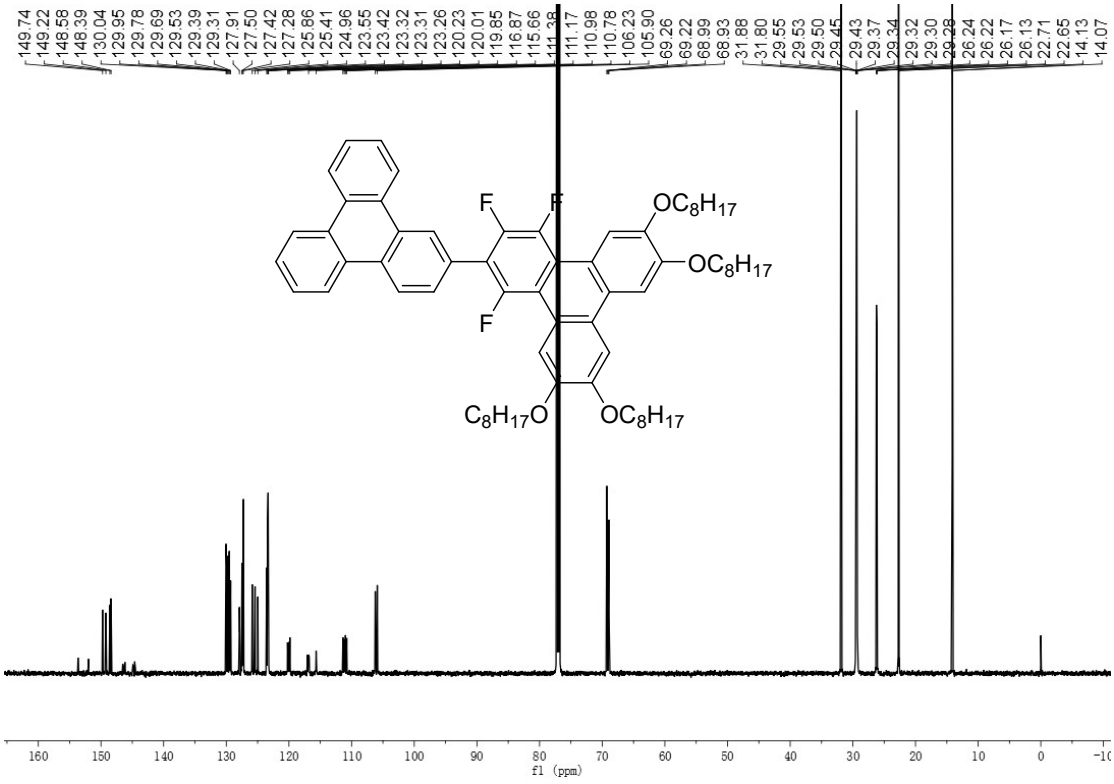

Figure S53 ^{13}C NMR ($CDCl_3$, 151 MHz) spectrum of **TP**8.

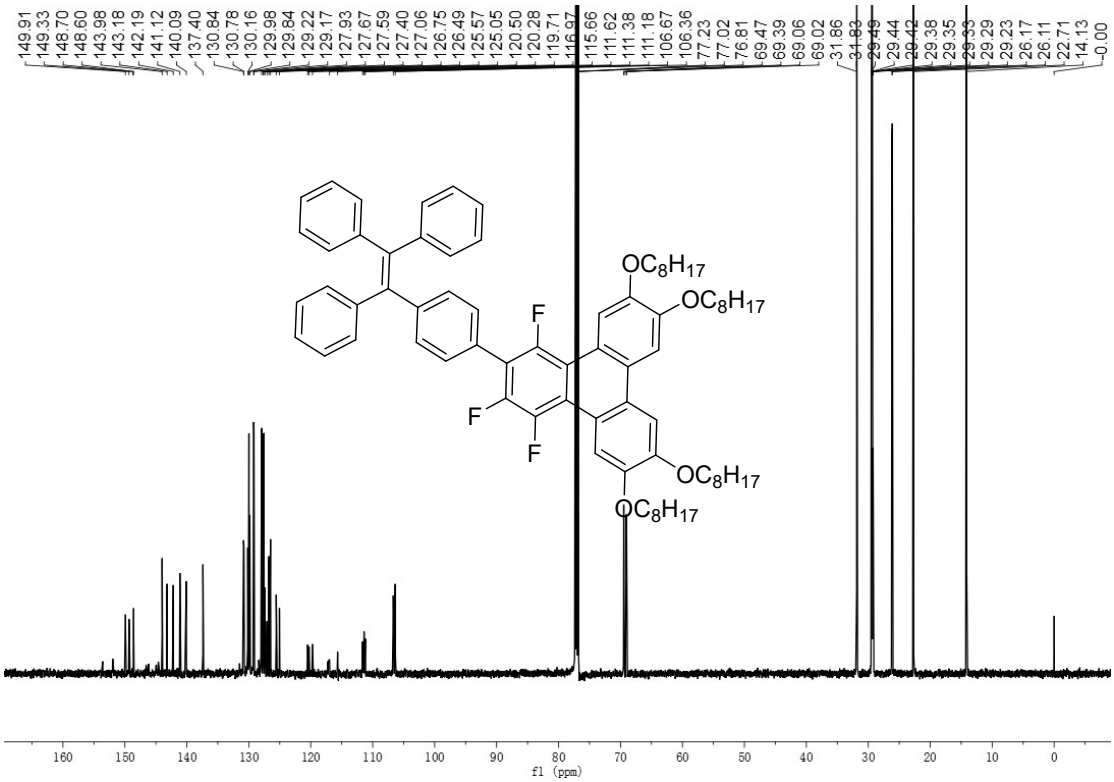

Figure S54 ^{13}C NMR ($CDCl_3$, 151 MHz) spectrum of **TPE**8.

4. HRMS

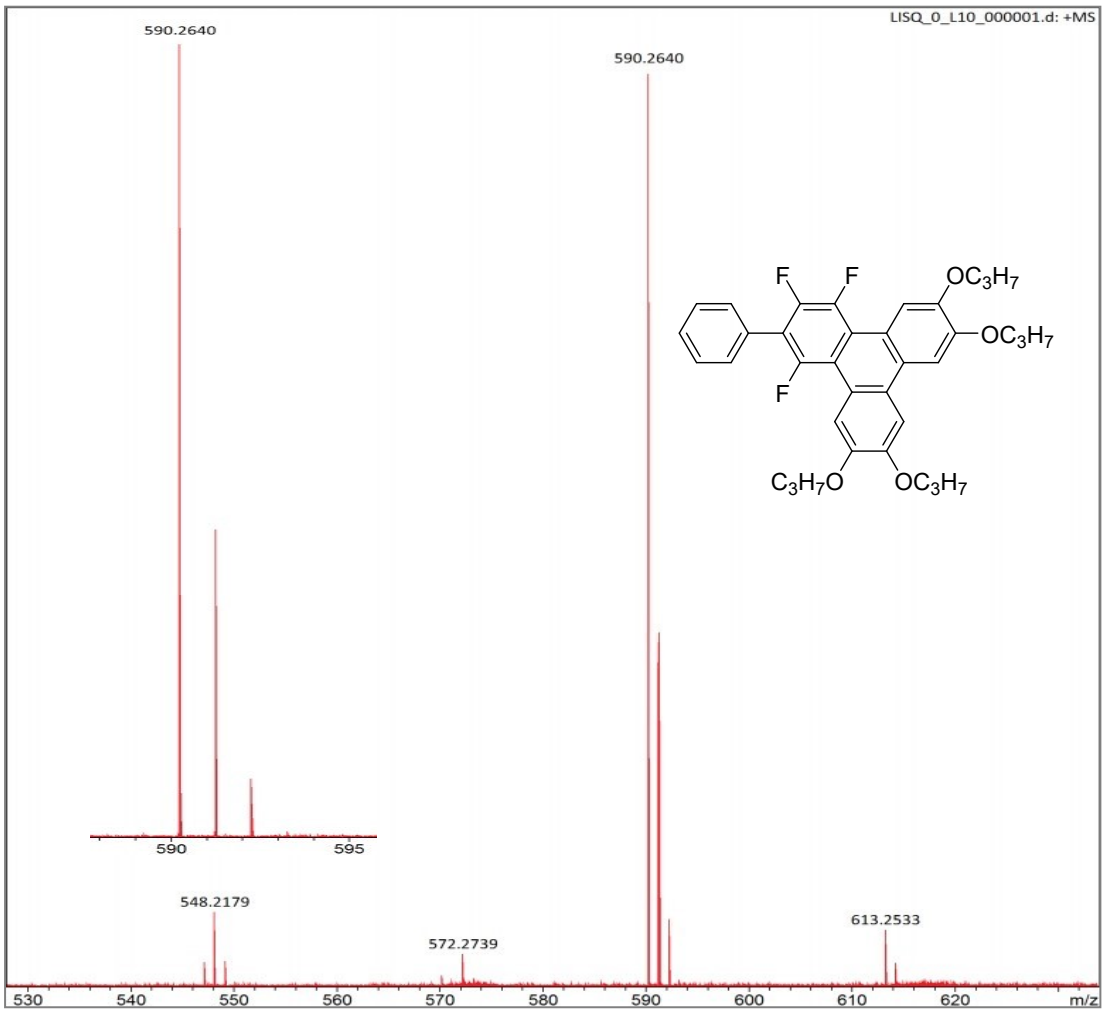

Figure S55 HRMS m/z (MALDI) spectrum of **PH**3.

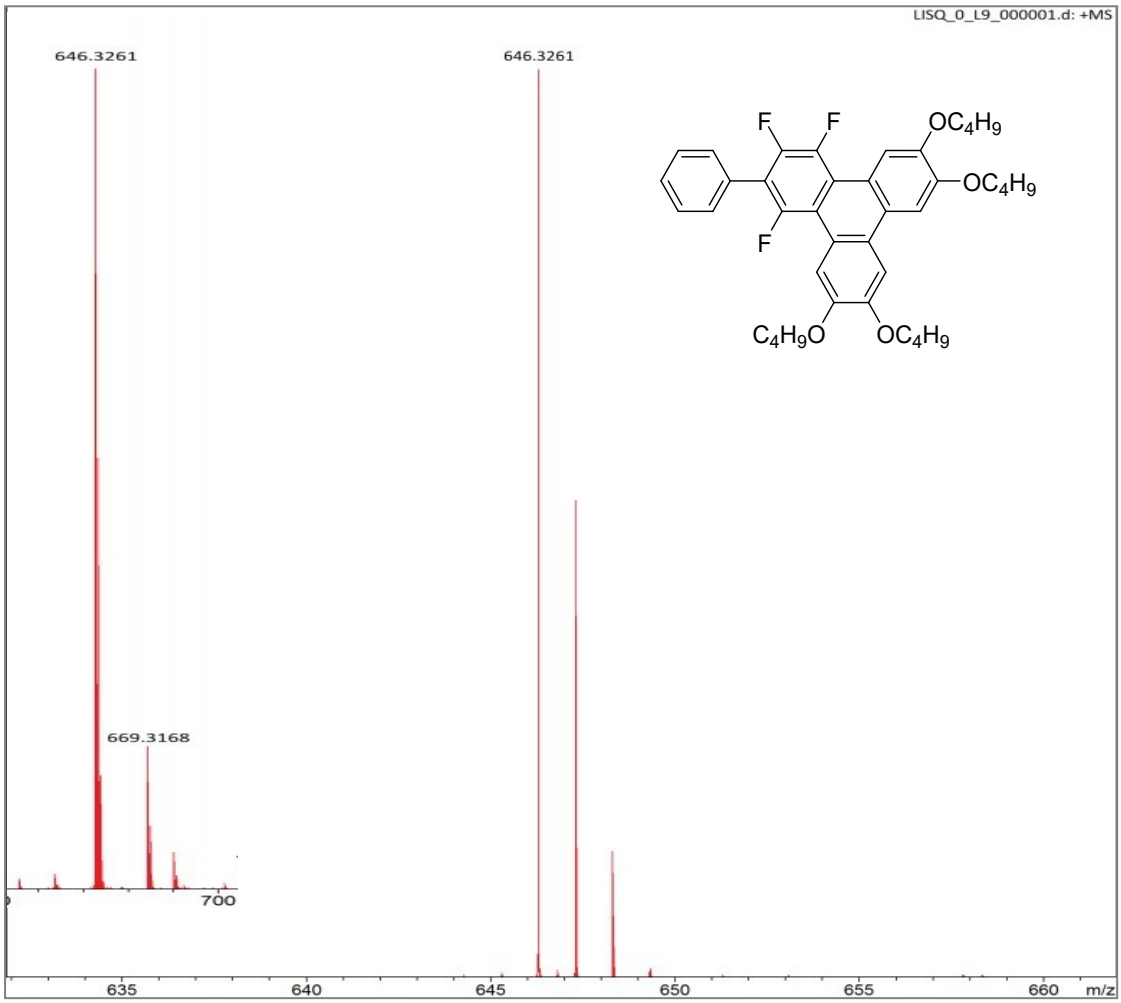

Figure S56 HRMS m/z (MALDI) spectrum of **PH**4.

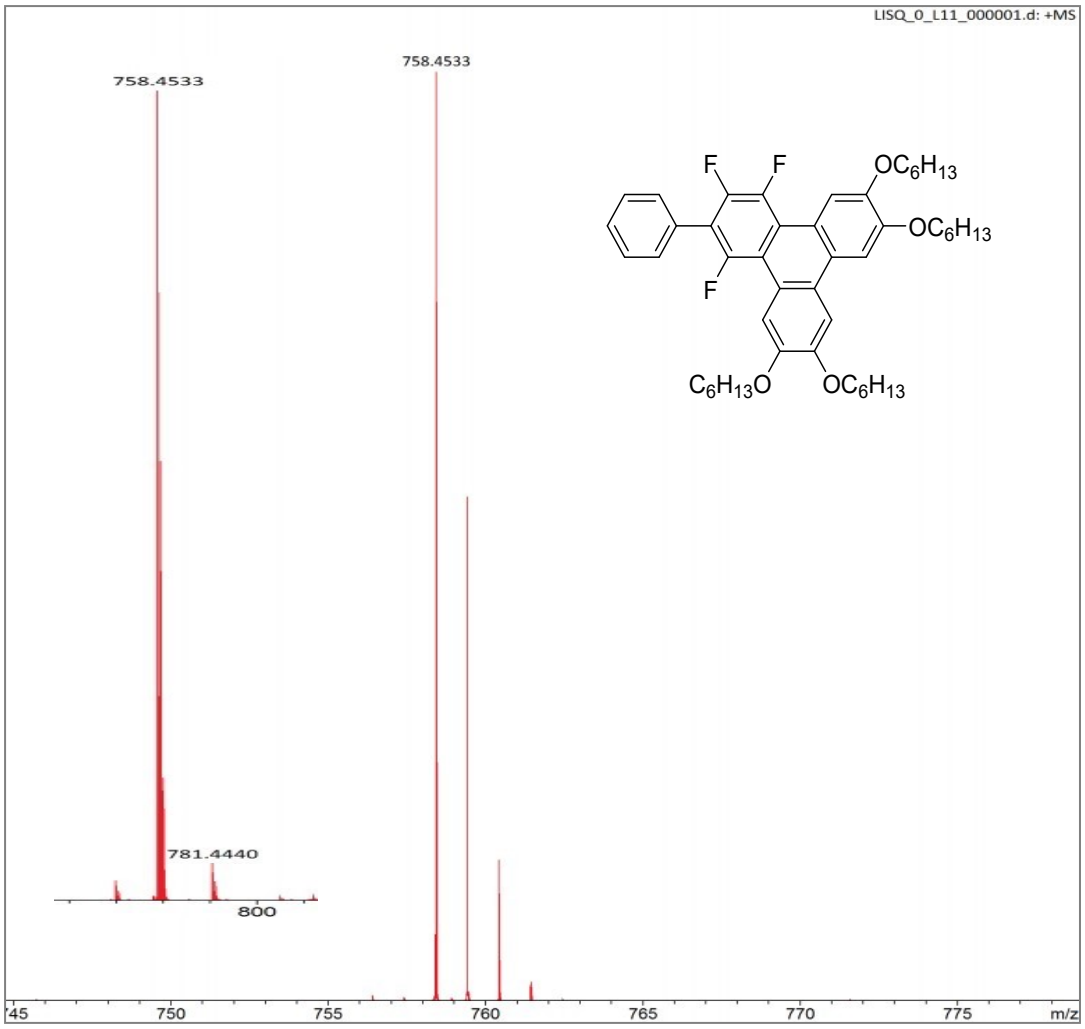

Figure S57 HRMS m/z (MALDI) spectrum of **PH**6.

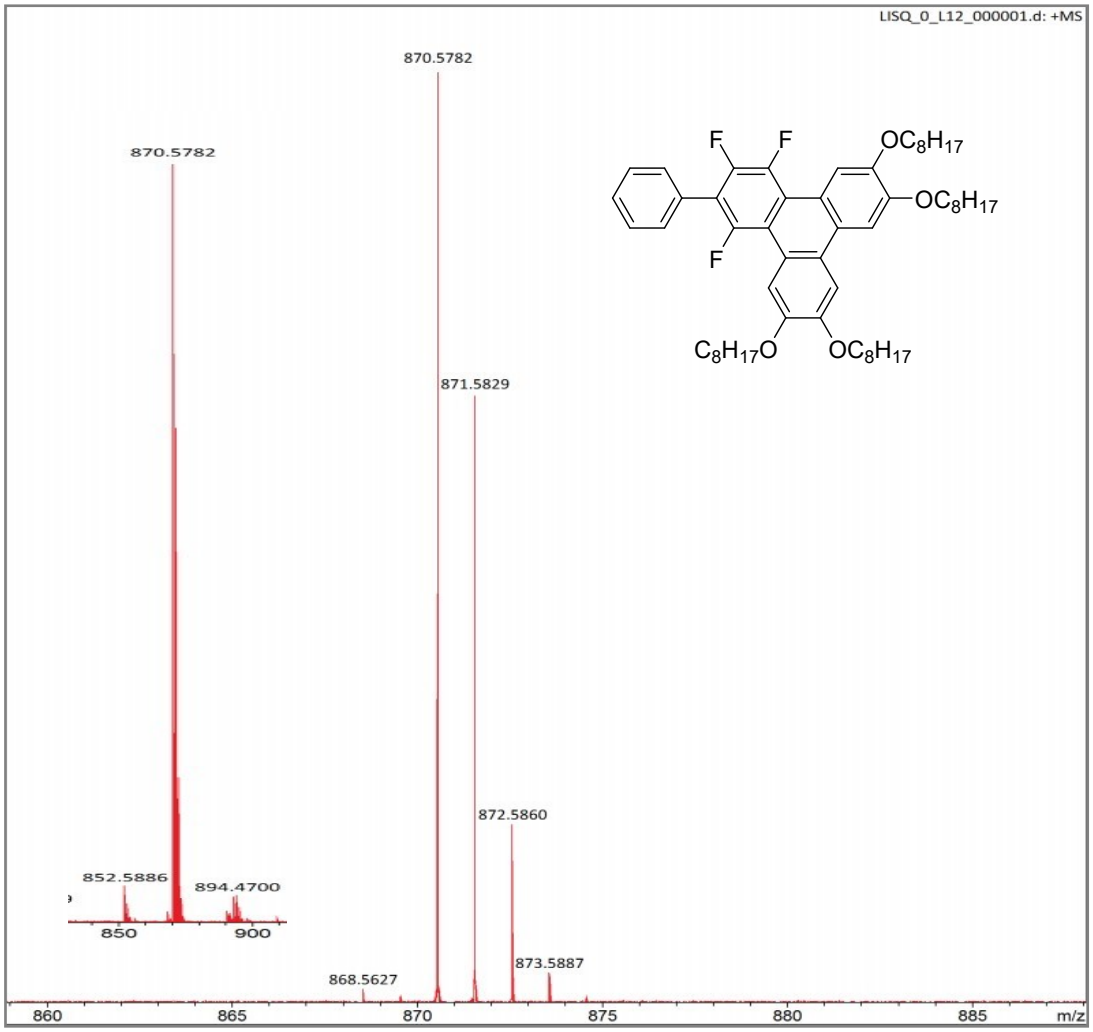

Figure S58 HRMS m/z (MALDI) spectrum of **PH**8.

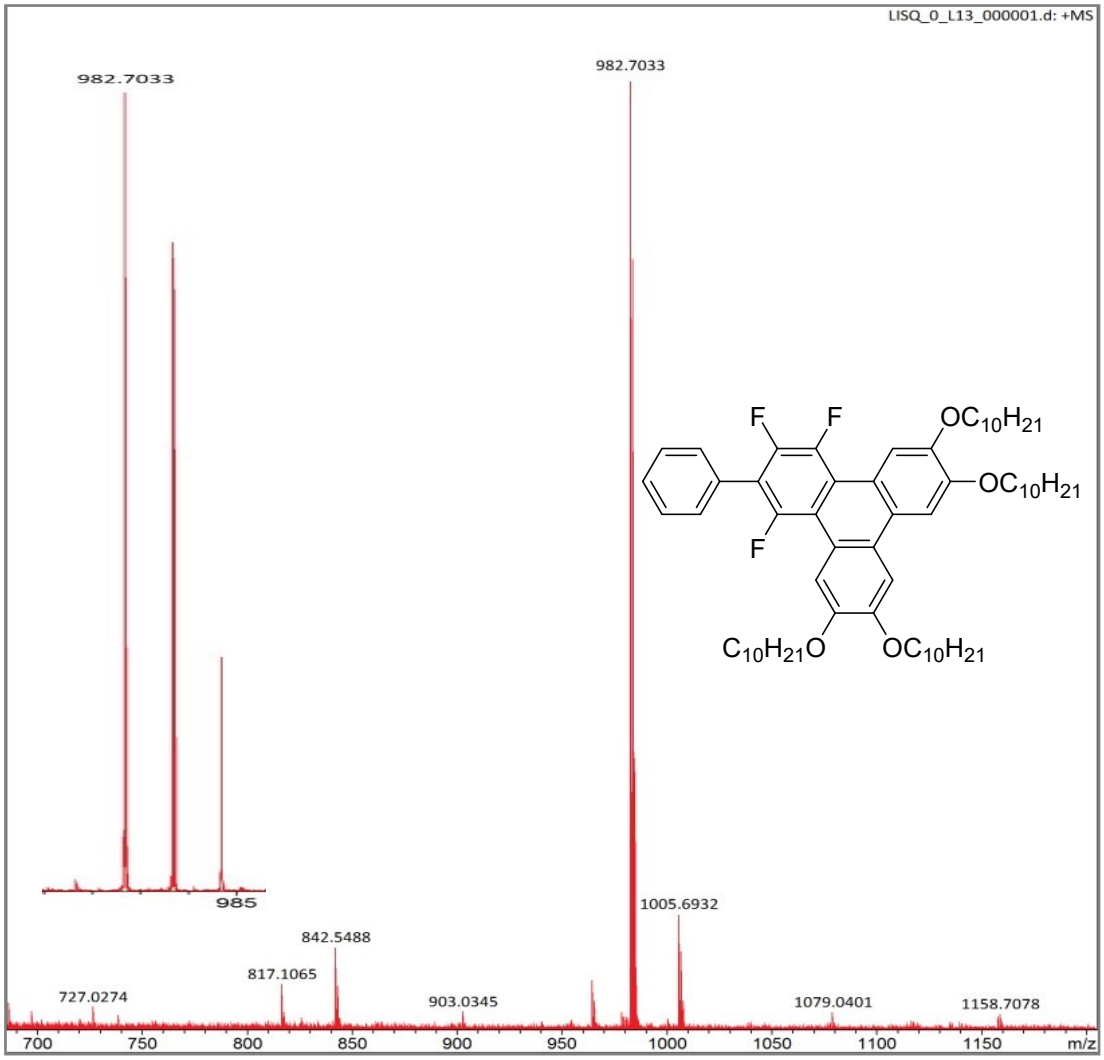

Figure S59 HRMS m/z (MALDI) spectrum of **PH**10.

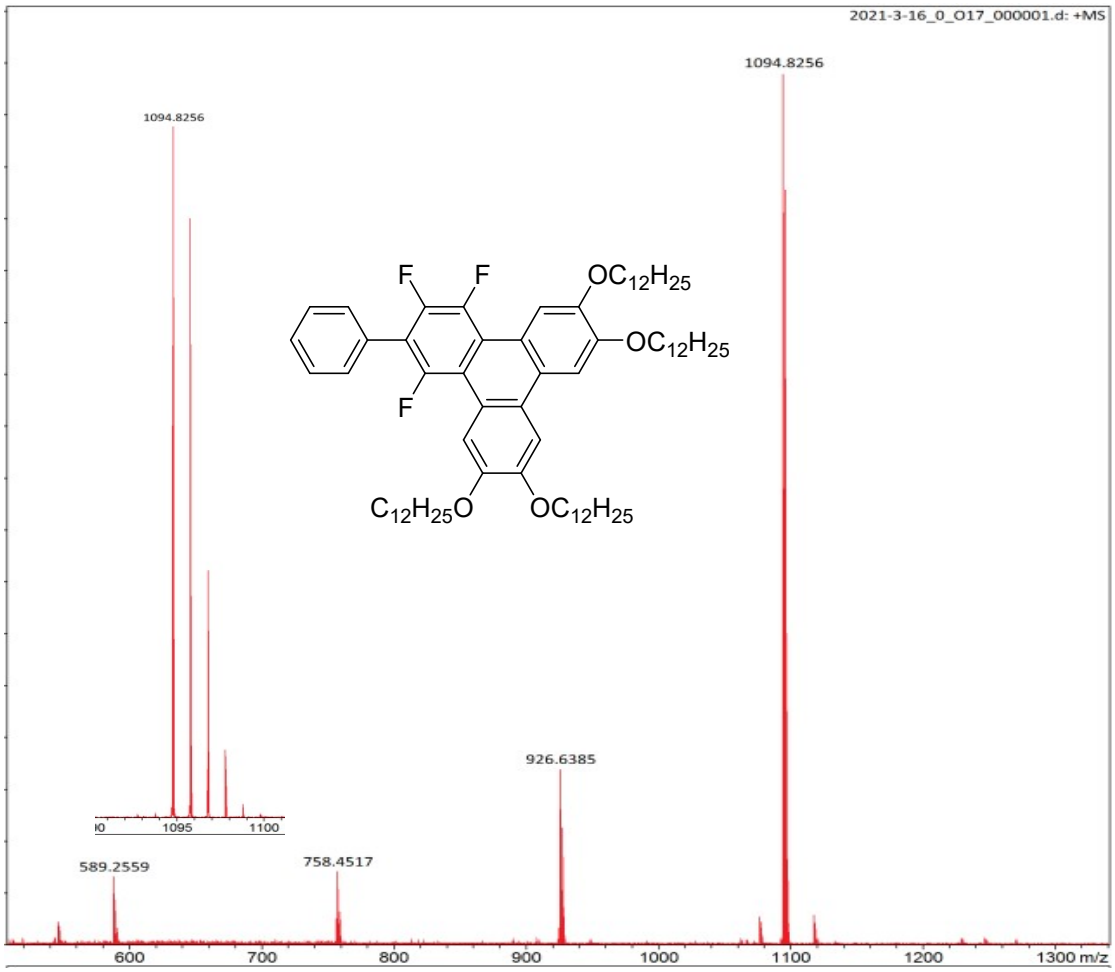

Figure S60 HRMS m/z (MALDI) spectrum of **PH**12.

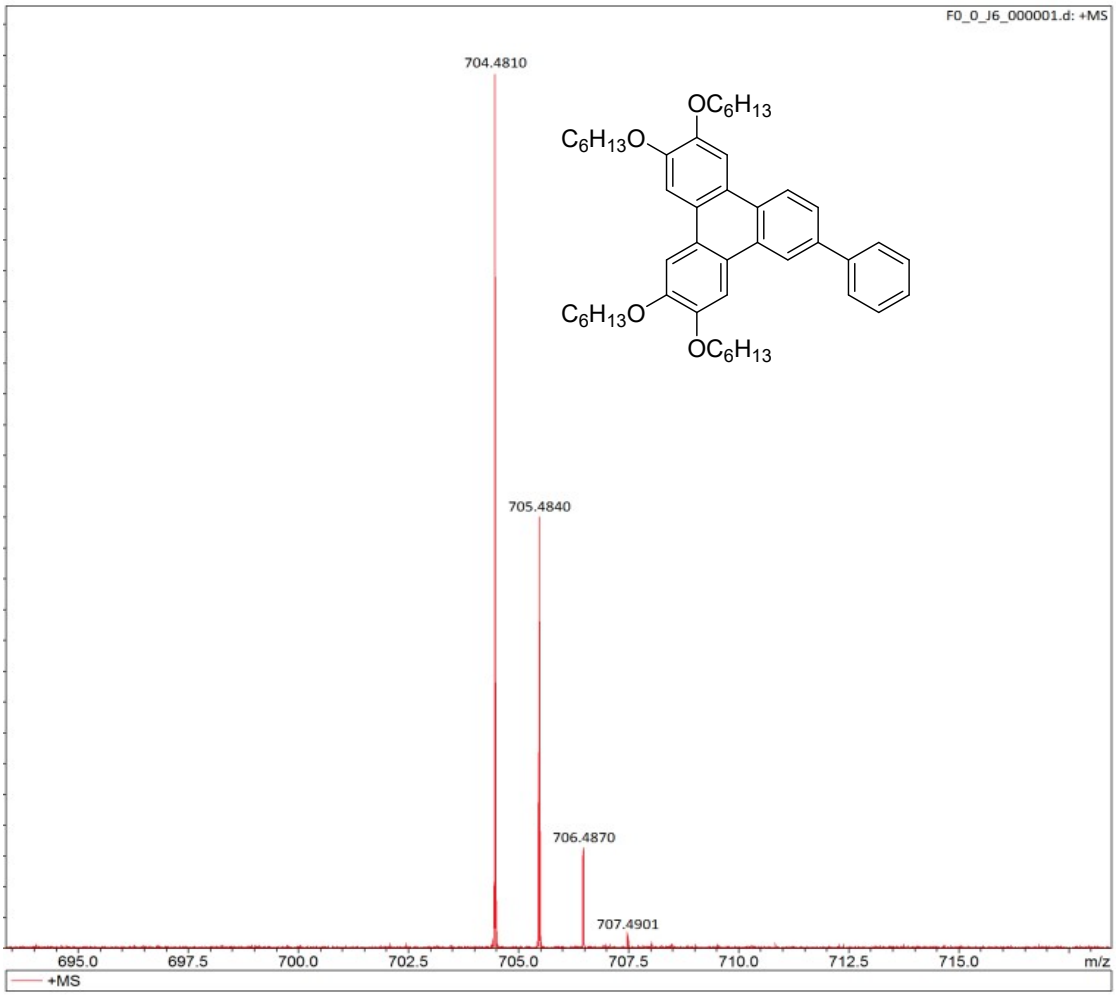

Figure S61 HRMS m/z (MALDI) spectrum of **BTP**6.

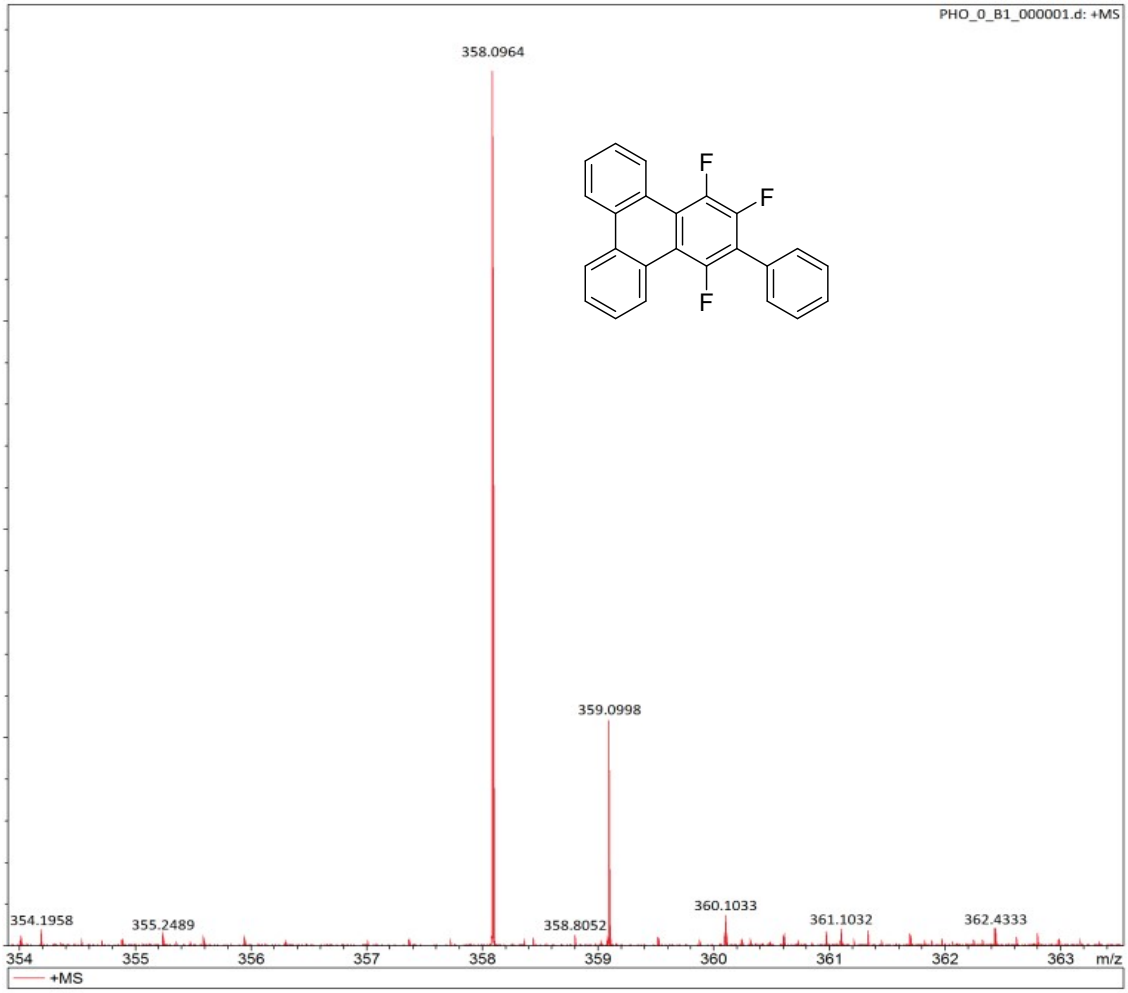

Figure S62 HRMS m/z (MALDI) spectrum of **PH**0.

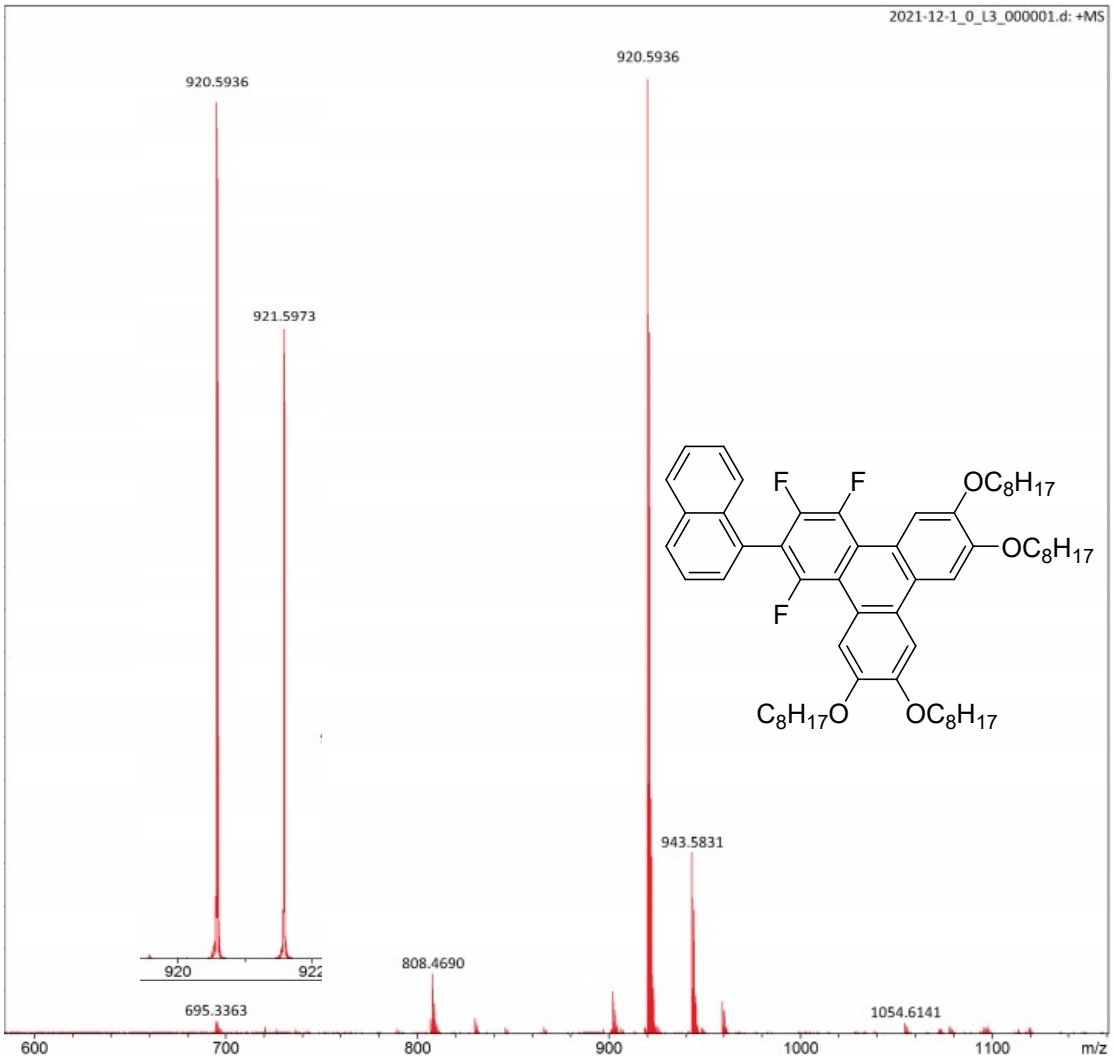

Figure S63 HRMS m/z (MALDI) spectrum of **NAA**8.

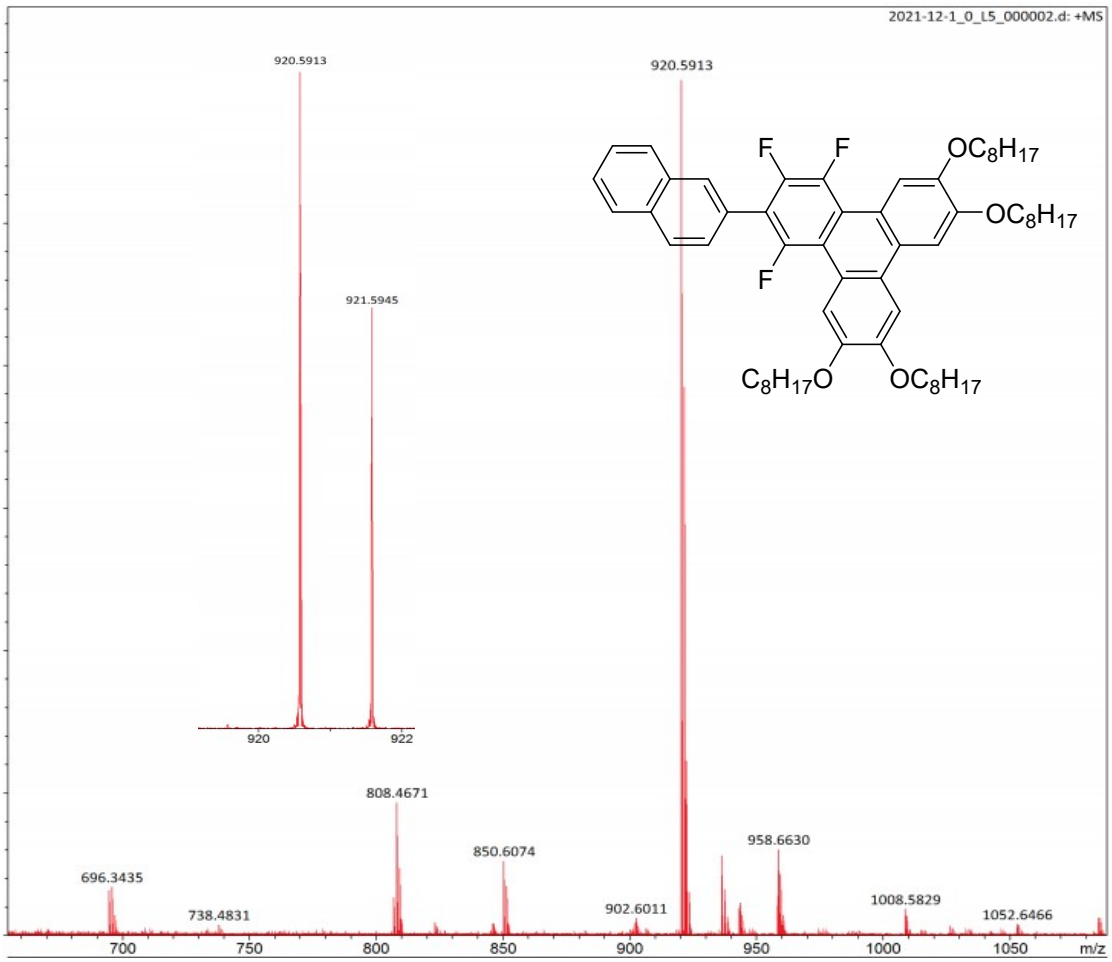

Figure S64 HRMS m/z (MALDI) spectrum of **NAB**8.

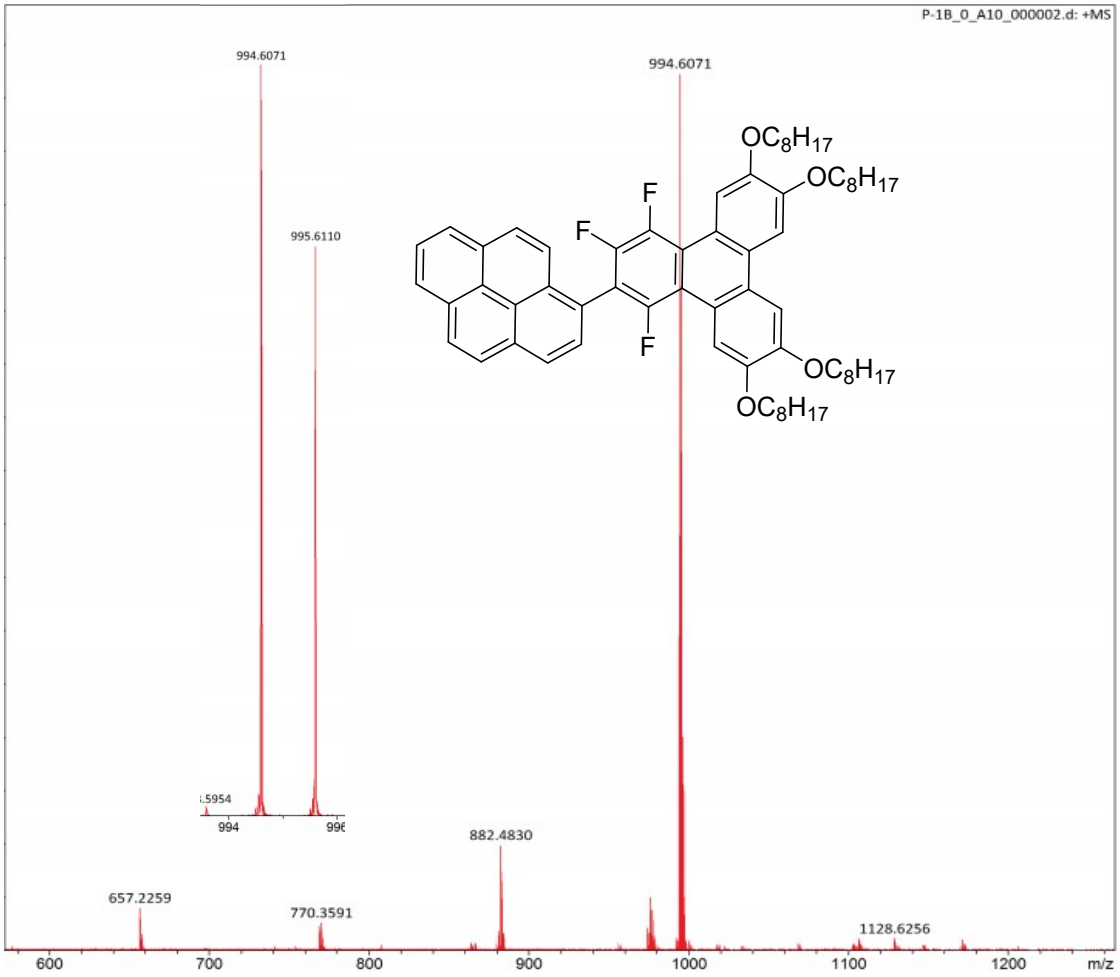

Figure S65 HRMS m/z (MALDI) spectrum of **PY**8.

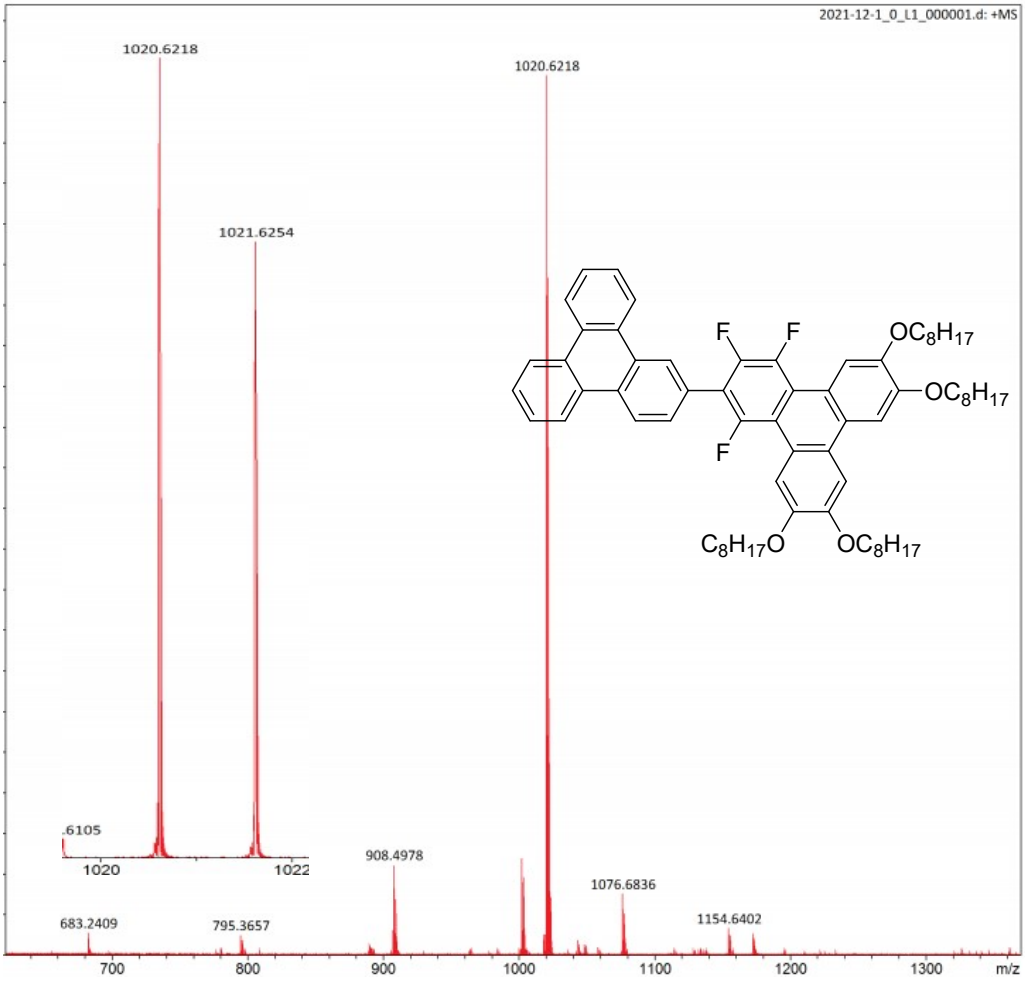

Figure S66 HRMS m/z (MALDI) spectrum of **TP**8.

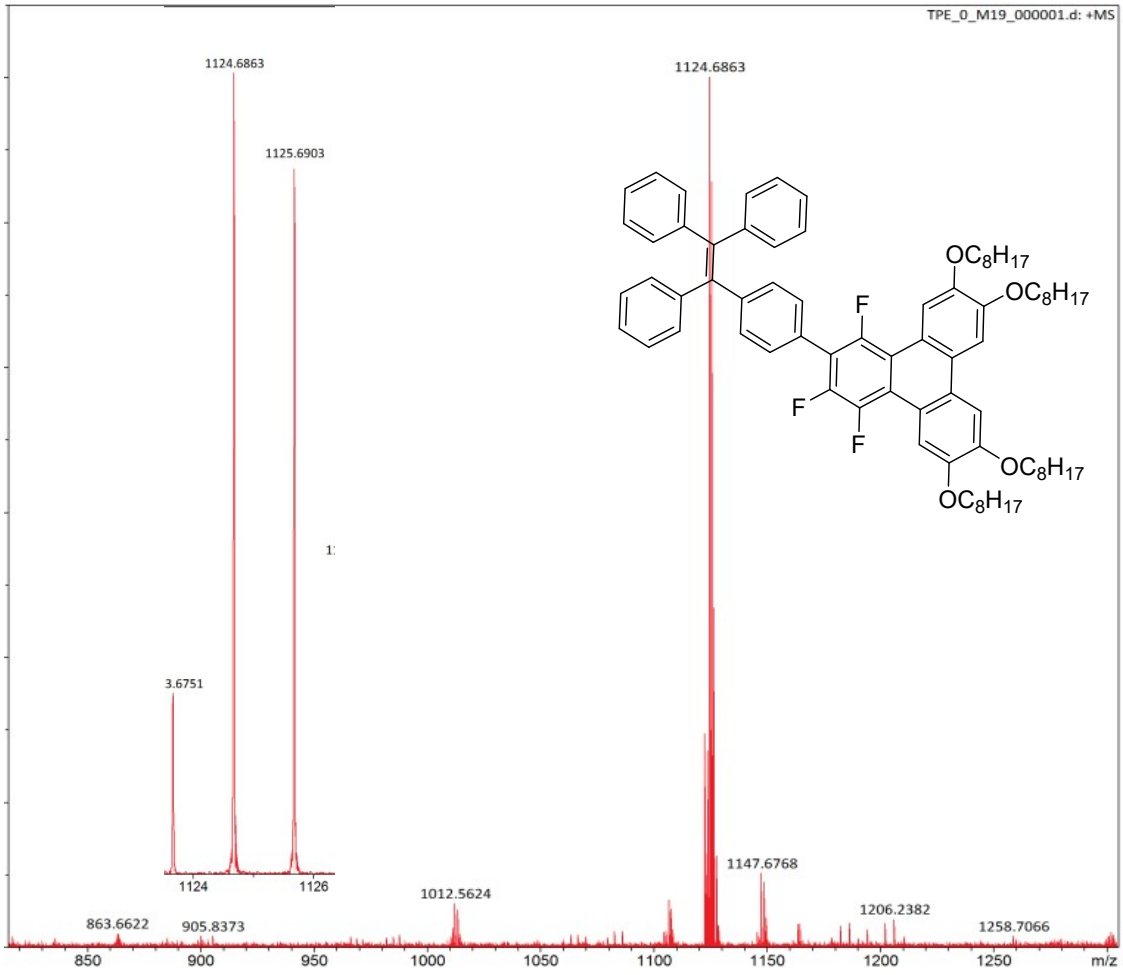

Figure S67 HRMS m/z (MALDI) spectrum of **TPE**8.

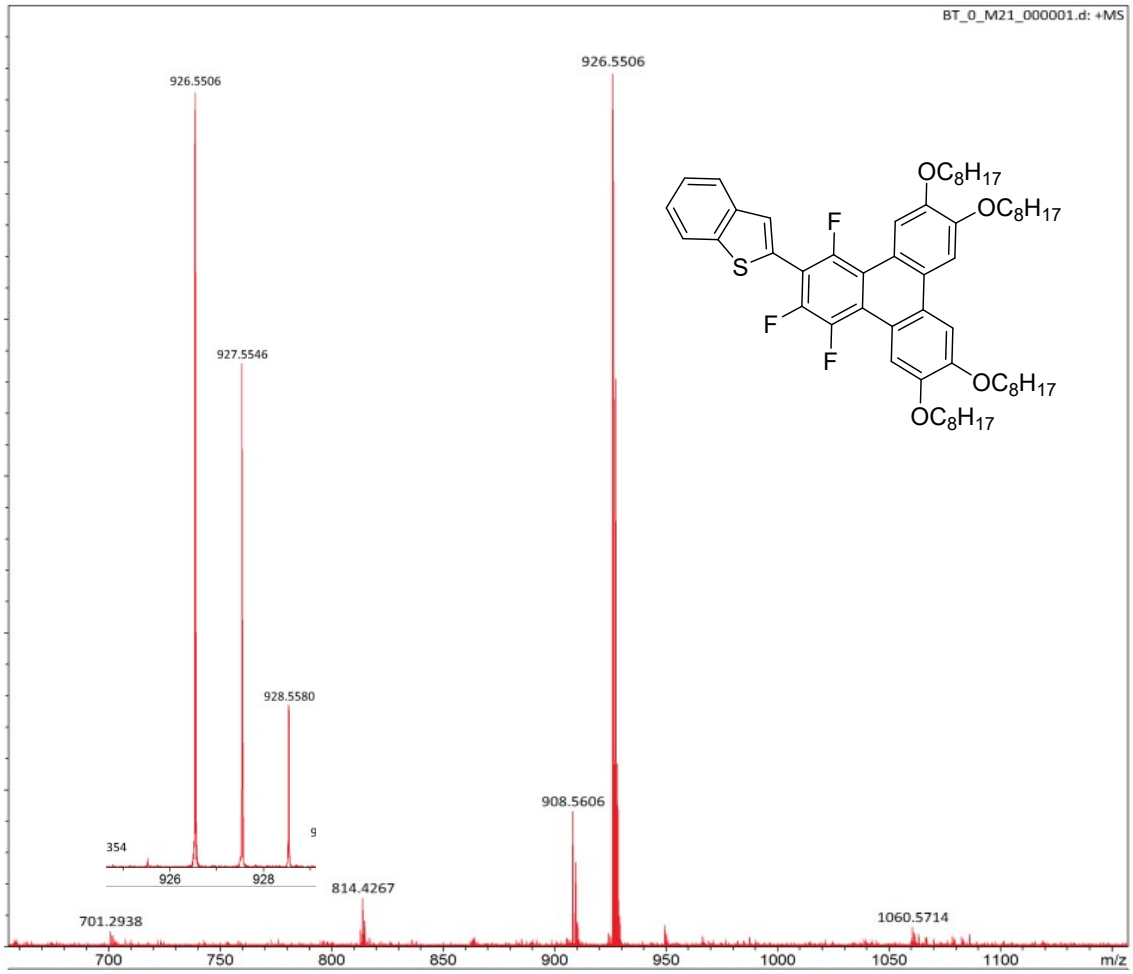

Figure S68 HRMS m/z (MALDI) spectrum of **BT**8.

5. X-ray Crystallography

Table S1. Crystal structure and refinement parameters of the compound **PH**0.

Compound	**PH**0
Empirical formula	$C_{24}H_{13}F_3$
Formula weight	358.34
Temperature/K	298.1(4)
Crystal system	monoclinic
Space group	$P2_1/n$
a/Å	13.2645(2)
b/Å	5.52840(10)
c/Å	22.7571(3)
α/°	90
β/°	102.6510(10)
γ/°	90
Volume/Å^3	1628.30(4)
Z	4
ρ_{calc}g/cm^3	1.462
μ/mm^{-1}	0.899
F(000)	736.0
Crystal size/mm^3	0.15 × 0.14 × 0.12
Radiation	CuKα (λ = 1.54184)
2Θ range for data collection/°	7.112 to 152.552
Index ranges	-16 ≤ h ≤ 16, -5 ≤ k ≤ 6, -27 ≤ l ≤ 28
Reflections collected	15594
Independent reflections	3314 [R_{int} = 0.0383, R_{sigma} = 0.0259]
Data/restraints/parameters	3314/0/244
Goodness-of-fit on F^2	1.035
Final R indexes [I>=2σ (I)]	R_1 = 0.0439, wR_2 = 0.1189
Final R indexes [all data]	R_1 = 0.0535, wR_2 = 0.1265
Largest diff. peak/hole / e Å^{-3}	0.17/-0.21
CCDC Deposition Number	2283240

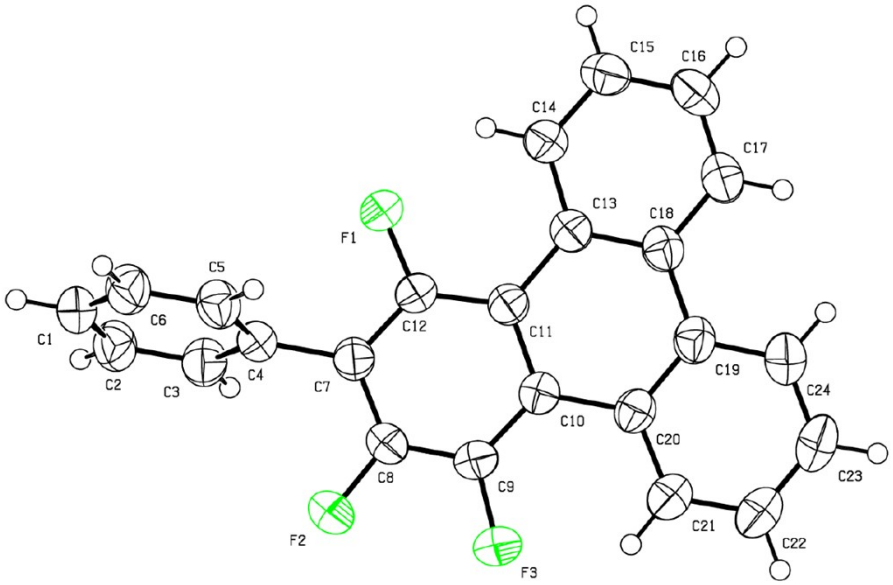

Figure S69 Atoms' numbering in **PH**0.

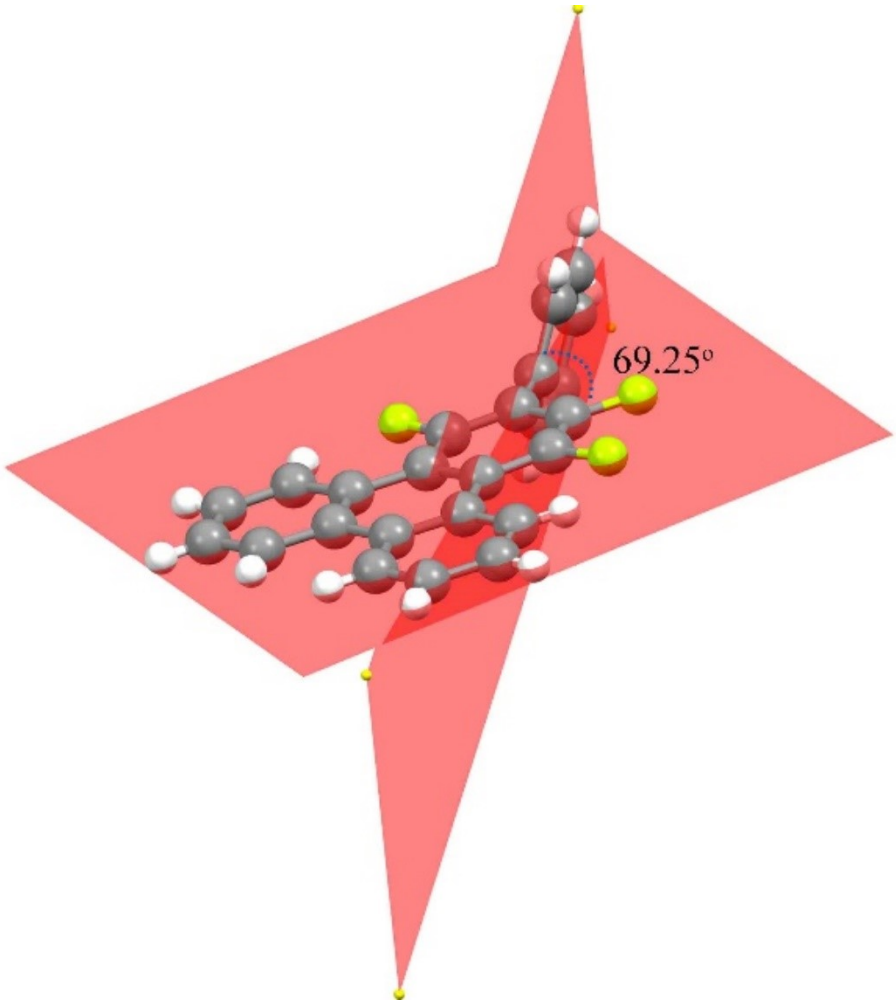

a

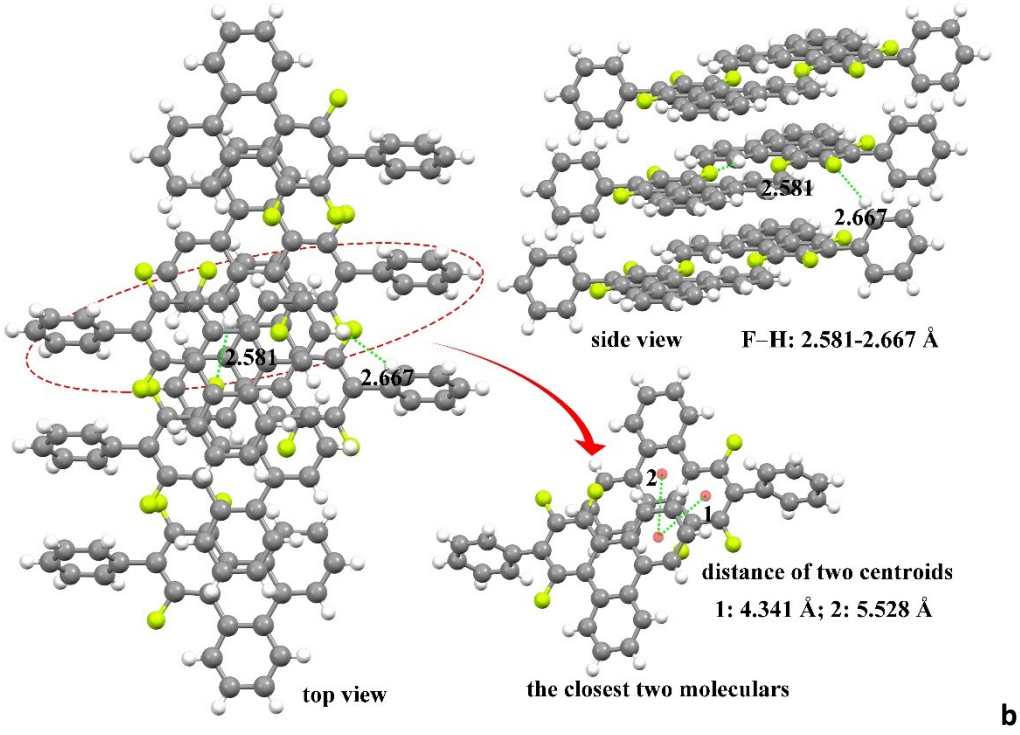

Figure S70 a) Torsional angle between triphenylene core and phenyl group in **PH**0 is 69.25°. The triphenylene moiety is perfectly planar, and all atoms of the TP core lie in one surface; b) Different views of molecular packing.

Table S2. Fractional atomic coordinates （A×104）and the equivalent isotropic displacement parameter (A2×103) of the compound **PH**0.

Atom	*x*	*y*	*z*	U(eq)
F2	3193.7(7)	1447.1(17)	6152.5(4)	66.2(3)
F3	4083.0(8)	1434.8(18)	5255.1(5)	69.6(3)
F1	1189.1(8)	8109.1(18)	5402.6(4)	73.6(3)
C10	3144.1(9)	4907(2)	4786.9(6)	40.3(3)
C4	1691.5(10)	4846(2)	6326.1(6)	42.9(3)
C13	2060.4(10)	8470(2)	4347.8(6)	41.4(3)
C11	2367.6(10)	6654(2)	4824.7(6)	40.2(3)
C20	3653.6(10)	4955(2)	4272.4(6)	43.0(3)
C7	2169.9(10)	4838(2)	5790.5(6)	43.2(3)
C8	2906.7(11)	3154(2)	5725.8(6)	46.0(3)
C18	2543.4(11)	8462(2)	3851.0(6)	45.4(3)
C9	3374.7(10)	3190(2)	5247.0(7)	45.9(3)
C12	1928.9(11)	6511(2)	5334.5(6)	45.2(3)
C19	3350.4(11)	6691(3)	3818.7(6)	48.4(3)
C14	1301.2(11)	10251(3)	4352.9(6)	49.6(3)
C5	1913.9(12)	6686(3)	6747.0(7)	51.5(3)

C1	822.8(12)	4852(3)	7329.7(7)	55.2(4)
C3	1027.8(12)	3011(3)	6412.6(7)	52.7(4)
C15	1032.1(12)	11927(3)	3902.6(7)	54.5(4)
C6	1486.9(13)	6674(3)	7251.0(7)	56.4(4)
C21	4436.1(12)	3306(3)	4216.6(7)	55.3(4)
C16	1510.4(12)	11912(3)	3421.0(7)	58.0(4)
C2	590.9(13)	3034(3)	6909.9(7)	57.5(4)
C17	2243.2(12)	10211(3)	3397.9(7)	57.8(4)
C22	4894.6(14)	3354(3)	3730.7(8)	64.9(4)
C24	3843.1(16)	6687(3)	3330.2(8)	70.1(5)
C23	4595.7(16)	5055(4)	3286.4(9)	75.5(5)

Table S3. anisotropic displacement parameters of the compound **PH0**(A2×103).

Atom	**U_{11}**	**U_{22}**	**U_{33}**	**U_{23}**	**U_{13}**	**U_{12}**
F2	75.2(6)	63.3(6)	65.8(6)	26.9(4)	27.9(5)	21.7(5)
F3	73.1(6)	67.3(6)	77.0(6)	21.4(5)	34.8(5)	33.7(5)
F1	97.8(7)	72.1(6)	63.2(6)	20.1(5)	44.1(5)	44.3(6)
C10	40.6(6)	40.4(7)	40.1(7)	-3.2(5)	9.2(5)	-3.3(5)
C4	48.9(7)	41.5(7)	39.5(7)	4.3(5)	11.9(5)	4.2(5)
C13	46.2(6)	38.6(7)	38.2(7)	-3.0(5)	6.8(5)	-2.9(5)
C11	44.6(6)	37.5(6)	38.6(7)	-2.9(5)	9.1(5)	-0.7(5)
C20	43.7(7)	43.9(7)	42.7(7)	-5.7(6)	12.0(5)	-2.8(5)
C7	48.1(7)	41.3(7)	41.7(7)	0.0(5)	13.0(5)	-0.9(5)
C8	50.4(7)	42.9(7)	45.6(8)	9.5(6)	12.1(6)	3.7(6)
C18	50.7(7)	44.9(7)	40.7(7)	-0.4(6)	10.3(6)	-3.8(6)
C9	43.9(6)	44.0(7)	51.1(8)	2.4(6)	13.0(6)	8.1(6)
C12	51.8(7)	41.5(7)	44.6(7)	-0.3(6)	15.5(6)	8.3(6)
C19	55.2(7)	48.9(8)	43.2(7)	-3.6(6)	15.4(6)	-3.5(6)
C14	54.1(8)	49.6(8)	45.1(8)	2.8(6)	10.9(6)	7.0(6)
C5	60.4(8)	46.3(8)	49.1(8)	-0.1(6)	14.8(6)	-7.1(6)
C1	65.8(9)	60.0(9)	44.6(8)	7.5(7)	22.4(7)	9.5(7)
C3	64.8(9)	43.2(7)	53.3(8)	-4.3(6)	20.1(7)	-4.5(6)
C15	56.0(8)	49.4(8)	55.4(9)	5.1(7)	6.4(7)	8.0(6)
C6	73.1(10)	53.2(8)	44.0(8)	-5.6(6)	15.5(7)	0.0(7)
C21	55.5(8)	58.9(9)	54.5(9)	-2.1(7)	18.8(7)	8.0(7)
C16	62.9(9)	56.0(9)	52.4(9)	16.1(7)	6.8(7)	2.9(7)
C2	67.6(9)	50.3(8)	60.9(9)	5.4(7)	28.1(7)	-5.9(7)
C17	63.4(9)	64.4(9)	48.1(8)	10.4(7)	17.7(7)	1.5(8)
C22	66.4(9)	70.7(11)	64.2(10)	-8.1(8)	28.7(8)	10.5(8)
C24	91.4(12)	72.8(11)	54.9(10)	11.0(8)	35.0(9)	14.6(10)

C23	89.8(13)	86.3(13)	63.4(10)	-1.8(10)	44.9(9)	11.3(11)

Table S4. The bond length of the compound **PH**0.

Atom	Atom	Length/Å	Atom	Atom	Length/Å
F2	C8	1.3476(15)	C7	C12	1.3742(19)
F3	C9	1.3479(15)	C8	C9	1.367(2)
F1	C12	1.3544(15)	C18	C19	1.464(2)
C10	C11	1.4280(18)	C18	C17	1.406(2)
C10	C20	1.4746(18)	C19	C24	1.408(2)
C10	C9	1.3968(19)	C14	C15	1.370(2)
C4	C7	1.4925(18)	C5	C6	1.386(2)
C4	C5	1.384(2)	C1	C6	1.375(2)
C4	C3	1.385(2)	C1	C2	1.375(2)
C13	C11	1.4692(19)	C3	C2	1.380(2)
C13	C18	1.4163(19)	C15	C16	1.381(2)
C13	C14	1.4101(19)	C21	C22	1.374(2)
C11	C12	1.4096(19)	C16	C17	1.362(2)
C20	C19	1.403(2)	C22	C23	1.374(3)
C20	C21	1.4077(19)	C24	C23	1.366(3)
C7	C8	1.3812(19)			

Table S5. The bond angle of the compound **PH**0.

Atom	Atom	Atom	Angle/˚		Atom	Atom	Atom	Angle/˚
C11	C10	C20	119.85(12)		C17	C18	C19	121.05(13)
C9	C10	C11	117.18(12)		F3	C9	C10	122.49(12)
C9	C10	C20	122.96(12)		F3	C9	C8	114.53(12)
C5	C4	C7	120.20(12)		C8	C9	C10	122.98(12)
C5	C4	C3	119.06(13)		F1	C12	C11	119.85(12)
C3	C4	C7	120.74(12)		F1	C12	C7	114.02(12)
C18	C13	C11	119.12(12)		C7	C12	C11	126.13(12)
C14	C13	C11	123.65(12)		C20	C19	C18	121.04(12)
C14	C13	C18	117.23(12)		C20	C19	C24	118.19(14)
C10	C11	C13	120.31(12)		C24	C19	C18	120.77(14)
C12	C11	C10	116.42(12)		C15	C14	C13	122.39(14)
C12	C11	C13	123.27(12)		C4	C5	C6	120.37(14)
C19	C20	C10	119.29(12)		C2	C1	C6	119.82(14)
C19	C20	C21	118.35(13)		C2	C3	C4	120.27(14)
C21	C20	C10	122.36(13)		C14	C15	C16	119.97(14)
C8	C7	C4	121.75(12)		C1	C6	C5	120.03(14)
C12	C7	C4	123.00(12)		C22	C21	C20	121.68(15)

C12	C7	C8	115.23(12)		C17	C16	C15	119.39(14)
F2	C8	C7	119.35(12)		C1	C2	C3	120.42(14)
F2	C8	C9	118.60(12)		C16	C17	C18	122.45(14)
C9	C8	C7	122.03(12)		C23	C22	C21	119.88(15)
C13	C18	C19	120.37(12)		C23	C24	C19	122.14(16)
C17	C18	C13	118.57(13)		C24	C23	C22	119.75(16)

Table S6. Hydrogen atomic coordinates (A×104) and the isotropic displacement parameters (A2×103).

Atom	***x***	***y***	***z***	**U(eq)**
H14	971	10288	4674	59
H5	2352	7937	6691	62
H1	531	4851	7666	66
H3	876	1759	6134	63
H15	528	13075	3921	65
H6	1650	7899	7536	68
H21	4648	2156	4516	66
H16	1334	13052	3115	70
H2	137	1811	6961	69
H17	2557	10206	3070	69
H22	5406	2238	3703	78
H24	3650	7834	3027	84
H23	4905	5094	2957	91

6. TGA

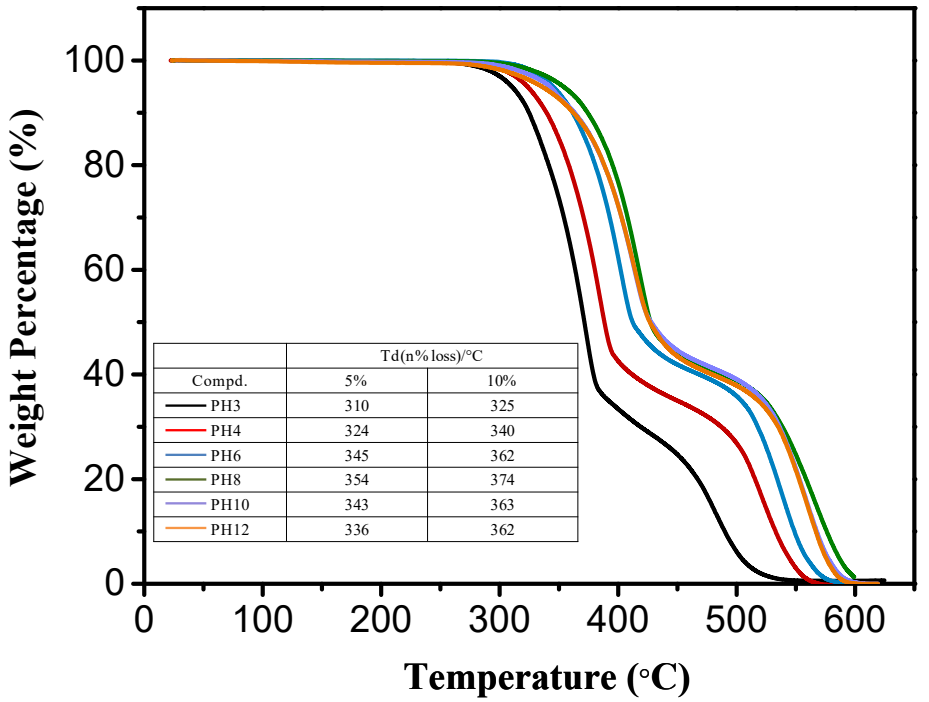

	Td(n% loss)/°C	
Compd.	5%	10%
PH3	310	325
PH4	324	340
PH6	345	362
PH8	354	374
PH10	343	363
PH12	336	362

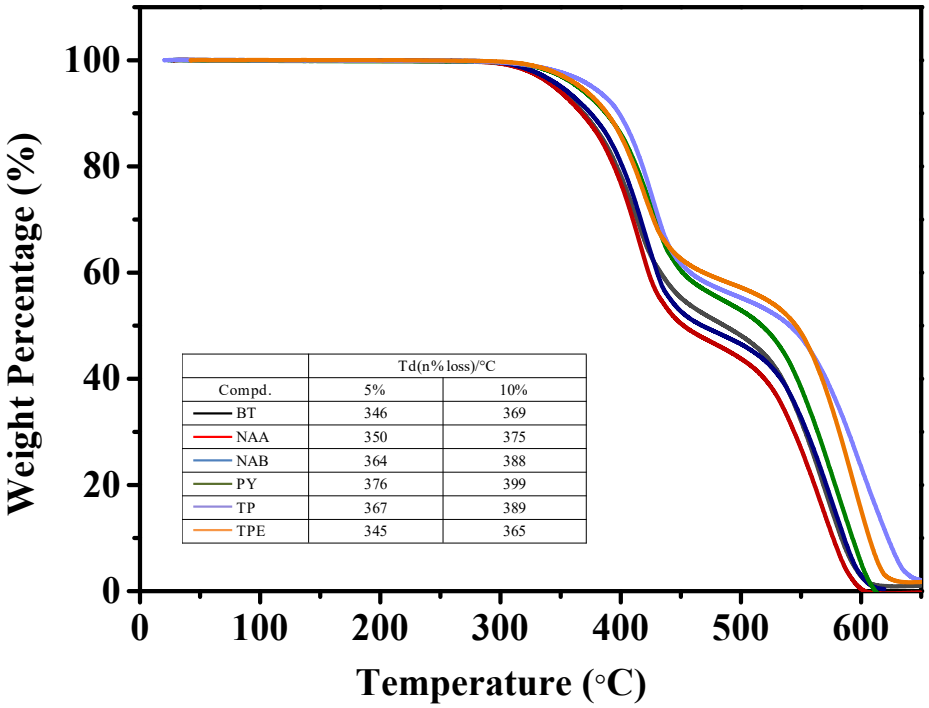

	Td(n% loss)/°C	
Compd.	5%	10%
BT	346	369
NAA	350	375
NAB	364	388
PY	376	399
TP	367	389
TPE	345	365

Figure S71 TGA thermograms of **PH***n* and 2-aryl-1,3,4-trifluorotriphenylenes (heating rate 10 °C/min).

7. POM

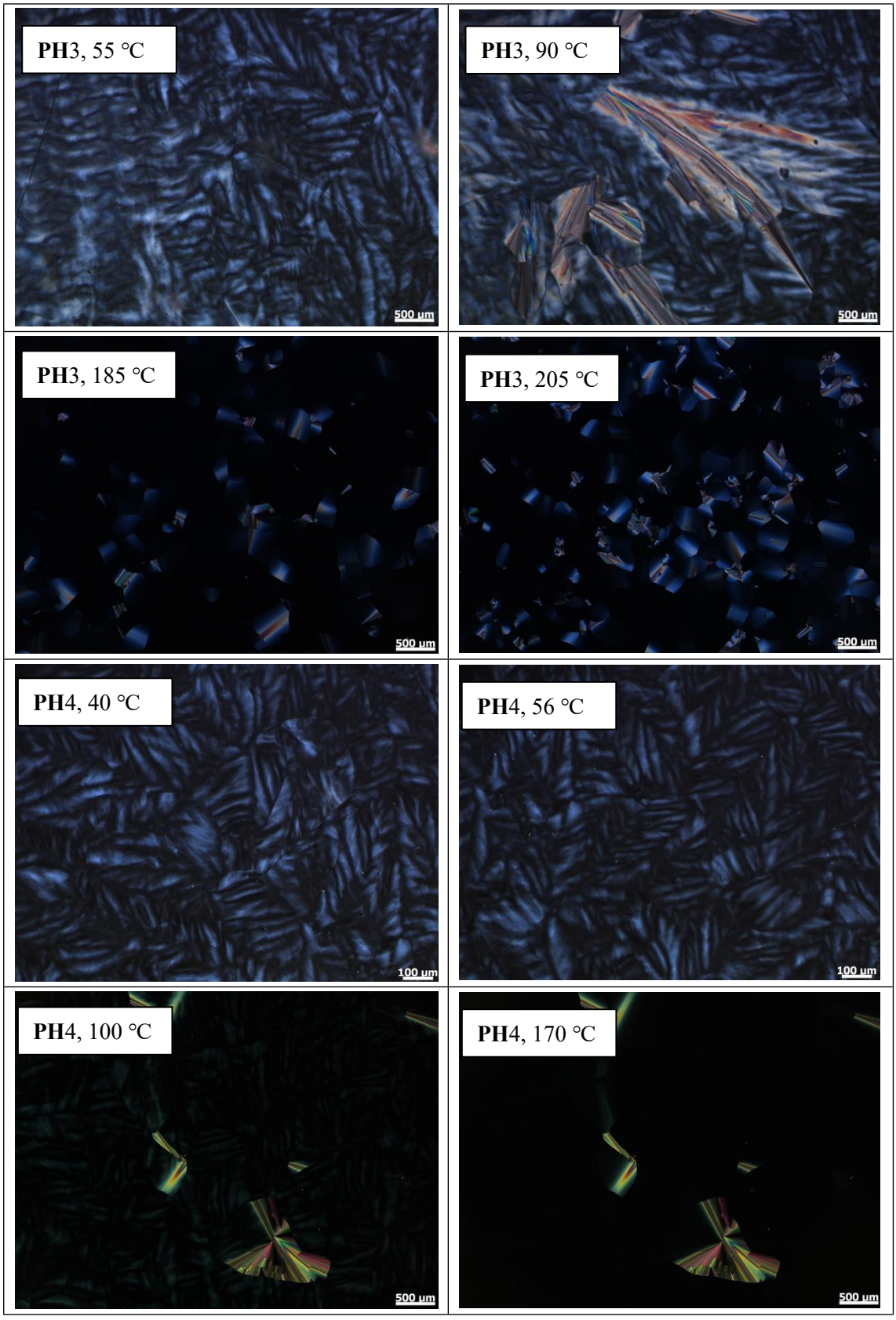
PH3, 55 ℃
500 μm
PH3, 90 ℃
500 μm
PH3, 185 ℃
500 μm
PH3, 205 ℃
500 μm
PH4, 40 ℃
100 μm
PH4, 56 ℃
100 μm
PH4, 100 ℃
500 μm
PH4, 170 ℃
500 μm

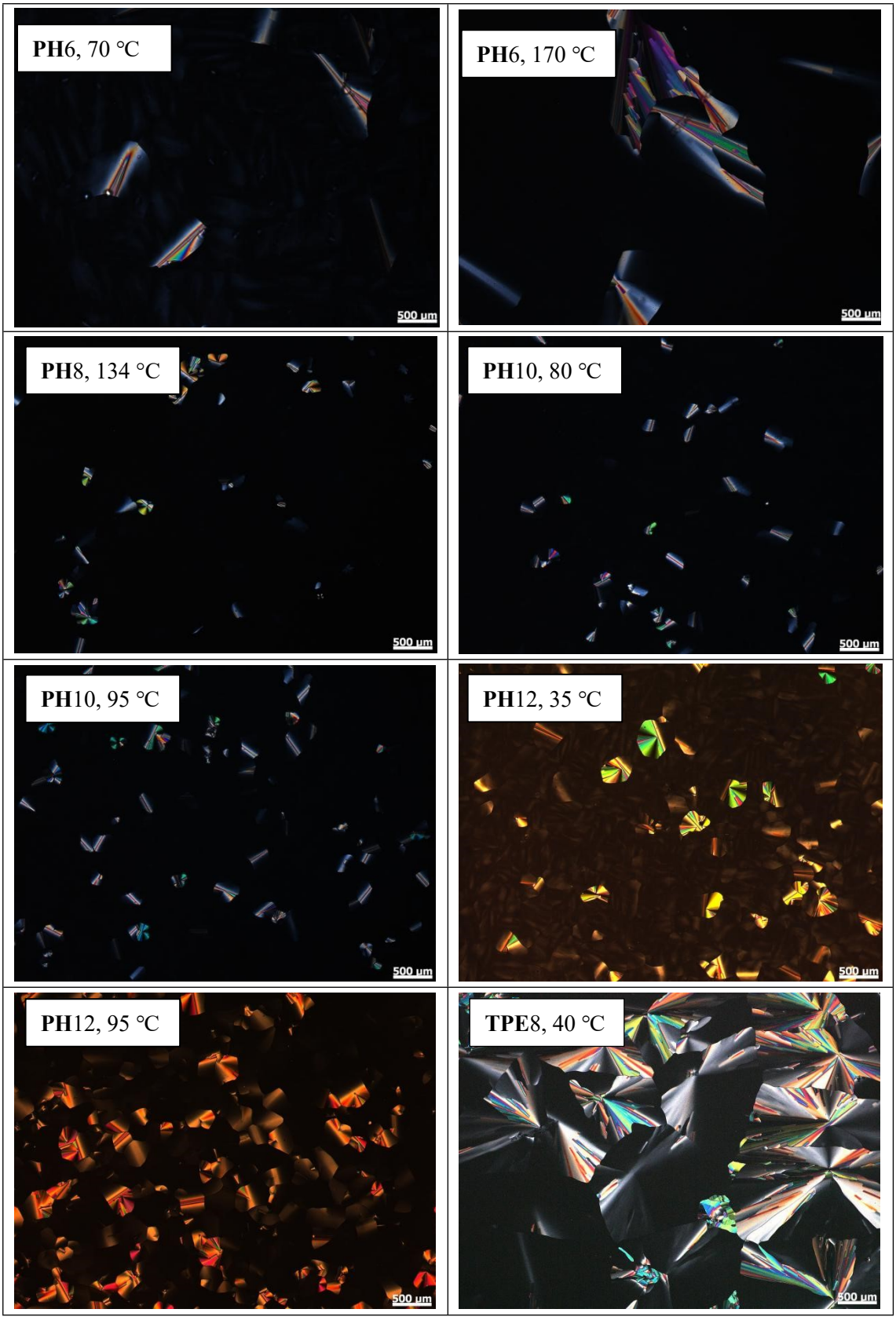
PH6, 70 °C
500 µm
PH6, 170 °C
500 µm
PH8, 134 °C
500 µm
PH10, 80 °C
500 µm
PH10, 95 °C
500 µm
PH12, 35 °C
500 µm
PH12, 95 °C
500 µm
TPE8, 40 °C
500 µm

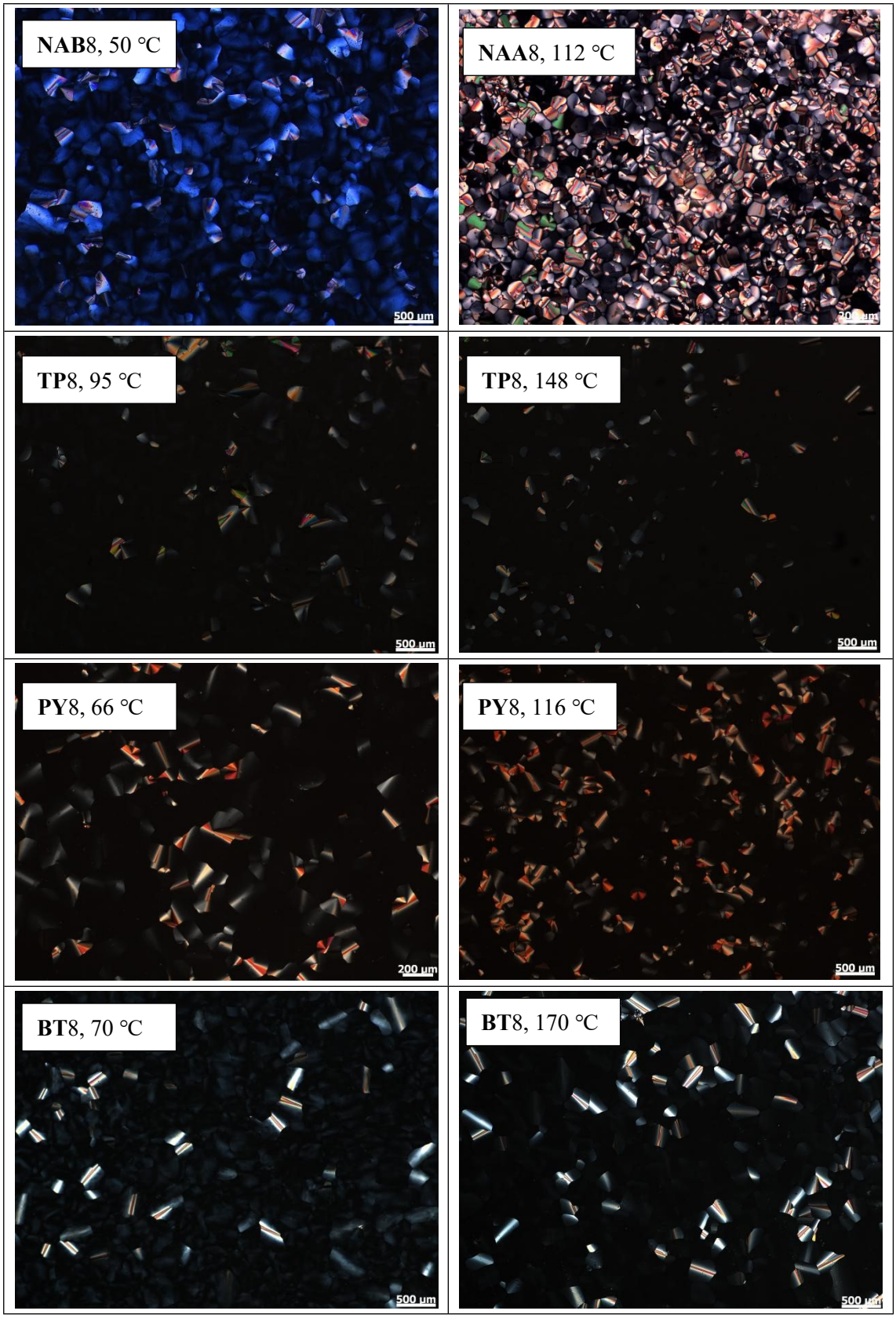

Figure S72 POM textures of **PH***n* and 2-aryl-1,3,4-trifluorotriphenylenes, taken at various temperatures on cooling from the isotropic liquid.

8. DSC

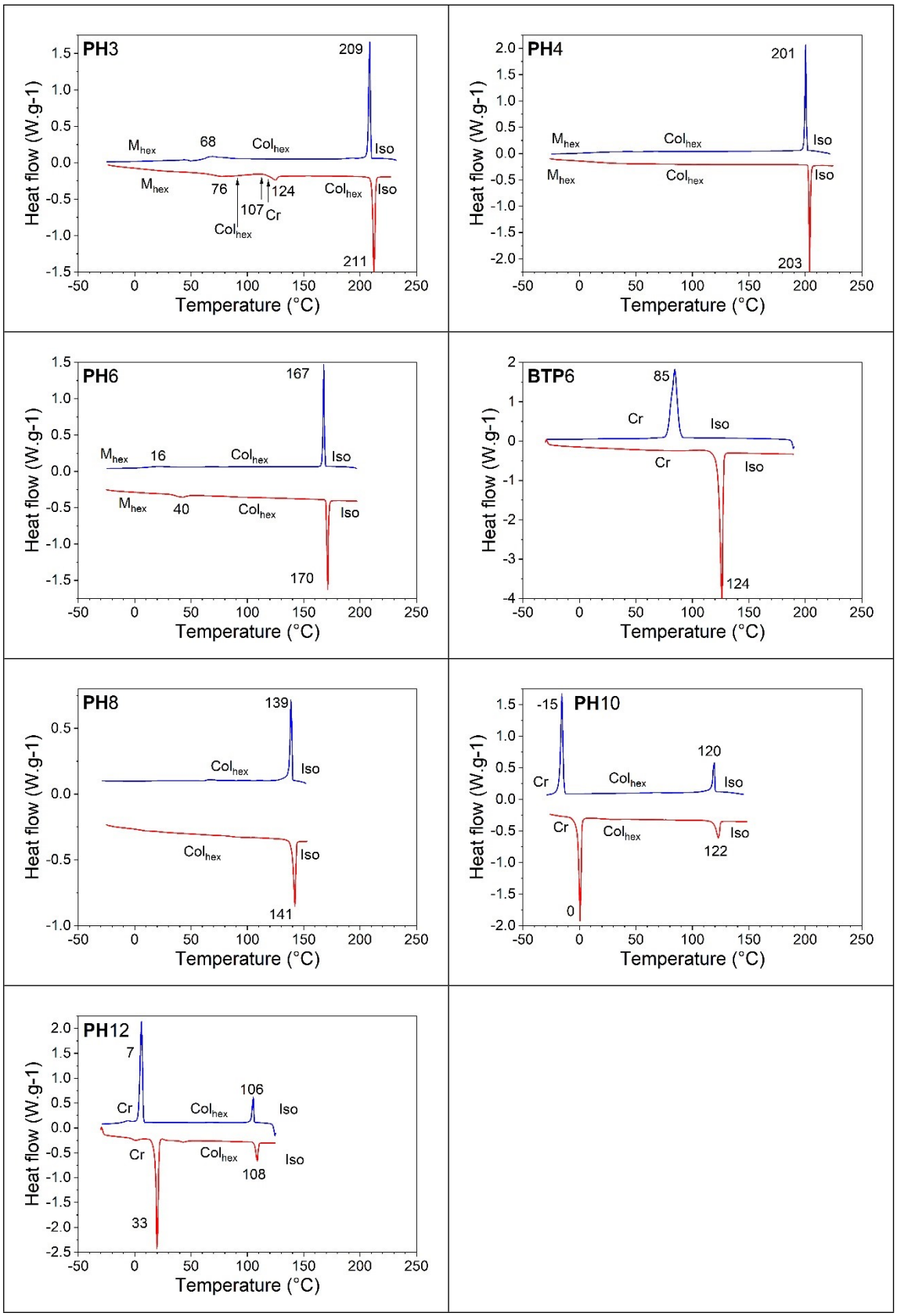

Figure S73 DSC of **PH***n* terms and **BTP**6 (heating/cooling rate 10 °C/min).

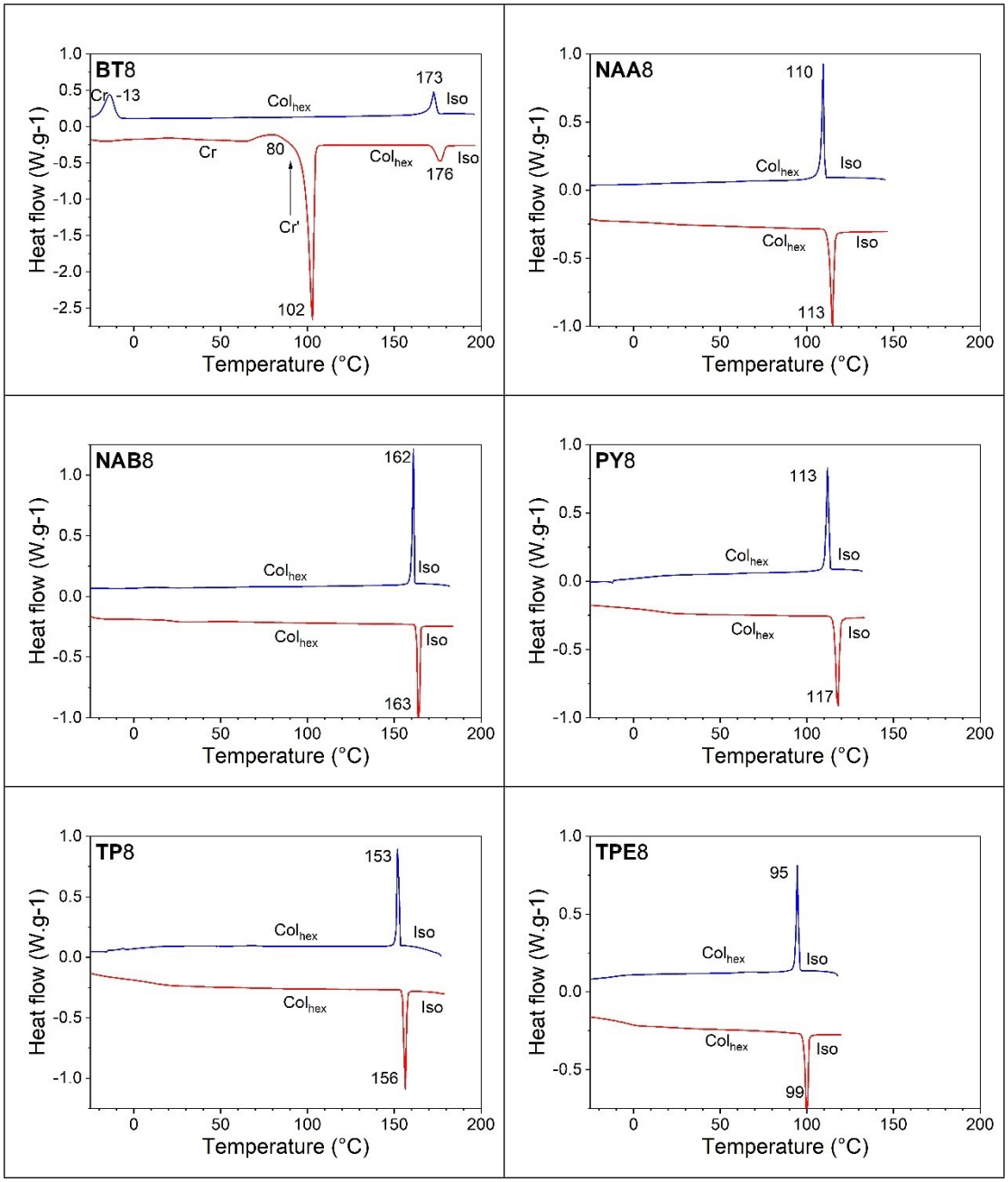

Figure S74 DSC of the 2-aryl-1,3,4-trifluorotriphenylenes (heating/cooling rate 10 °C/min).

Table S7. Phase transition parameters of **PH***n* and 2-aryl-1,3,4-trifluorotriphenylenes (heating and cooling rate of 10 °C/min).

Compds	2nd heating (1st cooling)/°C (ΔH, kJ·mol^{-1})	
PH3	M_{hex} 76 (-) Col_{hex} 107 Cr 124 (3.3) Col_{hex} 211 (11.8) I	I 209 (-11.2) Col_{hex} 68 (-) M_{hex}
PH4	M_{hex} 43 (-) Col_{hex} 203 (9.4) I	I 201 (-9.7) Col_{hex} 29 (-) M_{hex}
PH6	M_{hex} 40 (-) Col_{hex} 170 (8.3) I	I 167 (-8.3) Col_{hex} 16 (-)M_{hex}
BTP6	Cr 124 (44.4) I	I 85 (-52.8) Cr
PH8	Col_{hex} 141 (6.7) I	I 139 (-6.6) Col_{hex}
PH10	Cr -0 (25.5) Col_{hex} 122 (6.0) I	I 120 (-5.7) Col_{hex} -15 (-22.3) Cr

PH12	Cr 33 (35.8) Col_{hex} 108 (5.9) I	I 106 (-5.6) Col_{hex} 7 (-34.6) Cr
BT8	Cr 80 (-5.0) Cr' 102 (55.1) Col_{hex} 176 (5.9) I	I 173 (-5.2) Col_{hex} -13 (-5.9) Cr
NAA8	Col_{hex} 113 (8.2) I	I 110 (-7.6) Col_{hex}
NAB8	Col_{hex} 163 (7.7) I	I 162 (-7.5) Col_{hex}
PY8	Col_{hex} 117 (9.7) I	I 113 (-8.0) Col_{hex}
TP8	Col_{hex} 156 (8.1) I	I 153 (-7.6) Col_{hex}
TPE8	Col_{hex} 99 (7.0) I	I 95 (7.1) Col_{hex}

[a] Cr, Cr': crystalline phases; Col_{hex} : columnar hexagonal phase; M_{hex} : 3D columnar hexagonal phase; I: isotropic liquid

9. S/WAXS

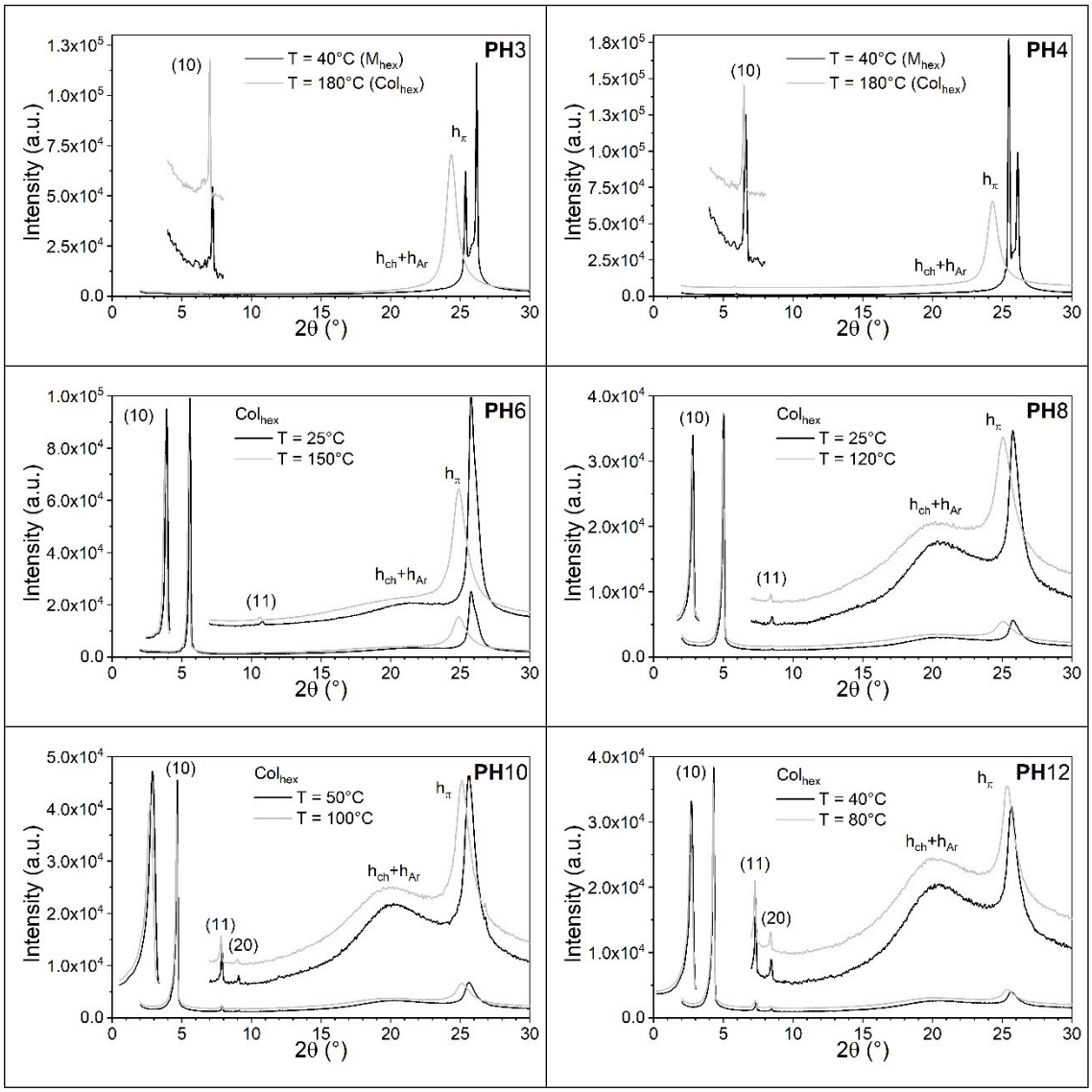

Figure S75 S/WAXS patterns of **PH***n*.

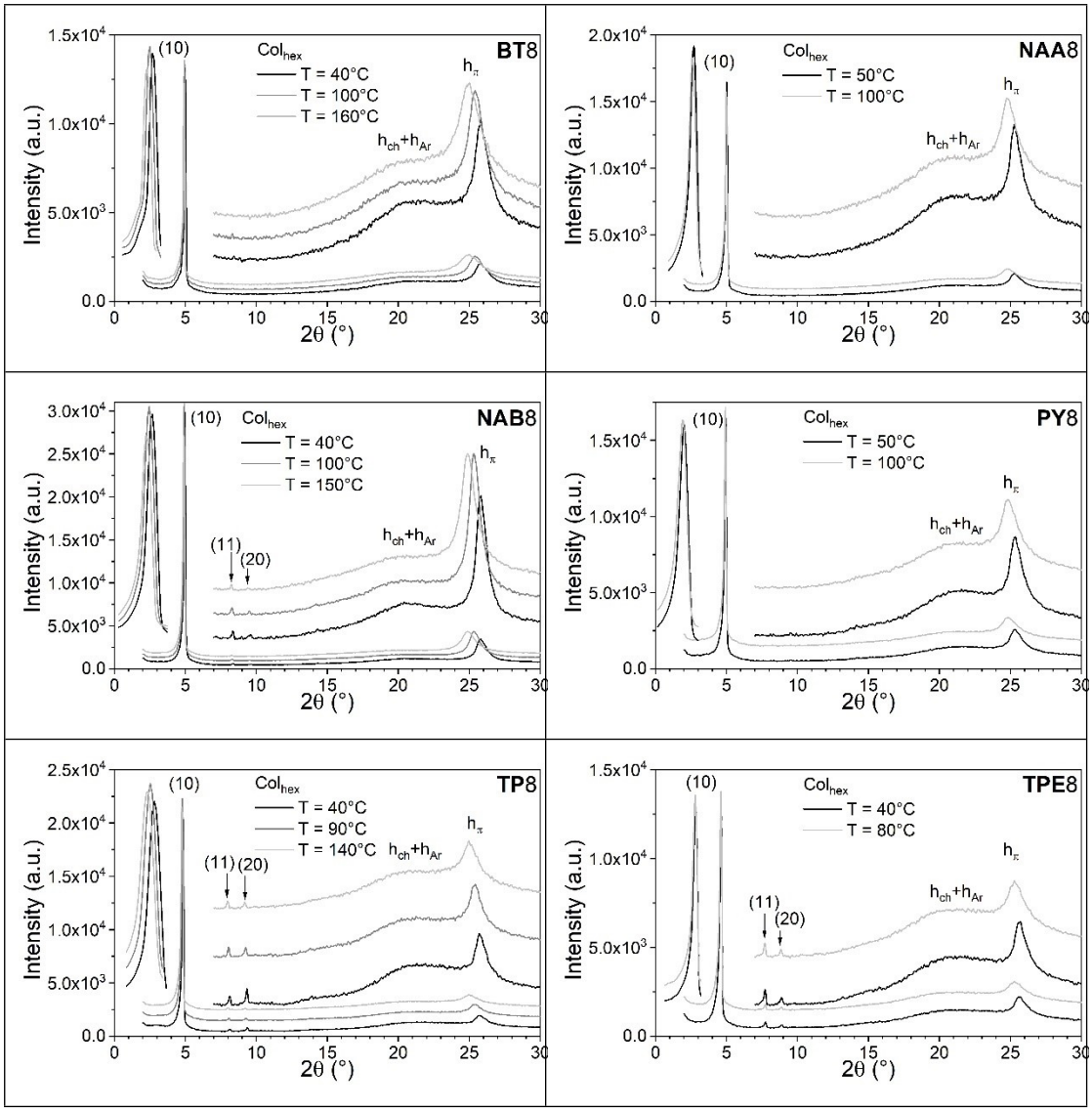

Figure S76 S/WAXS patterns of the mesophases of the 2-aryl-1,3,4-trifluorotriphenylenes compounds.

Table S8. Mesophases' parameters of **PH*n*** and 2-aryl-1,3,4-trifluorotriphenylenes

Compds	Temp. (°C)	$2\theta_{exp}$ (°)	d_{exp} (Å)	d_{calc} (Å)	I (shape)	*hk*/h(ξ)	Lattice parameters
PH3	180	6.249	14.13	14.13	VW (sh)	10	Col_{hex}
		24.36	3.65	-	VS (sh)	h_π (87)	a = 16.32 Å
		24.56	3.62	-	VW (br)	h_{ch}	A = 230.6 Å^2
PH4	180	5.848	15.10	15.12	VW (sh)	10	Col_{hex}
		24.31	3.66	-	VS (sh)	h_π (84)	a = 17.43 Å
		24.52	3.63	-	VW (br)	h_{ch}	A = 263.3 Å^2
PH6	150	5.531	16.50	16.49	VS (sh)	10	Col_{hex}
		10.727	8.24	8.24	VW (sh)	20	a = 19.04 Å
		21.28	4.17	-	VW (br)	h_{ch}	A = 314.0 Å^2
		24.94	3.57	-	VS (sh)	h_π (51)	
	25	5.417	16.30	16.31	VS (sh)	10	Col_{hex}
		10.838	8.16	8.15	VW (sh)	20	a = 18.83
		21.13	4.20	-	VW (br)	h_{ch}	A = 307.2
		25.89	3.44	-	VS (sh)	h_π (85)	

PH8	120	4.891	18.05	18.05	VS (sh)	10	Col_{hex}
		8.477	10.42	10.42	VW (sh)	11	a = 20.84 Å
		20.01	4.43	-	S (br)	h_{ch}	A = 376.2 Å^2
		25.05	3.54	-	VS (sh)	h_{π} (48)	
	25	4.950	17.84	17.85	VS (sh)	10	20.61
		8.565	10.31	10.30	VW (sh)	11	367.7
		20.49	4.34	-	S (br)	h_{ch}	
		25.88	3.44	-	VS (sh)	h_{π} (59)	
PH10	100	4.509	19.58	19.58	VS (sh)	10	Col_{hex}
		7.83	11.28	11.30	VW (sh)	11	a = 22.61 Å
		9.00	9.81	9.79	VW (sh)	20	A = 442.6 Å^2
		19.87	4.46	-	VS (br)	h_{ch}	
		25.13	3.54	-	VS (sh)	h_{π} (59)	
	50	4.589	19.24	19.24	VS (sh)	10	Col_{hex}
		7.957	11.10	11.11	VW (sh)	11	a = 22.22 Å
		9.174	9.63	9.62	VW (sh)	20	A = 427.6 Å^2
		20.04	4.43	-	VS (br)	h_{ch}	
		25.67	3.47	-	VS (sh)	h_{π} (68)	
PH12	80	4.27	20.95	20.95	VS (sh)	10	Col_{hex}
		7.307	12.09	12.09	VW (sh)	11	a = 24.19 Å
		8.425	10.48	10.47	VW (sh)	20	A = 506.8 Å^2
		19.92	4.45	-	VS (br)	h_{ch}	
		25.37	3.51	-	VS (sh)	h_{π} (50)	
	40	4.220	20.92	20.92	VS (sh)	10	Col_{hex}
		7.307	12.09	12.08	VW (sh)	11	a = 24.16 Å
		8.456	10.45	10.46	VW (sh)	20	A = 505.3 Å^2
		20.42	4.34	-	VS (br)	h_{ch}	
		25.70	3.46	-	VS (sh)	h_{π} (66)	
NAA8	100	4.908	17.99	17.99	VS (sh)	10	Col_{hex}
		19.90	4.46	-	VS (br)	h_{ch}	a = 20.77 Å
		24.83	3.58	-	VS (sh)	h_{π} (55)	A = 373.7 Å^2
	50	4.943	17.86	17.86	VS (sh)	10	Col_{hex}
		20.16	4.40	-	VS (br)	h_{ch}	a = 20.62 Å
		25.32	3.51	-	VS (sh)	h_{π} (67)	A = 368.4 Å^2
PY8	100	4.854	18.19	18.19	VS (sh)	10	a = 21.00 Å
		20.91	4.24	-	VS (br)	h_{ch}	A = 382.1 Å^2
		24.86	3.58	-	VS (sh)	h_{π} (50)	
	50	4.917	17.96	17.96	VS (sh)	10	a = 21.74 Å
		21.23	4.18	-	VS (br)	h_{ch}	A = 372.5 Å^2
		25.36	3.51	-	VS (sh)	h_{π} (68)	
TPE8	80	4.440	19.84	19.84	VS (sh)	10	Col_{hex}
		7.718	11.44	11.45	VW (sh)	11	a = 22.91 Å
		8.898	9.93	9.92	VW (sh)	20	A = 454.5 Å^2
		20.44	4.34	-	VS (br)	h_{ch}	
		25.28	3.52	-	VS (sh)	h_{π} (53)	
	40	4.474	19.73	19.73	VS (sh)	10	Col_{hex}
		7.755	11.39	11.39	VW (sh)	11	a = 22.79 Å
		8.952	9.87	9.7	VW (sh)	20	A = 449.7 Å^2
		20.76	4.27	-	VS (br)	h_{ch}	
		25.65	3.47	-	VS (sh)	h_{π} (63)	
BT8	160	4.880	18.09	18.09	VS (sh)	10	Col_{hex}
		19.98	4.44	-	VS (br)	h_{ch}	a = 20.89 Å
		24.95	3.56	-	VS (sh)	h_{π} (40)	A = 377.9 Å^2
	100	4.932	17.90	17.90	VS (sh)	10	Col_{hex}
		20.09	4.42	-	VS (br)	h_{ch}	a = 20.67 Å
		25.44	3.50	-	VS (sh)	h_{π} (54)	A = 370.0 Å^2

	40	4.984	17.71	17.71	VS (sh)	10	Col_{hex}
		20.38	4.35	-	VS (br)	h_{ch}	a = 20.45 Å
		25.84	3.44	-	VS (sh)	h_{π} (59)	A = 362.2 Å^2
NAB8	150	4.811	18.35	18.36	VS (sh)	10	Col_{hex}
		8.342	10.59	10.60	VW (sh)	11	a = 21.20 Å
		9.60	9.20	9.18	VW (sh)	20	A = 389.4 Å
		20.07	4.42	-	VS (br)	h_{ch}	
		24.91	3.57	-	VS (sh)	h_{π} (54)	
	100	4.830	18.28	18.28	VS (sh)	10	Col_{hex}
		8.373	10.55	10.56	VW (sh)	11	a = 21.11 Å
		9.66	9.15	9.14	VW (sh)	20	A = 386.0 Å
		20.29	4.37	-	VS (br)	h_{ch}	
		25.37	3.51	-	VS (sh)	h_{π} (72)	
	40	4.843	18.23	18.24	VS (sh)	10	Col_{hex}
		8.404	10.51	10.53	VW (sh)	11	a = 21.07 Å
		9.66	9.15	9.12	VW (sh)	20	A = 384.4 Å
		20.51	4.33	-	VS (br)	h_{ch}	
		25.84	3.44	-	VS (sh)	h_{π} (78)	
TP8	140	4.615	19.13	19.13	VS (sh)	10	Col_{hex}
		7.993	11.05	11.04	VW (sh)	11	a = 22.09 Å
		9.247	9.56	9.56	VW (sh)	20	A = 422.6 Å^2
		20.28	4.37	-	VS (br)	h_{ch}	
		24.98	3.56	-	VS (sh)	h_{π} (64)	
	90	4.655	18.96	18.96	VS (sh)	10	Col_{hex}
		8.081	10.93	10.95	VW (sh)	11	a = 21.90 Å
		9.304	9.50	9.48	VW (sh)	20	A = 415.3 Å^2
		20.44	4.34	-	VS (br)	h_{ch}	
		25.38	3.51	-	VS (sh)	h_{π} (73)	
	40	4.697	18.80	18.80	VS (sh)	10	Col_{hex}
		8.144	10.85	10.85	VW (sh)	11	a = 21.70 Å
		9.398	9.40	9.40	VW (sh)	20	A = 407.9 Å^2
		20.77	4.27	-	VS (br)	h_{ch}	
		25.76	3.45	-	VS (sh)	h_{π} (80)	

Annotation: $2\theta_{exp}$: measured diffraction angles; d_{exp} and d_{cal}: measured and calculated distances; VS, S, M, W, VW stand for very strong, strong, medium, weak, very weak; sh and br stand for sharp and broad; hk: Miller indices of columnar lattice reflection; h_{ch}: average distance between alkyl chains; h_{π}: average distance of π-π stacking of molecules, and ξ, correlation length; a: columnar lattice parameters; A: lattice area.

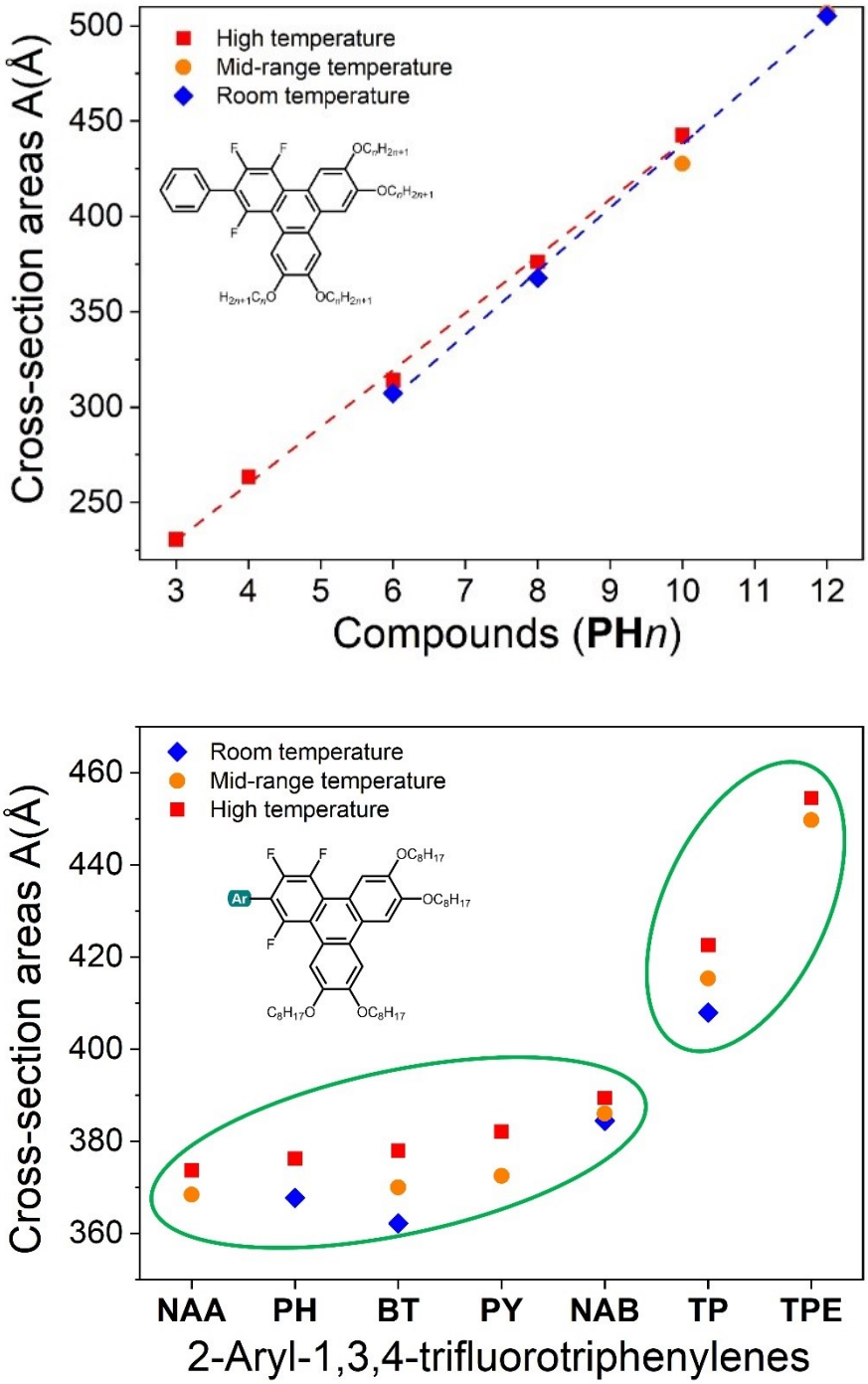

Figure S77 Columnar cross-sections of compounds **PH***n* (top) and 2-aryl-1,3,4-trifluorotriphenylenes (bottom).

10. DFT

Table S9. Molecular structures of compounds **BT**1, **PH**1, **NAA**1, **NAB**1, **PY**1, **TP**1 and **TPE**1.

Compounds	Molecular structure

BT1/**PH**1	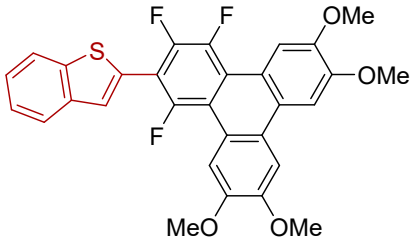	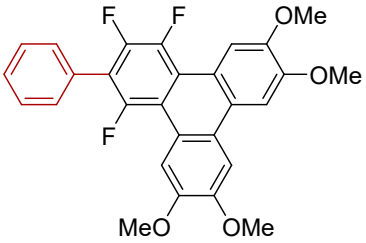
NAA1/**NAB** 1	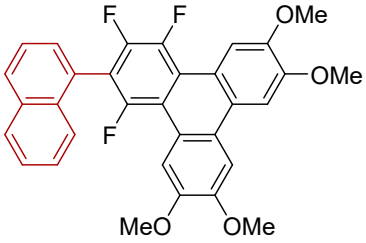	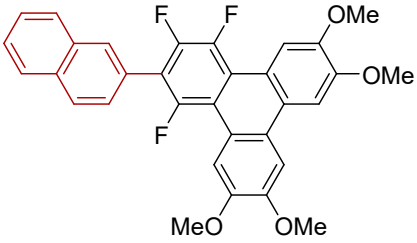
TP1/**PY**1	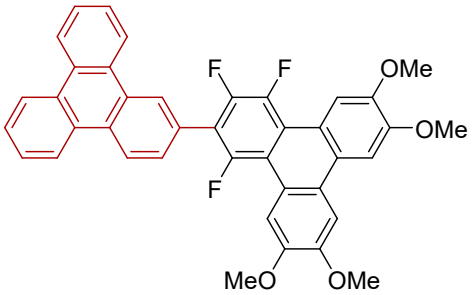	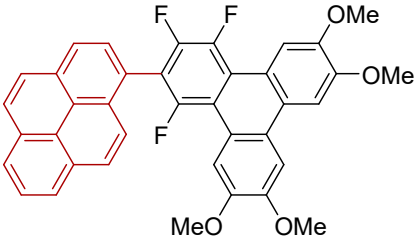
TPE1	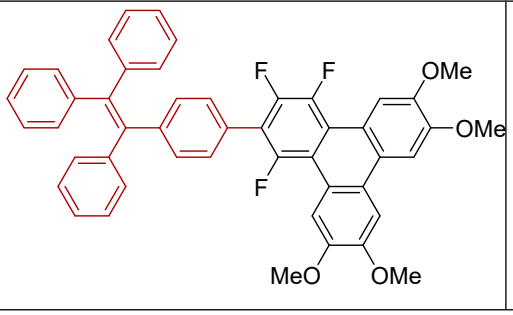	

Table S10. DFT calculated optimized molecular structures in THF of **BT**1, **PH**1, **NAA**1, **NAB**1, **PY**1, **TP**1 and **TPE**1.

Compounds	front views (in THF)	side views (in THF)
BT1	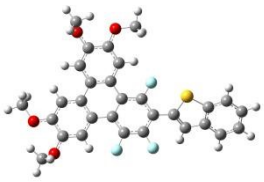	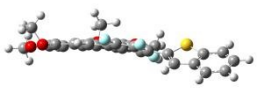
PH1	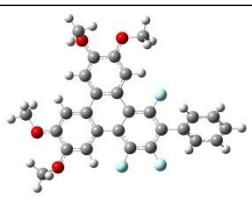	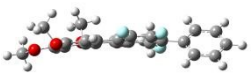

NAA1	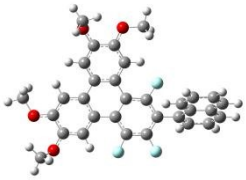	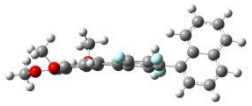
NAB1		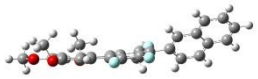
PY1		
TP1	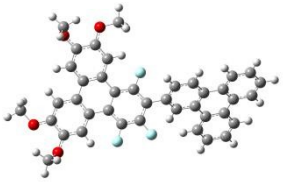	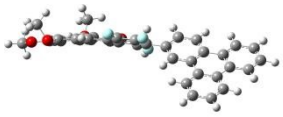
TPE1	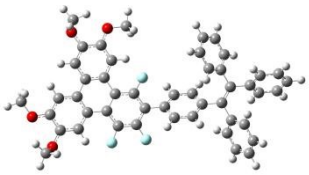	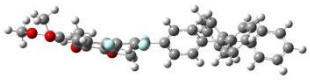

Table S11. DFT calculated optimized molecular structures in gas of **BT**1, **PH**1, **NAA**1, **NAB**1, **PY**1, **TP**1 and **TPE**1.

Compounds	front views (in GAS)	side views (in GAS)
BT1	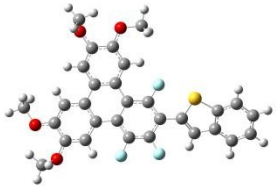	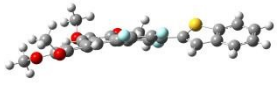

PH1	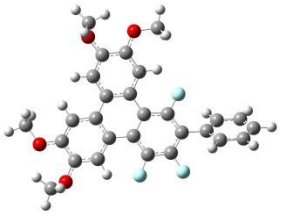	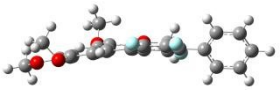
NAA1	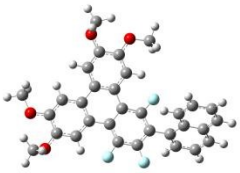	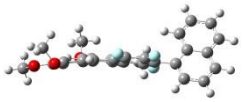
NAB1	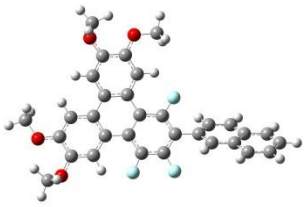	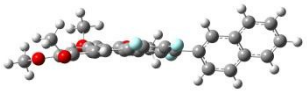
PY1		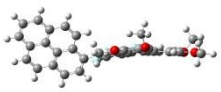
TP1	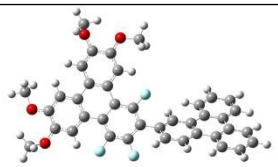	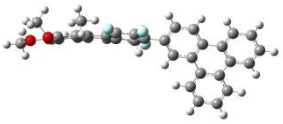
TPE1		

Table S12. List of selected molecular orbital energies for **BT**1, **PH**1, **NAA**1, **NAB**1, **PY**1, **TP**1 and **TPE**1 and the HOMO-LUMO energy gaps (△E).

	THF		**GAS**

	HOMO (eV)	LUMO (eV)	△E (eV)		HOMO (eV)	LUMO (eV)	△E (eV)
BT1	-5.88	-2.05	3.83		-5.77	-1.97	3.80
PH1	-5.89	-1.78	4.11		-5.76	-1.66	4.10
NAA1	-5.89	-1.82	4.07		-5.76	-1.72	4.04
NAB1	-5.88	-1.90	3.98		-5.75	-1.79	3.96
PY1	-5.78	-2.14	3.63		-5.68	-2.06	3.62
TP1	-5.88	-1.94	3.94		-5.75	-1.82	3.93
TPE1	-5.75	-1.95	3.80		-5.63	-1.85	3.78

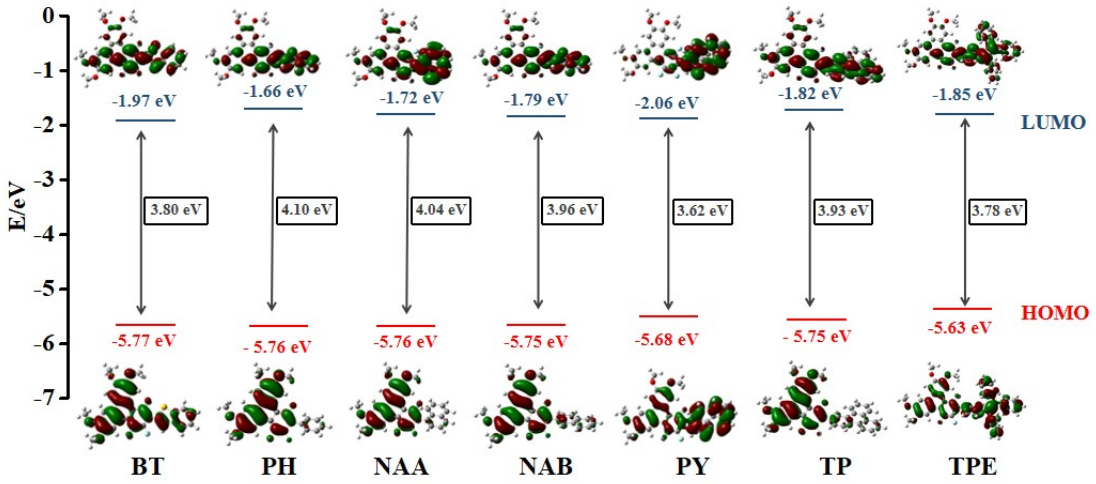

Figure S78 HOMO-LUMO and energy gap of the 2-aryl-1,3,4-trifluorotriphenylenes in gas state.

11. TOF

Table S13. TOF photoconductivity (hole) of **PY**8 recorded on heating (cell thickness 19.6 µm).

T (°C)	*E* (V cm^{-1})	τ_{hole} (s)	μ_{hole} (cm^2 V^{-1} s^{-1})	μaverage hole (cm^2 V^{-1} s^{-1})
30	2×10^4	4.18×10^{-3}	2.35×10^{-4}	4.47×10^{-4}
	3×10^4	4.40×10^{-3}	1.48×10^{-4}	
	4×10^4	4.60×10^{-3}	1.06×10^{-4}	
	5×10^4	4.69×10^{-3}	8.36×10^{-5}	
40	2×10^4	5.05×10^{-4}	1.94×10^{-4}	5.22×10^{-4}

	3×10^4	5.11×10^{-4}	1.28×10^{-4}	
	4×10^4	5.34×10^{-4}	9.18×10^{-5}	
	5×10^4	5.39×10^{-4}	7.28×10^{-5}	
50	2×10^4	5.76×10^{-4}	1.70×10^{-4}	5.74×10^{-4}
	3×10^4	5.71×10^{-4}	1.14×10^{-4}	
	4×10^4	5.74×10^{-4}	8.54×10^{-5}	
	5×10^4	5.74×10^{-4}	6.83×10^{-5}	
60	2×10^4	7.27×10^{-4}	1.35×10^{-4}	7.27×10^{-4}
	3×10^4	7.10×10^{-4}	9.20×10^{-5}	
	4×10^4	7.25×10^{-4}	6.76×10^{-5}	
	5×10^4	7.45×10^{-4}	5.26×10^{-5}	
70	2×10^4	7.94×10^{-4}	1.23×10^{-4}	8.06×10^{-4}
	3×10^4	7.94×10^{-4}	8.22×10^{-5}	
	4×10^4	8.25×10^{-4}	5.94×10^{-5}	
	5×10^4	8.11×10^{-4}	4.83×10^{-5}	
80	2×10^4	8.64×10^{-4}	1.13×10^{-4}	8.94×10^{-4}
	3×10^4	8.84×10^{-4}	7.39×10^{-5}	
	4×10^4	8.99×10^{-4}	5.45×10^{-5}	
	5×10^4	9.31×10^{-4}	4.21×10^{-5}	
90	2×10^4	1.04×10^{-3}	9.45×10^{-5}	1.01×10^{-3}
	3×10^4	9.96×10^{-4}	6.56×10^{-5}	
	4×10^4	1.02×10^{-3}	4.86×10^{-5}	
	5×10^4	1.00×10^{-3}	3.91×10^{-5}	
100	2×10^4	9.63×10^{-4}	1.02×10^{-4}	1.06×10^{-3}
	3×10^4	1.04×10^{-3}	6.31×10^{-5}	
	4×10^4	1.11×10^{-3}	4.43×10^{-5}	
	5×10^4	1.13×10^{-3}	3.46×10^{-5}	
110	2×10^4	9.63×10^{-4}	1.02×10^{-4}	1.06×10^{-3}
	3×10^4	1.04×10^{-3}	6.31×10^{-5}	
	4×10^4	1.11×10^{-3}	4.43×10^{-5}	
	5×10^4	1.13×10^{-3}	3.46×10^{-5}	
120	2×10^4	3.63×10^{-5}	2.70×10^{-3}	3.76×10^{-5}
	3×10^4	3.76×10^{-5}	1.74×10^{-3}	
	4×10^4	3.87×10^{-5}	1.27×10^{-3}	
	5×10^4	3.78×10^{-5}	1.04×10^{-3}	

Table S14. TOF photoconductivity (hole) of **PY**8 recorded on cooling (cell thickness 19.6 μm).

T **(°C)**	***E*** **(V cm^{-1})**	τ_{hole} **(s)**	μ_{hole} **(cm^2 V^{-1} s^{-1})**	μ**average hole (cm^2 V^{-1} s^{-1})**
120	2×10^4	3.63×10^{-5}	2.70×10^{-3}	3.76×10^{-5}
	3×10^4	3.76×10^{-5}	1.74×10^{-3}	
	4×10^4	3.87×10^{-5}	1.27×10^{-3}	
	5×10^4	3.78×10^{-5}	1.04×10^{-3}	

110	2×10^4	9.58×10^{-4}	1.02×10^{-4}	9.92×10^{-5}
	3×10^4	9.92×10^{-4}	6.58×10^{-5}	
	4×10^4	1.01×10^{-3}	4.88×10^{-5}	
	5×10^4	1.01×10^{-3}	3.87×10^{-5}	
100	2×10^4	8.27×10^{-4}	1.18×10^{-4}	9.66×10^{-4}
	3×10^4	9.95×10^{-4}	6.57×10^{-5}	
	4×10^4	1.19×10^{-3}	4.79×10^{-5}	
	5×10^4	1.02×10^{-3}	3.85×10^{-5}	
90	2×10^4	9.41×10^{-4}	1.04×10^{-4}	9.40×10^{-4}
	3×10^4	9.13×10^{-4}	7.15×10^{-5}	
	4×10^4	9.52×10^{-4}	5.15×10^{-5}	
	5×10^4	9.55×10^{-4}	4.11×10^{-5}	
80	2×10^4	8.48×10^{-4}	1.16×10^{-4}	8.47×10^{-4}
	3×10^4	8.42×10^{-4}	7.76×10^{-5}	
	4×10^4	8.49×10^{-4}	5.77×10^{-5}	
	5×10^4	8.49×10^{-4}	4.62×10^{-5}	
70	2×10^4	7.25×10^{-4}	1.35×10^{-4}	3.39×10^{-4}
	3×10^4	7.22×10^{-4}	9.04×10^{-5}	
	4×10^4	7.46×10^{-4}	6.57×10^{-5}	
	5×10^4	7.62×10^{-4}	5.14×10^{-5}	
60	2×10^4	6.20×10^{-4}	1.58×10^{-4}	6.45×10^{-4}
	3×10^4	6.61×10^{-4}	9.88×10^{-5}	
	4×10^4	6.43×10^{-4}	7.62×10^{-5}	
	5×10^4	6.55×10^{-4}	5.99×10^{-5}	
50	2×10^4	5.30×10^{-4}	1.85×10^{-4}	5.71×10^{-4}
	3×10^4	5.71×10^{-4}	1.14×10^{-4}	
	4×10^4	5.81×10^{-4}	8.43×10^{-5}	
	5×10^4	6.00×10^{-4}	6.53×10^{-5}	
40	2×10^4	4.79×10^{-4}	2.05×10^{-4}	4.90×10^{-4}
	3×10^4	4.90×10^{-4}	1.33×10^{-4}	
	4×10^4	4.99×10^{-4}	9.81×10^{-5}	
	5×10^4	4.93×10^{-4}	7.96×10^{-5}	
30	2×10^4	4.00×10^{-4}	2.45×10^{-4}	4.00×10^{-4}
	3×10^4	3.84×10^{-4}	1.70×10^{-4}	
	4×10^4	3.91×10^{-4}	1.25×10^{-4}	
	5×10^4	4.26×10^{-4}	9.21×10^{-5}	

T：test temperature；**E**：external electric field strength；τ_{hole}：hole drift time；μ_{hole}：charge drift times available at various electric fields；μ：average hole transport rate

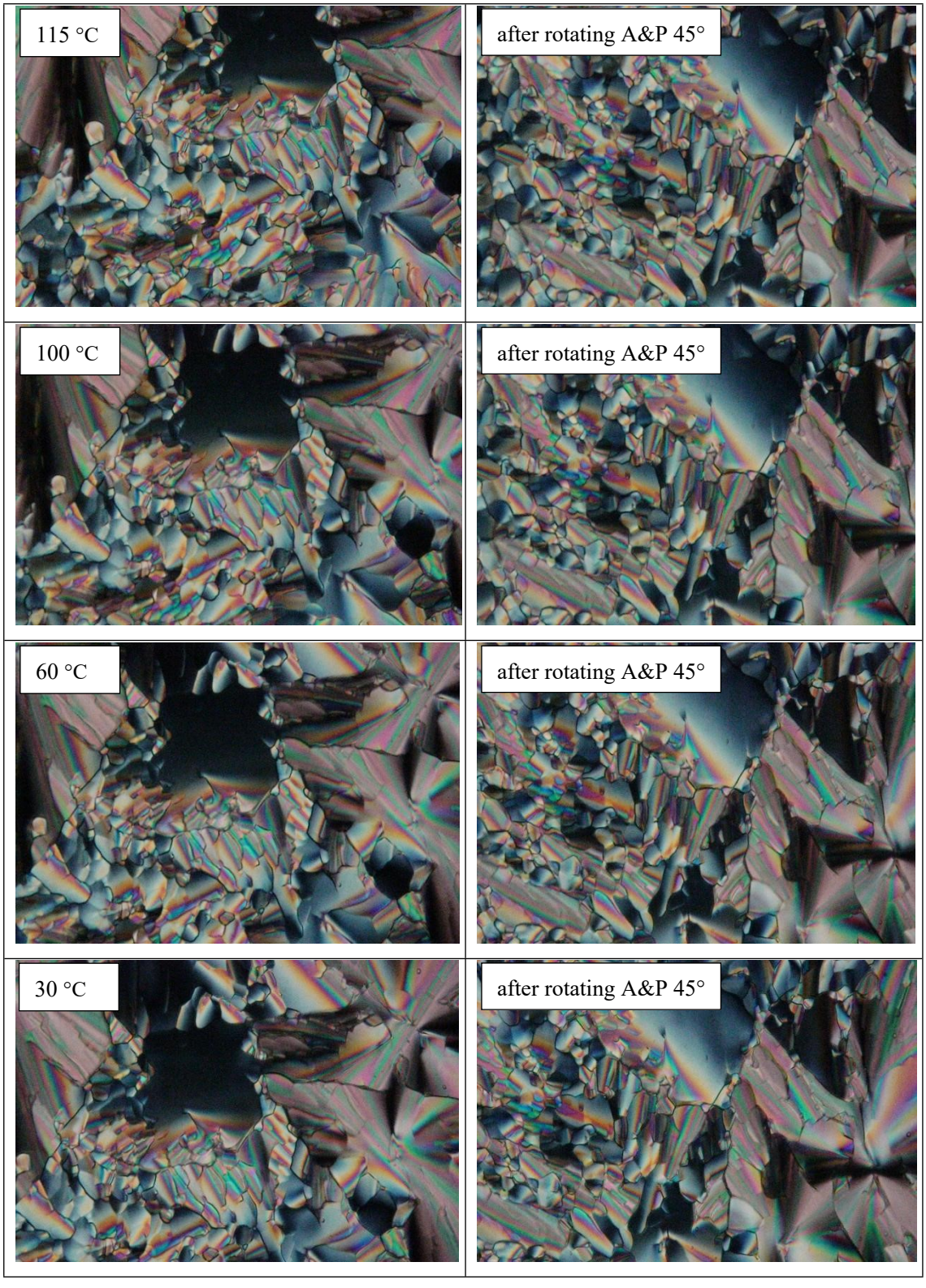
115 °C
after rotating A&P 45°
100 °C
after rotating A&P 45°
60 °C
after rotating A&P 45°
30 °C
after rotating A&P 45°

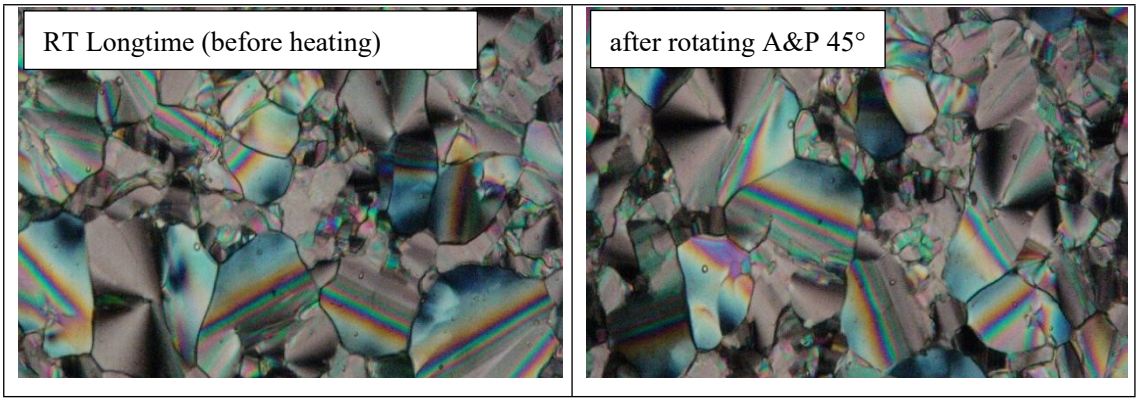

Figure S79 POM images of sample **PY**8 in ITO LC cell taken both on heating and cooling run during the TOF measurement.